TECHNISCHE UNIVERSITÄT MÜNCHEN

Lehrstuhl für Entwicklungsgenetik

Effects of a human ALS causative point mutation expressed in mouse – Generation and analysis

Carola Barbara Stribl

Vollständiger Abdruck der von der Fakultät Wissenschaftszentrum Weihenstephan für Ernährung, Landnutzung und Umwelt der Technischen Universität München zur Erlangung des akademischen Grades eines

Doktors der Naturwissenschaften

genehmigten Dissertation.

Vorsitzender: Univ.-Prof. Dr. E. Grill

Prüfer der Dissertation:

1. Univ.-Prof. Dr. W. Wurst
2. Univ.-Prof. Dr. Dr. h.c. C. Haass
   (Ludwig-Maximilians-Universität München)

Die Dissertation wurde am 31.07.2012 bei der Technischen Universität München eingereicht und durch die Fakultät Wissenschaftszentrum Weihenstephan für Ernährung, Landnutzung und Umwelt am 12.12.2012 angenommen.

CONTENT

1 Zusammenfassung

Amyotrophe Lateralsklerose (ALS) und frontotemporale Lobärdegeneration (FTLD) sind zwei schwerwiegende neurodegenerative Krankheiten für deren Behandlung es bis heute keine effektiven Methoden gibt. Neue Einblicke in diese Erkrankungen sowie deren gemeinsamen pathogenen Mechanismus wurden durch die Entdeckung von TDP-43 als Hauptkomponente der Ubiquitin-positiven Einschlüsse gewonnen. Bis heute wurden zahlreiche Punktmutationen in dem für TDP-43 kodierenden Gen *TARDBP* bei ALS Patienten entdeckt. Die zugrundeliegenden Mechanismen, die zu den Erkrankungen führen sind bis dato unbekannt, ebenso wie die Frage, ob ein Funktionsverlust oder ein toxischer Funktionsgewinn von TDP-43 für die Entstehung der Krankheiten verantwortlich ist.

Um neue Einblicke in die zugrundeliegenden pathogenen Mechanismen und die genaue Rolle von TDP-43 zu bekommen habe ich ein Mausmodell generiert welches eine humane TDP-43 cDNA mit der ALS auslösenden Mutation A315T unter Kontrolle des endogenen Promotors exprimiert. Mäuse, welche die Mutation homozygot exprimieren, sterben bereits im Embryonalstadium. Trotz der Expression der humanen cDNA unter Kontrolle des endogenen Promoters wird das humane TDP-43 etwa 3-fach überexprimiert während das endogene TDP-43 auf etwa 20% herunter reguliert wird. hTDP-43^{A315T} Mäuse entwickeln im Laufe der Zeit zahlreiche pathologische Veränderungen, wie die Entstehung von unlöslichen und ubiquitinierten TDP-43 Aggregaten im Gehirn und Rückenmark, eine veränderte Anzahl an Motoneuronen, sowie eine Abnahme des Körpergewichts. In Verhaltensanalysen zeigten die Tiere vor allem Anomalien im Gang. Des Weiteren wurde eine drastische Abnahme des Expressionslevels von Parkin, einem vermeintlichen Target von TDP-43, detektiert. In Übereinstimmung mit dem verringerten Level an Parkin wurde eine Abnahme von CD36, ein in den Fettmetabolismus involviertes Protein, festgestellt. Zudem wurden Abweichungen im Fetthaushalt erkannt. Die veränderte Expression von OPA-1 deutet zudem darauf hin, dass eine beeinträchtigte Funktion der Mitochondrien vorliegt.

Das beschriebene TDP-43 Mausmodell zeigt einige charakteristische Eigenschaften der neurodegenerativen Erkrankungen ALS und FTLD auf und bringt neue Einblicke in die Entstehung und zugrundeliegenden Mechanismen. Speziell im Hinblick auf die Rolle des Fettmetabolismus ist dieses Mausmodell geeignet um therapeutische Anwendungen zu testen.

2 Summary

Amyotrophic lateral sclerosis (ALS) and frontotemporal lobar degeneration (FTLD) are two fatal neurodegenerative diseases which can currently not be treated effectively. The discovery of TDP-43 as the major protein in ubiquitin-positive inclusions in ALS and FTLD was break through implying a common pathogenic mechanism. To date, several missense mutations in the gene *TARDBP*, encoding for TDP-43, were identified in ALS as well as in FTLD patients. However, the underlying mechanisms leading to the neurodegenerative diseases are still unknown, even if a loss-of-function or a toxic-gain-of-function of TDP-43 contribute to the development of the disorders remain unanswered up to now.

To gain new knowledge about the underlying pathogenic mechanisms and the role of mutant TDP-43, I generated a mouse model expressing human TDP-43 cDNA with the ALS causative mutation A315T under control of the endogenous promoter. Homozygous mutant mice were embryonic lethal indicating an essential role for TDP-43 in embryonic development or toxicity. Despite the expression of human TDP-43 under control of the endogenous promoter, a 3-fold overexpression of human TDP-43 was detectable in various tissues, while the endogenous mouse TDP-43 was reduced to 20%. Nevertheless, these mice developed a number of pathological and biochemical changes including insoluble and ubiquitinated TDP-43 inclusions in the brain and spinal cord, changes in the number of motor neurons and a loss of body weight that are reminiscent of the pathology found in ALS and FTLD patients. In the behavioral analysis, mutant mice revealed gait abnormalities. Furthermore, the expression level of Parkin, a putative TDP-43 target, decreased dramatically. In accordance with the decrease of Parkin, CD36, the fatty acid translocase which was previously correlated with a loss of Parkin, was also down-regulated in old hTDP-43^{A315T} mice. Moreover, analysis of blood plasma samples revealed changes in the lipid metabolism of mutant mice. An abnormal regulation of OPA-1, a protein involved in mitochondrial fusion and fission, was discovered indicating mitochondrial dysfunction in mutant animals.

This new TDP-43 mouse model shows several characteristic features of ALS and FTLD and provides new hints into the underlying mechanisms involved in the development of the diseases. It may be useful for testing therapeutic approaches especially regarding the role of lipid metabolism.

3 Introduction

3.1 TDP-43 proteinopathies

3.1.1 Amyotrophic lateral sclerosis (ALS)

First described by Jean-Martin Charcot (Rowland, 2001) in 1869, amyotrophic lateral sclerosis (ALS), also known as Lou Gehrig's disease, is a devastating neurodegenerative disorder characterized by the progressive loss of upper and lower motor neurons. The degeneration of motor neurons in the primary motor cortex, brain stem and anterior horn of the spinal cord leads to progressive muscle atrophy, weakness and spasticity. Paralysis of respiratory muscles leads to death within one to five years after the diagnosis. In Europe amyotrophic lateral sclerosis (ALS) has an incidence of 2-3 cases per 100,000 individuals, with a lifetime risk of 1:400 to develop the disease (for review see Hardiman et al. 2011).

ALS type	onset	Gene	Locus	References
ALS1	adult	*SOD1*	21q22.11	Rosen et al. 1993
ALS2	juvenile	*ALS2*	2q33.1	Hadano et al. 2001
ALS3	adult	unknown	18q21	
ALS4	juvenile	*SETX*	9q34.13	Chen et al. 2004
ALS5	juvenile	*SPG11*	15q21.1	Orlacchio et al. 2010
ALS6	adult	*FUS*	16p11.2	Vance et al. 2009 Kwiatkowski et al. 2009
ALS7	adult	Unknown	20p13	
ALS8	adult	*VABP*	20q13.33	Niskimura et al. 2004
ALS9	adult	*ANG*	14q11	Greenway et al. 2006
ALS10	adult	*TARDBP*	1p36.22	Neumann et al. 2006
ALS11	adult	*FIG4*	6q21	Chow et al. 2009
ALS12	adult	*OPTN*	10p13	Maruyama et al. 2010

Tab. 1: Genetic heterogeneity of ALS

The majority of cases occur sporadically (90%) and only 10% show a familial history with a Mendelian inheritance (Mitchell and Borasio, 2007). The inheritance pattern is often autosomal dominant, but cases of autosomal recessive pedigrees have also been observed

(Gros-Louis et al. 2006). The mean age of onset for amyotrophic lateral sclerosis varies between 55 – 65 years whereas the median age of onset is at 64 years. For sporadic ALS (sALS) 5% of the cases have an onset before the age of 30 (Haverkamp et al. 1995). The identification of mutations in *SOD1* (encoding superoxide dismutase 1) as a risk factor for familiar amyotrophic lateral sclerosis (fALS) remarkably advanced ALS research (Rosen et al. 1993). Over the past years several other putative genes were identified as risk factors for ALS (Tab.1). Interestingly, all ALS patients show inclusions of TDP-43 in brain and spinal cord neurons except those carrying a mutation in SOD1 (Neumann et al. 2006, Arai et al. 2006).

3.1.2 Frontotemporal lobar degeneration (FTLD)

Frontotemporal lobar degeneration (FTLD), formerly known as Pick's disease (PiD), is characterized by the loss of neurons in the frontal and temporal lobe of the brain. FTLD is the third most common form of dementia after Alzheimer's disease and Lewy body dementia (Ratnavalli et al. 2002). Three clinical syndromes are summarized in FTLD: Frontotemporal Dementia (FTD), Semantic Dementia (SD) and Progressive Nonfluent Aphasia (PNFA). Frontotemporal dementia is the most common clinical syndrome and is characterized by profound alteration in personality and behavior, while semantic dementia and progressive nonfluent aphasia manifest as language dysfunctions (Neary et al., 1998). The age of onset ranges between 40 – 60 years with a very slow progress.

FTLD type	Gene	Locus	References
FTLD-tau	*MAPT*	17q21.1	Hutton et al. 1998
FTLD-TDP	*VCP*	9p13.3	Watts et al. 2004
FTLD-TDP	*GRN*	17q21.31	Baker et al. 2006 Cruts et al. 2006
FTLD-UPS	*CHMP2B*	3p11.2	Skibinski et al. 2005
FTLD-TDP	*TARDBP*	1p36.22	Benajiba et al. 2009
FTLD-TDP	unknown	9q21-q22	Morita et al. 2006
FTLD-TDP	TMEM106B	7p21.3	Van Deerlin et al. 2010

Tab. 2: Genetic heterogeneity of FTLD

A characteristic hallmark of FTLD is the formation of abnormal protein inclusions in neurons and glial cells. Histologically, FTLD can be divided into three groups: (1) FTLD with tau-positive and ubiquitin-negative inclusions, termed FTLD-tau (approximately 50% of all cases); (2) FTLD with tau-negative and ubiquitin-positive, TDP-43-positive inclusions termed FTLD-TDP and (3) FTLD with tau-negative and ubiquitin-positive, FUS-positive inclusions termed FTLD-FUS. Most cases occur sporadically with only a small number ascribed to familial history. During the last decade several genes were identified as a risk factor for FTLD. Mutations in the gene *MAPT* encoding for TAU are known to be involved in FTLD-tau (Hutton et al. 1998). Mutations in the genes TARDBP, FUS and GRN were found in patients with FTLD-TDP and several other genes have been identified as listed in table 2.

3.1.3 The link between ALS and FTLD

As mentioned, patients suffering from ALS develop a form of motor neuron degeneration (MND). Interestingly, 15 – 20% of ALS patients display signs of frontotemporal lobar degeneration (FTLD) characterized by behavioral and cognitive impairments (ALS-dementia). The same connection was found in FTLD patients, where 15-20% of them develop symptoms of motor neuron disease (FTLD-MND) (Lillo and Hodges 2009). The breakthrough in understanding the link between the two neurodegenerative diseases was the discovery of TDP-43 being the major protein in ubiquitinated inclusions for most cases of ALS and FTLD (Neumann et al. 2006, Arai et al. 2006). “Overlap” cases of FTLD with MND or ALS with cognitive impairment reveal a TDP-43 pathology situated somewhere between the pathology observed at FTLD-TDP and ALS (Brandmeir et al. 2008, Geser et al. 2009). Whereas mutations in *TARDBP* encoding for TDP-43 are often found in sporadic and familial ALS patients, patients with FTLD-U rarely display mutations in the TDP-43 associated gene.

3.2 TAR DNA-binding protein 43 (TDP-43)

3.2.1 Structure of TDP-43

TAR DNA-binding protein 43 (TDP-43) is a 414 amino acid protein with an estimated molecular mass of 43kDa encoded by *TARDBP* on chromosome 1p36.2. It was first identified in 1995 as a binding protein to the TAR DNA sequence motif of HIV Type1 (Ou et al. 1995). The gene *TARDBP* encoding for TDP-43 consists of six exons while the first exon is untranslated and has up to 11 different alternative splice forms, the predominant being the 43kDa form (Buratti and Baralle, 2008). TDP-43 contains two RNA recognition motifs (RRM1 and RRM2) and a C-terminal glycine-rich region (Fig.1). RRM1 is essential for binding to single-stranded RNA (ssRNA) with a minimum of five UG repeats, while the function of RRM2 is still unclear. Interactions with other proteins are mediated by the C-terminal glycine-rich region (Ou et al. 1995, Wang et al. 2004, Ayala et al. 2005). TDP-43 is predominantly located in the nucleus, but there is also a continuous shuttling between the nucleus and the cytoplasm mediated by the N-terminal nuclear localization signal (NLS) and nuclear export signal (NES) (Ayala et al. 2008).

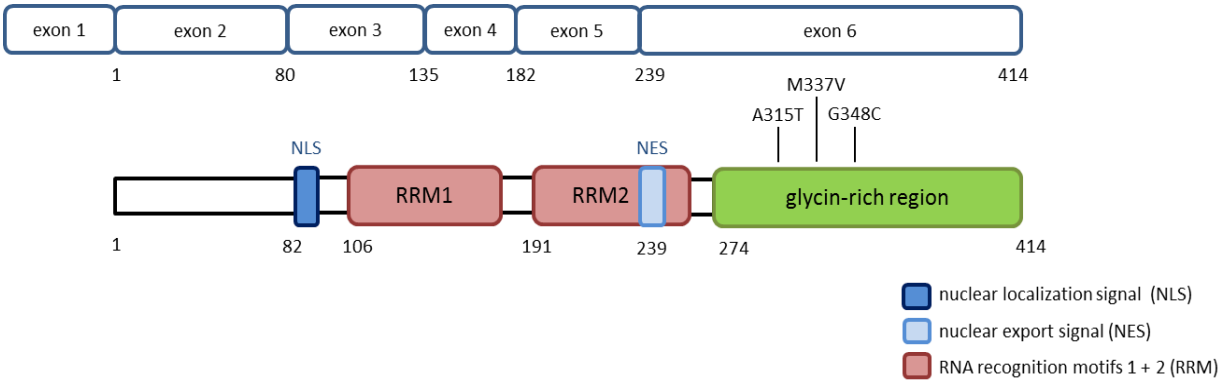

Fig. 1: Structure of TDP-43. The gene TARDBP consists of six exons encoding for a 414 amino acids protein (upper panel). The protein TDP-43 contains two RRMs, a C-terminal gylcine-rich region, a NLS and a NES (lower panel).

The majority of the mutations identified for ALS and FTLD patients are located in the C-terminal glycine-rich region. All but one are dominant missense mutations, leading to an exchange of one amino acid. In 2008, Gitcho et al. identified the mutation A315T in a cohort of MND patients. This point mutation leads to an exchange of the highly conserved alanine to threonine (c.1077 G>A) in the C-terminus of TDP-43. The patients carrying the A315T

mutation displayed a slowly progressive variant of ALS with no cognitive impairments (Gitcho et al. 2008). Sreedharan et al. (2008) identified the mutation M337V in familiar ALS patients, which is also located in the C-terminal region of TDP-43. As for the A315T mutation no cognitive impairments could be diagnosed. The mutation G348C leading to an amino acid exchange from glycine to cysteine was identified 2008 in a cohort of sporadic ALS patients (Kabashi et al. 2008). To date, about 40 mutations in *TARDBP* were identified in sporadic and familiar ALS patients indicating an essential role of TDP-43 in the development of the disease.

3.2.2 TDP-43 autoregulation

TDP-43 expression levels must be tightly regulated in embryogenesis and adulthood because of severe consequences due to TDP-43 overexpression or down-regulation in animal models. Knockout of TDP-43 in mice resulted in early peri-implantation lethality during embryogenesis suggesting an essential role of the protein in embryonic development (Wu et al. 2010, Sephton et al. 2009). An overexpression of TDP-43 leads to phenotypes similar to ALS and FTLD patients (for review, see Wegorzewska and Baloh 2010). Recently, Ayala et al. (2011) claimed that TDP-43 can regulate its own mRNA levels by binding to its own 3'UTR sequence. The interaction of TDP-43 with its 3'UTR was confirmed by two studies using UV-CLIP analyses (Polymenidou et al. 2011, Tollervey et al. 2011). In summary, these studies indicate that TDP-43 regulates itself through a negative feedback loop by binding on its own 3'UTR sequence. The exact mechanism of the negative feedback is still under consideration. One hypothesis is the involvement of nonsense mediated decay (NMD), where TDP43-mediated splicing of its own 3'UTR would introduce a premature stop codon and thereby targets the mRNA for degradation (Polymenidou et al. 2011). Another hypothesis is that the exosome system plays a role in reducing the levels of TDP-43 (Ayala et al. 2011).

3.2.3 Functions of TDP-43

Due to its structure, TDP-43 is a member of the heterogenous nuclear ribonucleoprotein (hnRNP) family of proteins (Lagier-Tourenne and Cleveland 2009). hnRNPs are known to regulate splicing and TDP-43 was found to regulate splicing of several mRNAs. Additionally, TDP-43 is involved in the regulation of mRNA levels and in RNA trafficking (for review, see Lee et al. 2011). Furthermore, TDP-43 binds to FUS, a protein similar to TDP-43 and also involved in ALS and FTLD (Ling et al. 2010). Both proteins are recruited to stress granules indicating a role in RNA stability and RNA transport (Colombrita et al. 2009). TDP-43 was also found to play a role in microRNA (miRNA) biogenesis concerning the binding to the Drosha and Dicer complexes (Kawahara et al. 2012, Gregory et al. 2004) and altered miRNA levels after TDP-43 knockdown (Buratti et al. 2010). In addition to its role in RNA pathways, TDP-43 interacts with single-stranded DNA (ssDNA) via its C-terminal glycin-rich region and thereby inhibiting transcription through an unknown mechanism (Fig.2A).

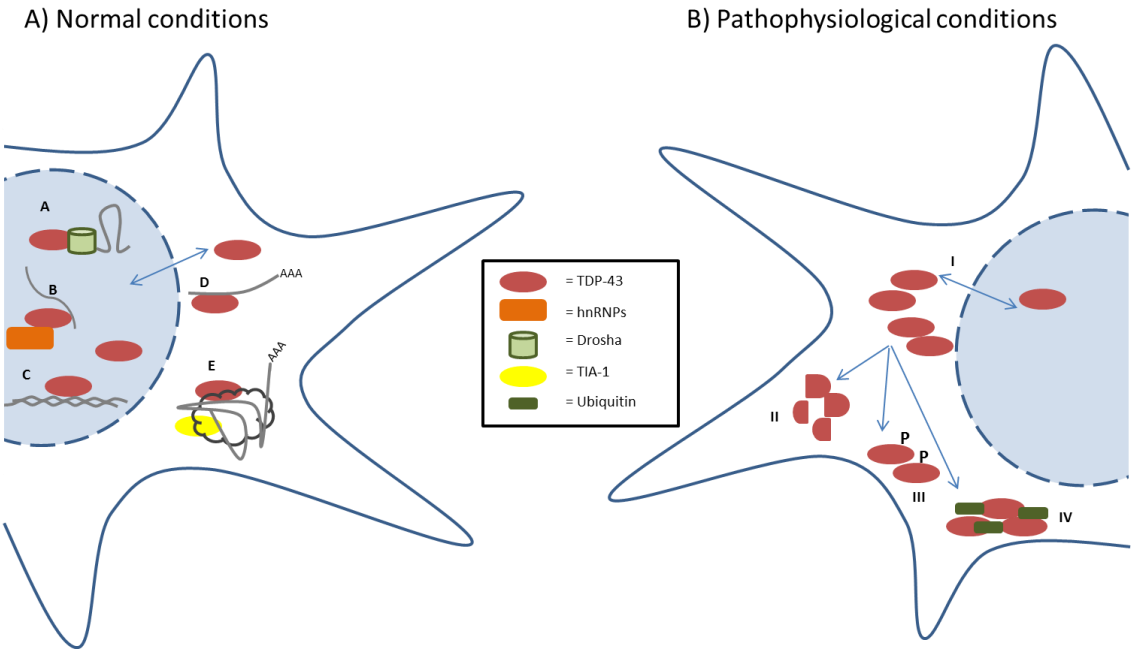

Fig. 2: TDP-43 under normal and pathophysiological conditions. (A) Under normal conditions TDP-43 is involved in several nuclear cellular processes as miRNA biogenesis (A), mRNA splicing (B) and inhibition of transcription (C). TDP-43 is also involved in mRNA transport (D) and is recruited to stress granules (E). (B) Under pathophysiological conditions, TDP-43 is sequestered to the cytoplasm (I), where it is abnormally cleaved (II), hyper-phosphorylated (III) and ubiquitinated (IV) leading to the formation of insoluble cytoplasmic inclusions.

Several interesting targets were identified via iCLIP assays after TDP-43 knockdown or overexpression, such as the disease-related transcripts *Fus*, *Grn*, *Htt, Parkin, Hdac6* and *Casein kinase I* and *II* (Polymenidou et al. 2011, Tollervey et al. 2011). Furthermore, TDP-43 mediates exon skipping of the cystic fibrosis transmembrane conductance regulator (CFTR) and apolipoprotein A2 (APOA2) (Buratti et al. 2001, Mercado et al. 2005). TDP-43 mediates not only exon skipping but also exon inclusion of the Progranulin receptor sortilin 1 (Sort1) and the survival motor neuron protein 2 (SMN2) (Polymenidou et al. 2011, Bose et al. 2008). However, most target genes found to not necessarily provide association or even a hint to the human diseases.

3.2.4 TDP-43 pathology

In the neurodegenerative diseases ALS and FTLD, TDP-43 was found to be the main part of ubiquitinated aggregates in neurons and glial cells (Neumann et al. 2006). Under normal circumstances, TDP-43 is mainly located to the nucleus where it functions in several cellular processes (Fig.2A). Under pathophysiological conditions, neurons exhibit a clearance of TDP-43 from the nucleus (Fig.2B). In the cytoplasm, TDP-43 is abnormally cleaved, leading to 25kDa C-terminal fragments missing their NLS sequence (Neumann et al. 2006). In addition, cytosolic TDP-43 is ubiquitinated. TDP-43 is thought to be degraded by the ubiquitin-proteasome system (UPS). The inhibition of the UPS may lead to an increase of ubiquitinated TDP-43 (for review, see Levine and Krömer 2008). Moreover, TDP-43 is hyper-phosphorylated at specific serine residues (Hasegawa et al. 2008, Neumann et al. 2009). This phosphorylation potentially contributes to a longer half-life, suggesting that degradation is inhibited and formation of inclusions is advanced (Zhang et al. 2010). In contrast, Li et al. claim that hyper-phosphorylation acts as a defense mechanism (Li et al. 2011). All these post-translational modifications lead to a characteristic biochemical profile of insoluble TDP-43 in ALS and FTLD (Fig.3B). Histological, TDP-43 can be detected in neurons and glial cells of brain and spinal cord sections as cytoplasmic inclusions and can be classified into four subtypes of FTLD-TDP as shown in figure 3. Subtype 1 is characterized by the formation of long neuritic profiles predominantly in the superficial cortical laminae with few or no neuronal cytoplasmic inclusions (NCIs) or neuronal intranuclear inclusions (NIIs). In subtype 2 cases, NCIs are predominant in superficial and deep cortical layers with the presence of few

neurites and few or no NIIs. The abundance of small neuritic profiles and NCIs predominantly in the superficial cortical layers characterizes subtype 3. Subtype 4 is characterized by the abundance of NIIs and dystrophic neurites with few NCIs in affected cortical regions and the absence of inclusions in the hippocampal dentate granule cells. In sALS cases TDP-43 pathology is characterized by the formation of round and skein-like neuronal and glial inclusions in affected brain regions (Fig.3A) (for review see Neumann et al. 2007).

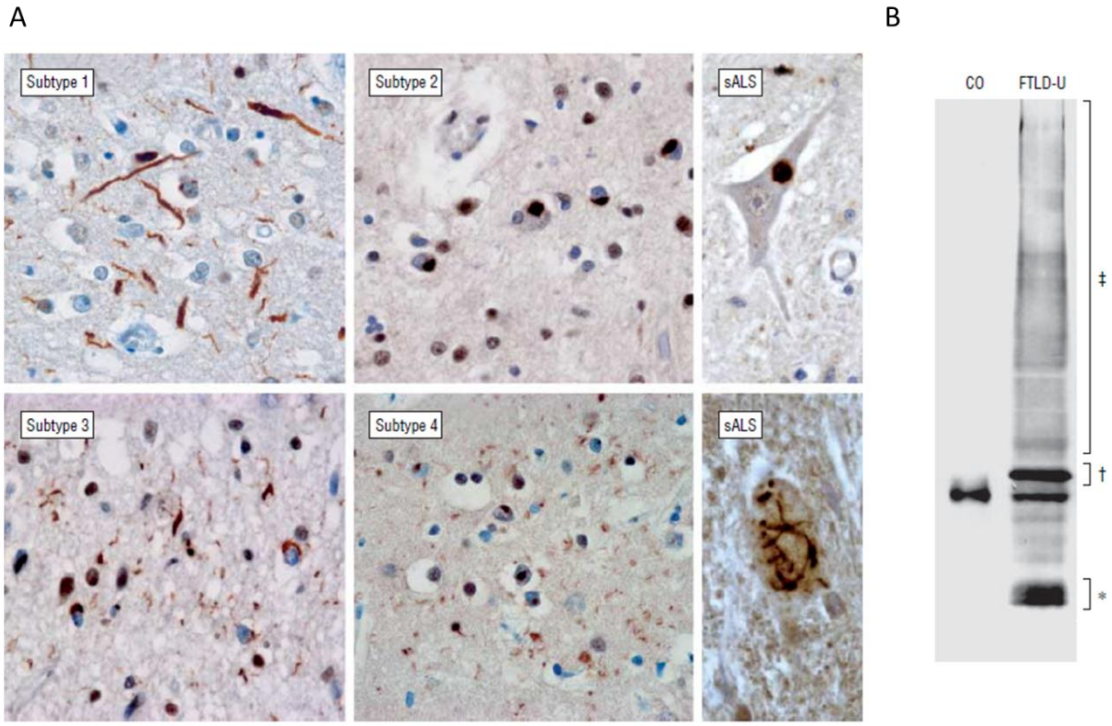

Fig. 3: TDP-43 pathology in ALS and distinct subtypes of FTLD-U. (A) Types of TDP-43 inclusions of FTLD-U subtype 1-4 and sporadic ALS. (B) Biochemical profile of TDP-43 in urea extracts from FTLD-U brains, presence of disease-specific TDP-43 species. C-terminal fragments are represented by the approximately 25kDa bands (*), hyper-phosphorylated TDP-43 at approximately 45kDa (†) and high molecular weight smear represents ubiquitination of TDP-43 (‡), which are not detectable in control (CO) brains. Reprinted with permission from American Medical Association © Neumann et al. TDP-43 Proteinopathy in Frontotemporal Lobar Degeneration and Amyotrophic Lateral Sclerosis. Arch Neurol. 64(10):1388-94 (2007).

TDP-43 pathology is not only detectable in ALS and FTLD; other neurodegenerative diseases also exhibit TDP-43 inclusions as secondary pathological features. TDP-43 pathology was reported in 50% of all Alzheimer's disease cases and in 60% of all Parkinson's disease cases as well as in several rare disorders, including Guam ALS and Guam ALS-PD (for review, see Chen-Plotkin et al. 2010). In these cases, TDP-43 inclusions co-exist, but only partially co-localize with tau or α-synuclein aggregates (Uryu et al. 2008, Amador-Ortiz et al. 2007, Geser et al. 2008 and Hasegawa et al. 2007). In addition, TDP-43 pathology occurs also in

polyglutamine diseases as Huntington's disease (HD) and spinocerebellar ataxias (SCAs). One study reported that in all cases of HD examined (10 in total), TDP-43 co-localized with mutant huntingtin in cytoplasmic inclusions (Schwab et al. 2008). Furthermore, Elden et al. (2010) could show that TDP-43 associates with ataxin 2, a polyglutamine (polyQ) protein mutated in SCA2, in a RNA dependent complex and thereby abnormally localizes.

3.3 TDP-43 mouse models

In the last years, several TDP-43 transgenic rodent models were published (for review, see Wegorzweska and Baloh, 2010). In order to mimic the disease course of amyotrophic lateral sclerosis, human TDP-43 cDNAs were expressed in rodents under control of exogenous promoters. Either wildtype cDNA or cDNAs with ALS associated mutations were used to gain insight into the mechanisms of the fatal disorder. Wegorzweska et al. (2009) published the first TDP-43 transgenic mouse model. Under control of the mouse prion promoter (mPrp) a human TDP-43 cDNA transgene was expressed with the mutation A315T, 3-fold over endogenous TDP-43. With an age of 3 months, transgenic mice exhibited gait abnormalities and started losing weight leading to death at the age of 5 months. Despite the discovery of ubiquitin-positive inclusions and a reduction in motor neurons, no TDP-43 aggregates could be detected. Several other TDP-43 transgenic mouse models were published expressing human wildtype or mutant TDP-43 cDNA under control of the mPrp promoter, leading to an ALS associated phenotype with TDP-43 inclusions and a reduced lifespan (Xu et al. 2010, Stallings et al. 2010). Similar results were obtained expressing human TDP-43 cDNA under control of the murine Thy-1 promoter (Wils et al. 2010, Shan et al. 2010). Rodent models with an expression of TDP-43 cDNA under control of the endogenous promoter exhibited a more slightly or even no motor neuron pathology (Zhou et al. 2010, Swarup et al. 2011). All these animal studies indicate that the expression level of TDP-43 is tightly regulated and that the higher the TDP-43 expression level the more severe the phenotype of the rodents.

3.4 Objective of the thesis

The aim of this study was to generate a mouse model expressing an amyotrophic lateral sclerosis (ALS) causative mutation under control of the endogenous promoter and to analyze the effects caused by the human mutation.

TDP-43 was identified as the major part of ubiquitin-positive inclusions of amyotrophic lateral sclerosis (ALS) and frontotemporal lobar degeneration (FTLD). In order to investigate the role of TDP-43 in these neurodegenerative diseases, human TDP-43 cDNA was used to generate a new mouse model. Therefore, FlEx gene trap vectors were constructed carrying human wildtype or mutant (A315T, G348C, M337V and 82aaa) TDP-43 cDNA. In combination with Flp recombinase mediated cassette exchange the human cDNAs were inserted in the Tardbp mouse locus using adequate gene trap ES cell clones. As basis for all further analyses the newly generated mouse model was crossed with Rosa26Cre mice to initiate human TDP-43 expression ubiquitously. Young and aged animal cohorts were used for histological analyses and in a behavioral test battery aiming for revealing changes in ALS/FTLD related behavior caused by the inserted mutation.

With this study, I intended to gain new insights into the role of TDP-43 in ALS/FTLD and its associated mutations contributing to develop new approaches for the therapeutic treatment of the neurodegenerative diseases.

4 Material

4.1 Chemicals

Chemicals	Company
3,3'-diaminobenzidine (DAB)	Sigma
β-mercaptoethanol	Sigma
acetic acid	Merck
agarose (for gelelectrophoresis)	Biozym
ampicillin	Sigma
Ampuwa	Fresenius
aquapolymount	Polysciences
bacto agar	Difco
bis-tris	Sigma
boric acid	Merck
bovine serum albumin	Sigma
bromphenol blue	Sigma
CHAPS	Biomol
chloroform	Sigma
citric acid	Sigma
colcemid	Roche
cresyl violet acetate	Sigma
dimethyl formamide	Sigma
dimethyl sulfoxide (DMSO)	Sigma
dithiotreitol (DTT)	Roche
DMEM	Gibco
dNTP	Fermentas
EDTA	Sigma
EGTA	Sigma
ethanol absolute	Merck
ethidiumbromide	Fluka
ethylene glycol	Sigma

fetal calf serum (FCS)	PAN
Ficoll 400	Sigma
formaldehyde	Sigma
glycerol	Sigma
gelatin	Sigma
hematoxylin (according to Mayer)	Sigma
HEPES	Gibco
hydrochloric acid (HCl)	Merck
hydrogen peroxide (H_2O_2, 30%)	Sigma
isopropanol	Merck
Kanamycin	Sigma
magnesium chloride	Merck
maleic acid	Sigma
MEM nonessential amino acids	Gibco
MES hydrate	Sigma
methanol	Merck
mineral oil	Sigma
MOPS	Sigma
Nonidet P40 (NP-40)	Fluka
paraformaldehyde	Sigma
pertex mounting medium	HDscientific
PIPES	Sigma
potassium ferricyanide ($K_3Fe(CN)_6$)	Sigma
potassium ferrocyanide ($K_4Fe(CN)_6 \cdot 3H_2O$)	Sigma
potassium hydroxide (KOH)	Sigma
potassium phosphate	Roth
RNaseZAP®	Sigma
Skim milk powder	BD Biosciences
sodium acetate	Merck
sodium chloride	Merck
sodium citrate	Sigma
sodium desoxycholate	Sigma

sodium dodecyl sulfate (SDS)	Sigma
sodium hydrogen carbonate	Sigma
sodium hydroxide	Roth
Stempan E14 GMEM medium	PAN
thiourea	Invitrogen
TriReagent	Sigma
tris	Sigma
Trizol	Invitrogen
Trypsin (TBV-2)	Gibco
Trypsin/EDTA (E14)	PAN
tween-20	Sigma
urea	Sigma
X-Gal	Fermentas
xylol	Roth

4.2 Instruments

Instrument	Type	Company
autoclave	667-1ST	Aigner
balances	LC6201S, LC220-S	Sartorius
centrifuges	Evolution RC	Sorvall
	5417 R, 5424	Eppendorf
	Varifuge 3.0R	Heraeus
chambers for electrophoresis		Peqlab
developing machine	Curix 60	Agfa
digital camera	AxioCam MRc	Zeiss
electric homogenizer	Ultra-Turrax T25 basic	IKA
electroporation system	Gene Pulser XCell	BioRad
freezer (-20°C)		Liebherr
freezer (-80°C)	HFU 686 Basic	Heraeus
fridges (4°C)		Liebherr

gel documentation system	E.A.S.Y.	Herolab
gel blotting system	XCell SureLock™ MiniCell	Invitrogen
glass homogenizer (2ml)		KIMBLE
glass pipettes		Hirschmann
glassware		Schott
ice machine	AF 30	Scotsman
imaging analyzer	FLA-3000	Fuji
incubators (bacteria)	Innova 4230	New Brunswick Scientific
incubators (cells)		Heraeus
IntelliCage system	V1.4	NewBehavior AG
light source for microscopy	KL 1500	Leica
magnetic heater	MR3001	Heidolph
magnetic stirrer		Heidolph
microscope	Axioplan2 imaging	Zeiss
microscope (fluorescent)	Axiovert 200M	Zeiss
microtom	SM2000R	Leica
microwave oven		Sharp
Neubauer counting chamber		Brand
PCR machine	MasterCycler Gradient	Eppendorf
perfusion pump	401U/D1	Watson-Marlow Bredel
pH meter	pH Level 1	InoLab
photometer	Biophotometer 6131	Eppendorf
pipette filler, electronic	Easypet	Eppendorf
pipettes		Gilson
power supplies for	E443	Consort
electrophoresis	EC250-90, EC3000-90	Thermo
	EPS200	Pharmacia Biotech
real-time PCR system	7900HT	Applied Biosystems
Rotating rod apparatus	Letice LE 8200	Bioseb
shaker	Polymax 1040	Heidolph
slide warmer	BV SW 85	Adamas instrument
sonifier	cell disrupter B15	Branson

software microscope	Axiovision	Zeiss
thermomixer	comfort	Eppendorf
UV-lamp	N-36	Benda
vortex	Vortex genie 2	Scientific industries
water bath	U3	Julabo
	AQUAline AL 12	LAUDA
water conditioning system	MilliQ biocel	Millipore

4.3 Consumables & others

Consumables	Company
1kb DNA ladder	Invitrogen
cell culture dishes	Nunc
cell strainer	BD Biosciences
centrifuge tubes	Corning
coverslips	Roth
cuvettes for electroporation	BioRad
embedding pots	Polysciences
filter paper	Whatman 3mm
filter tips	Starlab
gloves	Meditrade
gloves, nitrile	Kimtech Science
hyperfilm	Amersham
multiwell plates	Nunc
one way needles	Terumo
one way syringes	Terumo
pasteur pipettes	Brand
PCR reaction tubes	Biozym
PCR reaction lids	Biozym
phase lock gel	Eppendorf
pipette tips	Gilson

plastic pipettes	Greiner
PVDF membrane	Millipore
reaction tubes (0.5 ml, 1.5 ml, 2 ml)	Eppendorf
reacton tubes (15 ml, 50 ml)	Sarstedt
SeeBlue Plus 2	Invirtrogen
SmartLadder	Eurogentec
superfrost Plus slides	Menzel Gläser
tissue cassettes	Merck
tissue embedding molds	Polysciences
wipes	Kimtech Science

4.4 Commonly used stock solutions

Solution	Ingredients
fast digestion buffer (1x)	5 mM KCl 10 mM Tris 0.5% NP-40 0.5% Tween-20
Loading buffer for agarose gels	15% Ficoll 400 200 mM EDTA 1-2% Orange G
Paraformaldehyde (PFA, 4%)	4% PFA w/v in PBS
PBS (1x), pH 7.4	171 mM NaCl 3.4 mM KCl 10 mM Na_2HPO_4 1.8 mM KH_2PO_4
TAE (10x)	0.4 M Tris base 0.1 M acetate 0.01 M EDTA
Tris-HCl , pH 7.5	1 M Tris base

4.5 Kits

Kit	Company
ECL detection kit	Amersham
FirstChoice® RLM RACE Kit	Ambion
Gateway® LR clonase™ II enzyme mix	Invitrogen
High capacity cDNA reverse transcription Kit	Applied Biosystems
iScript™ Select cDNA Synthesis Kit	BioRad
Pierce® BCA Protein Assay Kit	Thermo Scientific
Qiagen Plasmid Maxi Kit	QIAGEN
Qiaprep Spin Miniprep Kit	QIAGEN
QIAquick Gel extraction Kit	QIAGEN
QIAquick PCR purification Kit	QIAGEN
RNeasy® Mini Kit	QIAGEN
TOPO TA Cloning® Kit (Dual promoter)	Invitrogen
Vectastain Elite ABC Kit	Vector Labs
Wizard genomic DNA purification Kit	Promega

4.6 Enzymes

Enzyme	Company
alkaline phosphatase, calf intestinal (CIP)	NEB
antarctic phosphatase	NEB
casein kinase I	NEB
Cre recombinase	NEB
DNA polymerase (Taq)	QIAGEN
DNase I	Roche
Klenow fragment of DNA polymerase I	NEB
PCR mastermix	5 PRIME
Proteinase K	Roche
restriction enzymes	NEB, Roche

RNase A	Serva
T4 DNA ligase	NEB

4.7 Oligonucleotides

4.7.1 Oligonucleotides for genotyping

Name	Sequence	Annealing temp.	Product size
SR2	5'-GCCAAACCTACAGGTGGGGTCTTT-3'	60°C	321 bp insertion
TPO6	5'-ATCAAGGAAACCCTGGACTACTG-3'		261 bp insertion + hygro
D045for	5'-CTGTTGTCGGATTCCTTCCC-3'		712 bp original Tardbp
D045rev	5'-CTCGTCATTTCTTACCTGGAG-3'	56°C	588 bp insertion (TBV-2)
LTRfor	5'-CAACTGCAAGAGGGTTTATTGG-3'		220 bp insertion (E14)
B045	5'-CTCCGCCTCCTCTTCCTCCATC-3'		651 bp original betageo
B048	5'-CCTCCCCCGTGCCTTCCTTGAC-3'	58°C	359 bp inverted betageo
B050	5'-TTTGAGGGGACGACGACAGTAT-3'		426 bp successful exchange
pCre1	5'-ATGCCCAAGAAGAAGAGGAAGGT-3'	60°C	447 bp Cre insertion
pCre2	5'-GAAATCAGTGCGTTCGAACGCTAGA-3'		

4.7.2 Oligonucleotides for PCR amplification

Name	Sequence	Annealing temp.
mTDP-UTR-for	5'-ATATTCTGCCATAGGAATAC-3'	54°C
Dclk1for	5'-AGAGATTTTCAGCCGTGCAG-3'	54°C
Dclk1rev	5'-GGGAGTAGTCCTCCGATTCC-3'	
Dstfor	5'-AAGCACAGTGATGGTTCGTG-3'	52°C
Dstrev	5'-TAGGATGAACTTTTCCCGCA-3'	
Kcnd3for	5'-GGCAAGACCACCTCACTCAT-3'	56°C
Kcnd3rev	5'-AGTGGCTGGACAGAGAAGGA-3'	

Kcnip2for	5'-CGGCTCCTATGACCAGCTTA-3'	56°C
Kcnip2rev	5'-GGAGTTGTTCCAGACCCTCA-3'	
Sema3Ffor	5'-ACAACCCCATGTGCACCTAT-3'	54°C
Sema3Frev	5'-AGGGATGAGCTCAGCATGTA-3'	
Sort1for	5'-CAGGAGACAAATGCCAAGGT-3'	54°C
Sort1rev	5'-TGGCCAGGATAATAGGGACA-3'	

4.8 Vectors and plasmids

Plasmid	Construct from	Description
pCRII-TOPO	Invitrogen	TOPO TA cloning vector
pDest^{+1}	L. Schebelle	destination vector for gateway cloning
pEx-FLP-hTDP-43^{WT}BGHpA		exchange vector for RMCE
pEx-FLP-hTDP-43^{A315T}BGHpA	T. Javaheri	exchange vector for RMCE
pEx-FLP-hTDP-43^{G348C}BGHpA	T. Javaheri	exchange vector for RMCE
pEx-FLP-hTDP-43^{M337V}BGHpA	T. Javaheri	exchange vector for RMCE
pEx-FLP-hTDP-43^{82aaa}BGHpA	T. Javaheri	exchange vector for RMCE
pEx-FLP-hTDP-43^{WT}-3'UTR		exchange vector for RMCE
pEx-FLP-hTDP-43^{A315T}-3'UTR		exchange vector for RMCE

4.9 Taqman Gene Expression Assays

Gene	Assay ID / Cat.No.	Company
mouse ACTB (endogenous control)	4352933E	Applied Biosystems
Tardbp human	Hs00606522_m1	Applied Biosystems
Tardbp mouse	Mm00523866_m1	Applied Biosystems
Fus	Mm01271304_m1	Applied Biosystems
Grn	Mm0433848_m1	Applied Biosystems

Park2	Mm0450186_m1	Applied Biosystems
Htt	Mm01213820_m1	Applied Biosystems

4.10 Work with bacteria

4.10.1 E. coli Strains

Strain	Company
DH5α	Invitrogen
TOP10	Invitrogen

4.10.2 Solutions

Solution	Ingredients
LB medium (Luria-Bertani)	10 g bacto peptone 5 g yeast extract 5 g NaCl ad 1 l H_2O
LB agar	98.5% LB medium 1.5% bacto agar
Ampicillin selection medium	LB medium with 50 µg/ml ampicillin
Kanamycin selection medium	LB medium with 25 µg/ml kanamycin
Ampicillin selection agar	LB agar with 100 µg/ml ampicillin
Kanamycin selection agar	LB agar with 50 µg/ml kanamycin

4.11 ES cell culture

4.11.1 ES cell lines

ES cell line	Clone
TBV-2	D045A10
E14TG2A.4	E304C05

4.11.2 Media & Solutions

Solution	Ingredients
E14 medium	10% FCS (Hybond) 1000 U/ml LIF in E14 medium
F1 medium	15% FCS (PAN) 20 mM HEPES 1x MEM nonessential amino acids 0.1 mM β-mercaptoethanol 1500 U/ml LIF in DMEM
feeder medium	10% FCS in DMEM
freezing medium (1x)	15% FCS (PAN) 10% DMSO in DMEM
gelatin solution	1% gelatin in H_2O
LacZ-staining solution	5mM potassium ferricyanide 5mM potassium ferrocyanide 1 mg/ml X-Gal in LacZ-washing buffer
LacZ-washing buffer	1mM MgCl2

	0.01% sodium desoxycholate 0.02% NP-40 in PBS

4.12 Western blot analysis

4.12.1 Solutions

Solution	Ingredients
Blocking solution	5% skim milk powder in 1x TBS-T
Loading buffer (5x)	5x sample loading buffer, Invitrogen 4% β-mercaptoethanol
RIPA buffer	50 mM Tris-HCl 150 mM NaCl 3 mM EDTA 1% Triton-X 100 0.5% SDS 0.5% sodium desoxycholate 1 tablet complete protease inhibitor 1 tablet phosphatase inhibitor
Running buffer (1x)	5% 20x NuPAGE® Running buffer, Invitrogen
Stripping buffer (1x)	200 mM glycine 3.5 mM SDS 1% Tween-20 pH 2.2
10 x TBS	0.25 M Tris-HCl pH 7.5 1.37 M NaCl
1x TBS-T	1x TBS 0.05% Tween-20
Transfer buffer (1x)	5% 20x NuPAGE® Transfer buffer, Invitrogen 10% methanol

4.12.2 Antibodies

Antibody	Dilution	Company
anti-CD36, mouse polyclonal	1: 500	R&D Biosciences
anti-TDP-43 human, mouse monoclonal	1 : 1,000	Abcam
anti-TDP-43 mouse/human, rabbit polyclonal	1 : 1,000	Proteintech
anti-FUS/TLS (4H11), mouse monoclonal	1 : 500	Santa Cruz Biotechnology
anti-GRN, rat polyclonal	1 : 50	gift from Dr. E. Kremmer
anti-Parkin, mouse monoclonal	1 : 1,000	Santa Cruz Biotechnology
anti-Huntingtin, rabbit polyclonal	1 : 10,000	Abcam
anti-phospho-TDP-43, mouse-monoclonal	1 : 50	gift from Dr. E. Kremmer

4.13 Immunohistochemistry

4.13.1 Solutions

Solution	Ingredients
Blocking solution	1x PBS 10% FCS
cresylviolet solution (Nissl staining)	0.5% cresylviolet 2.5 mM sodium acetate 0.31% acetic acid
PBS-T	1x PBS 0.25% Triton-X 100

4.13.2 Antibodies

Antibody	Dilution	Company
anti-TDP-43 human, mouse monoclonal	1 : 500	Abcam
anti-TDP-43 mouse/human, rabbit polyclonal	1 : 500	Proteintech
anti-Ubiquitin (clone Ubi-1), mouse monoclonal	1 : 500	Millipore

4.14 Mouse strains

4.14.1 Wild type and other used mouse strains

Mouse strain	Description
C57Bl/6J	wild type mouse line
C57Bl/6J-Tg(pPGKneobpA)Ems/J	Wild type mouse line containing a neomycin resistance vector (for feeder cells)
Gt(ROSA)26Sor$^{tm16(Cre)Arte}$ (Taconic)	ubiquitous activity; general deleter knock-in of "Splice-Acceptor – NLS^{SV40T} – Cre polyadenylation site" in the ROSA26 locus
Nestin-Cre (Tronche et al. 1999)	mouse line expressing Cre recombinase under control of the Nestin promoter and enhancer, active in the CNS and additional tissue starting at E11.0

4.14.2 Generated mouse strains

Mouse strain	Description
hTDP-43^{A315T}	
hTDP-43^{A315T}Rosa	hTDP43^{A315T} x Rosa26Cre
hTDP-43^{A315T}Nes	hTDP43^{A315T} x *Nestin-Cre*

5 Methods

5.1 Molecular biology methods

5.1.1 Cloning and work with plasmid DNA

Transformation of chemically competent bacteria

For transformation chemically competent E. coli DH5α bacteria were used. For one transformation a 100 µl aliquot of DH5α bacteria was slowly thawed on ice and 2 µl of plasmid were added to the bacterial suspension. For mixing the tube was flipped carefully and the suspension was incubated for 30 min on ice. Afterwards a heat-shock was performed for 45 sec at 42°C to permeabilize the plasma membrane. After a recovering time of 2 min on ice 700 µl of LB medium was added and incubated for 1 h at 37°C. The suspension was shortly centrifuged and the pellet was resuspended in 100 µl LB medium. The bacteria solution was plated on LB agar plates containing the appropriate antibiotic and incubated overnight at 37°C. In general, ampicillin (100 µg/ml) or kanamycin (50 µg/ml) were used for selection.

Gateway® Cloning reaction

To transfer DNA fragments efficiently between plasmids, we used the Gateway® Cloning System from Invitrogen. The following reaction batch was used:

1 µl	entry clone (100 ng/µl)
1 µl	destination vector (150 ng/µl)
6 µl	TE buffer, pH 8.0

After thawing LR Clonase™ II enzyme mix on ice, 2 µl were added to the reaction and incubated at 16°C overnight. To stop the reaction, 1 µl of Proteinase K solution were applied and incubated at 37°C for 10 min. Afterwards, 1 µl of each reaction were transformed into DH5α cells and plated on ampicillin selection plates. Grown clones were picked, analyzed via restriction digest and putative positive clones were sequenced additionally.

Preparation of plasmid DNA

To extract plasmid DNA of transformed bacteria the subsequent Qiagen Kits were used following manufacturer's instructions: The Qiagen Plasmid MiniPrep Kit for selecting correctly transformed colonies and the Qiagen Plasmid Maxi Kit for higher yield plasmid preparation.

For MiniPrep production, one colony was inoculated in 3 ml LB medium containing the appropriate antibiotic overnight at 37°C. For MaxiPrep production, 1 ml of the Miniprep culture was added to 200 ml LB medium with antibiotic and incubated overnight at 37°C.

The concentration of DNA was determined with a spectrophotometer. The optical density (OD) was measured at a wavelength of 260 nm and the concentration was calculated. Purity of DNA was assessed by the relation of OD_{260}/OD_{280}, which should not exceed a value of 1.8.

Restriction digest of plasmid DNA

To digest plasmid DNA, enzymes and buffers were used following manufacturer's instructions. For one µg of DNA 2 units (U) of restriction enzyme were added and incubated for 2 h or overnight at the appropriate temperature. If blunt ends were required, the Klenow fragment of Taq polymerase I was used. Therefore, 5 units of Klenow fragment and 25 nM of NTPs were added to the digested DNA and incubated for 20 min at room temperature. To inactivate the Klenow fragment the solution was incubated at 75°C for 20 min.

If necessary, de-phosphorylation was performed to prevent unwanted re-ligation of the digested DNA. Therefore, 10 units alkaline phosphatase (CIP) were added and incubated for 45 min at 37°C.

Isolation of DNA fragments

To isolate digested DNA fragments according to their size, a gel electrophoresis was performed. The DNA probes were supplemented with loading buffer and loaded on 1-2% agarose gels containing ethidium bromide. The run was performed in 1xTAE buffer at 100 V for 30 – 60 min depending on the size of the fragments. As a length standard a 1kb ladder or Smartladder were used. For visualization a UV desk was utilized with a wavelength of 366nm and the correct bands were cut out using a scalpel.

The DNA was extracted using the Qiagen Gel Extraction Kit following manufacturer's instructions.

Ligation of DNA fragments

The linearized vector and the DNA insert were mixed in a ratio of 1:3. The restriction fragments were ligated by adding 600 U T4 DNA ligase and T4 DNA ligase buffer in a total volume of 20 µl. The reaction was incubated for 2 h or overnight at RT depending on sticky end or blunt end ligation.

5.1.2 Analysis of genomic DNA

Isolation of genomic DNA

Genomic DNA from cells and mouse tails was isolated with the Promega Wizard genomic DNA purification kit following manufacturer's instructions. For a "quick and dirty" isolation of genomic DNA the mouse tails were shacked 5h - overnight at 55°C with fast digestion buffer and proteinase K (0.1 mg/ml). The next day proteinase K was inactivated at 95°C for 10 min. For PCR analysis 1 µl of isolated DNA was used.

Polymerase Chain Reaction (PCR)

For amplification of DNA fragments from either genomic or complementary or plasmid DNA, a PCR analysis was performed. The basic approach included the following:

1 µl	template DNA
1 µl	forward Primer (10 pmol)
1 µl	reverse Primer (10 pmol)
10 µl	5x MasterMix
ad 25 µl	H_2O

The following program was used for every PCR:

94°C	5 min	
94°C	30 sec	⎫
X °C	60 sec	⎬ x35
72°C	60 sec	⎭
72°C	10 min	
4°C	∞	

The specific annealing temperatures for each primer pair can be found in the material section (see 4.7).

5.1.3 Analysis of RNA

Isolation of RNA

For RNA work the material was treated with RNaseZap® and only RNase free solutions, tubes and pipette tips were used. For the tissue preparation a single mouse was emphasized with CO_2 and the required organs were extracted and immediately frozen on dry ice. Organs were stored at -80°C or immediately processed. Therefore, the tissue was homogenized in Trizol or TriReagent and total RNA was isolated following manufacturer's instructions. RNA concentration was determined with a spectrophotometer, where an OD_{260} of one corresponds to 40 µg RNA per ml.

Reverse Transcription Polymerase Chain Reaction (RT-PCR)

Isolated RNA was transcribed into complementary DNA (cDNA) using iScript™ Select cDNA Synthesis Kit (BioRad). Therefore, the following reaction batch was used:

x µl	RNA (1 µg)
4 µl	5x iScript select reaction mix
2 µl	oligo$(dT)_{20}$ primer
1 µl	iScript reverse transcriptase
ad 20 µl	nuclease-free H_2O

The cDNA reaction was incubated at 42°C for 60-90 min and reverse transcriptase was inactivated at 85°C for 5 min. The cDNA was processed immediately or frozen at -20°C. An amount of 1 µl of cDNA template was used for further RT-PCR analysis.

Quantitative Real-Time Polymerase Chain Reaction (qRT-PCR)

For generation of cDNA the High Capacity cDNA reverse transcription Kit (Applied Biosystems) was used. Therefore, the following reaction batch was used:

10 µl	RNA template (1 µg)
2 µl	10x RT buffer
2 µl	10x RT random primers
0.8 µl	25x dNTP Mix (100mM)
1 µl	MultiScribe™ reverse transcriptase
ad 20 µl	nuclease-free H_2O

To perform reverse transcription the reaction was incubated at 25°C for 10 min, followed by 37°C for 2h and 5 min inactivation of the reverse transcriptase at 85°C. cDNA was stored at 4°C or -20°C until further progression.

For qRT-PCR we used TaqMan® Gene Expression assays. For the quantitative analysis of cDNA the following reaction batch was used:

10 µl	cDNA (30 ng)
9 µl	2x TaqMan® Universal Master Mix
1 µl	20x TaqMan® Assay

The TaqMan® Gene Expression Assays were analyzed on a 7900HT Fast Real-Time PCR system with the SDS software v2.3 (Applied Biosystems). The further calculation and statistical analysis were calculated with Microsoft Office Excel.

Rapid Amplification of cDNA Ends (3'RACE)

To amplify and clone sequence at the 3' end of an mRNA we used the FirstChoice® RLM-RACE Kit (Ambion). First total RNA is reverse transcribed into cDNA with the following reaction batch:

2 µl	RNA (1 µg)
4 µl	dNTP Mix
2 µl	3'RACE adapter
2 µl	10x RT buffer
1 µl	RNase inhibitor
1 µl	M-MLV reverse transcriptase
8 µl	nuclease-free H_20

The mix was incubated for 1h at 42°C. Afterwards, an outer 3'RLM-RACE was performed using the RT reaction mix from the previous step at following batch:

1 µl	RT reaction mix
5 µl	10x PCR buffer
4 µl	dNTP Mix
2 µl	3'RACE gene specific outer primer (mTDPUTRfor)
2 µl	3'RACE outer primer
1 µl	Taq DNA polymerase
ad 50 µl	nuclease-free H_2O

The outer 3'RLM-RACE reaction was performed with the following cycles:

94°C	3 min	
94°C	30 sec	x35
60°C	30 sec	
72°C	30 sec	
72°C	7 min	
4°C	∞	

The amplified products were separated with gel electrophoresis and sequenced after performing a gel extraction protocol.

5.1.4 Analysis of protein samples

Isolation of protein

Mice were emphasized with CO_2 and decapitated. The brain or other tissues were removed and immediately stored on dry ice. The homogenization of the tissue was performed in RIPA buffer with protease and phosphatase inhibitors (1 tablet/10 ml buffer) with a glass homogenizer. Afterwards the protein suspension was incubated for 20 min at 4°C, sonicated and centrifuged for 15 min at 12000 rpm at 4°C. The supernatant was transferred into a new tube and used for quantification of protein concentration as the soluble protein fraction. Two times the pellet was washed with RIPA buffer, sonicated and centrifuged for 30 min at 14000 rpm at 4°C. The supernatants were collected as S1 and S2 fraction. After the second washing step the pellet was resuspended in Urea buffer, sonicated and centrifuged for 30 min at 12000 rpm at 22°C. The resulting supernatant was collected as the insoluble protein fraction and stored at 4°C.

The protein concentration of the soluble protein fraction was determined by bicinchoninic acid (BCA). Therefore, 1:5 and 1:10 protein dilutions were generated together with a standard dilution of BSA. The BCA reagents were mixed and added to the dilutions on a 96-well plate following manufacturer's instructions. After an incubation of 30 min at 37°C the absorption was measured at a wavelength of 562nm with a photometer. On the basis of the values from the standard curve the protein concentration was determined for each sample with Microsoft Office Excel.

Western blot analysis

Proteins were separated according to their size on SDS polyacrylamide gel electrophoresis (Laemmli, 1970). The NuPAGE® Novex gel system from Invitrogen was used. 20 µg of total protein samples were mixed with 5x sample loading buffer (Invitrogen) and incubated at 95°C for 5 min. After 2-5 min on ice, the samples were loaded onto the gel. SDS-PAGE was performed at 200 V for 30 – 90 min, depending on the protein size and the concentration of the used gel. Afterwards, the gel was blotted on a PDVF membrane which was activated by incubation in 100% methanol for 1 min. After blotting (1h, 30 V), the membrane was blocked with 5% milk in TBS-T for about 60 min. Then, the membrane was incubated overnight at 4°C with the specific primary antibody in blocking solution. The next day three washing steps were performed with TBS-T (10 min each) that followed incubation with the specific secondary antibody for 1h in blocking solution and afterwards three washing steps with TBS-T (10 min each). For detection of bands the membrane was incubated with ECL reagents for 1 min and transferred into a hyperfilm cassette. After exposure to a chemieluminescent film for 15 sec to 10 min (depending on signal intensity), the film was developed with a developing machine and quantified using ImageJ (Abramoff et al. 2004).

Protein phosphorylation in vitro

To generate a positive control for the phospho-specific TDP-43 antibody, a synthetic phosphorylation of a protein lysate with casein kinase I was performed. The following reaction batch was used:

1 µl	brain protein lysate (15 µg)
2 µl	10x CKI reaction buffer
5 µl	casein kinase I
ad 20 µl	H_2O

The reaction was incubated for 18 hours at 30°C and immediately used for western blot analysis.

5.2 Histology

5.2.1 Perfusion and Dissection

First the mice were asphyxiated with CO_2 and fixed with their paws onto a polystyrene board. After opening the thoracic cavity, the tip of the left heart ventricle was cut and a blunt needle was inserted in the ascending aorta. With a perfusion pump blood vessels were rinsed with ice-cold PBS until the liver turned pale. Afterwards the perfusion was carried out with ice-cold 4% paraformaldehyde (PFA) for 5 min until the body stiffened. To dissect the brain, the mice were decapitated and the brains were stored in 4% PFA. For preparation of the spinal cord, the whole spinal column was dissected and stored in 4% PFA. For post-fixation the tissue was kept in 4% PFA overnight at 4°C.

5.2.2 Dehydration and Paraffin embedding

After one day 4% PFA fixation the spinal cord was dissected out of the spinal column and as well as the brain stored in 70% ethanol until further progression. Following, the dehydration in an ascending ethanol scale, equilibration and embedding in paraffin is described:

Reagents	Temperature	Time
4% PFA	4°C	Overnight
70 % ethanol	4°C	Overnight
96% ethanol	RT	2 h
100% ethanol	RT	2 h
Xylol	RT	1 – 2 h
Xylol/Paraffin	RT	1 h
Paraffin	60°C	overnight

After the overnight incubation in paraffin, the tissue was embedded in tissue cassettes and stored at 4°C.

For preparation of paraffin sections, the tissue cassettes were fixed at a microtome and 8 µm thick sections were cut. The sections were transferred to a water bath (39°C) for

flattening and mounted on slides. Afterwards the slides were dried in an incubator (36°C) overnight and stored at 4°C until use.

5.2.3 Nissl staining

To prepare the spinal cord sections for counting of the motor neurons, the sections were stained with the Nissl reagent cresyl violet. Staining was performed according to the following protocol:

Step	Reagents	Time
dewaxing	Xylol	30 min
rehydration	100% ethanol	5 min
rehydration	96% ethanol	5 min
rehydration	70% ethanol	5 min
staining	Cresyl violet	30 min
rinse	H_2O	1 min
differentiation	70% ethanol	2 x 10 sec
differentiation	96% ethanol + 0.5% acetic acid	5 sec
dehydration	96% ethanol	2 x 10 sec
dehydraton	100% ethanol	2 x 10 sec
embedding	Xylol	2 x 5 min

The slides were covered immediately with pertex and dried overnight at room temperature.

5.2.4 Motor neuron counting

After paraffin embedding serial 8 µm spinal cord sections from the L3-L5 region were cut (four section series). One series of each spinal cord was stained with Nissl reagent (see 5.2.3) and used for spinal motor neuron quantification. Therefore, motor neurons of the sciatic motor pool were counted form each second section harboring a clearly definable nucleolus.

5.2.5 Immunohistochemistry

DAB-staining

3-3'Diaminobenzidine (DAB) is a commonly used compound for immunohistochemical staining of proteins. The staining was performed according to the following protocol:

Step	Solution	Time	Remarks
dewaxing	Xylol	30 min	
rehydration	100% ethanol	2 x 5 min	
rehydration	96% ethanol	2 x 5 min	
rehydration	70% ethanol	2 x 5 min	
rinse	H2O	10 min	
antigen retrieval	0.01 M Na-citrat	3 min	
antigen retrieval	0.01 M Na-citrat	5 min	microwave, 630 W
antigen retrieval	0.01 M Na-citrat	10 min	cool down
antigen retrieval	0.01 M Na-citrat	3 min	microwave, 630 W
antigen retrieval	0.01 M Na-citrat	20 min	cool down
wash	0.1 M PBS	2 x 5 min	
quenching	0.1% H_2O_2 / PBS	5 min	destruction of endo-genous peroxidases
wash	0.1 M PBS	2 x 5 min	
blocking	10% FCS/PBS + 0.25% Triton-X	1 h	humid chamber
1st Antibody	10% FCS/PBS + primary AB	o/n	humid chamber, 4°C
wash	0.1 M PBS	3 x 5 min	
2nd antibody	10% FCS/PBS + biotinylated second antibody	1 h	humid chamber
wash	0.1 M PBS	3 x 5 min	
intensifying	10% FCS/PBS + ABC reagents	30 min	
wash	0.1 M PBS	2 x 5 min	
wash	0.1 M Tris-HCl	5 min	
DAB-staining	0.1 M Tris-HCl + 5% DAB +	30 min	humid chamber, dark

	H2O2		
wash	0.1 M PBS	2 x 5 min	stop staining
dehydration	70% ethanol	2 x 5 min	
dehydration	96% ethanol	2 x 5 min	
dehydration	100% ethanol	2 x 5 min	
embedding	Xylol	2 x 10 min	

Slides were covered immediately with pertex and dried at room temperature under the hood. For some cases a hematoxylin staining was performed additionally, to stain the nuclei independent from the DAB staining. For this reason, the following protocol was used after stopping the staining with DAB:

Step	Solution	Time
nuclei staining	hematoxylin	10 min
differentiation	70% ethanol + 1% HCl	30 sec
blueing	H_2O	10 min

Afterwards, the dehydration was carried out as described above and the slides were covered with pertex and dried overnight.

Immunofluorescence

To stain paraffin sections with fluorescent secondary antibodies, on the first day the same protocol was used as described for the DAB staining. The second day was performed according to the following protocol:

Step	Solution	Time	Remarks
wash	0.1 M PBS + 0.25% Triton-X	3 x 10 min	
2^{nd} antibody	10% FCS/PBS + 0.25% Triton-X	1 h	humid chamber, dark
wash	0.1 M PBS	2 x 10 min	dark

nuclei staining	DAPI	5 min	dark
wash	0.1 M PBS	10 min	dark

The slides were covered immediately with aqua polymount and dried in the dark at 4°C.

5.3 Embryonic stem cell culture

Embryonic stem (ES) cells represent the inner cell mass (ICM) of a blastocyst and are pluripotent. They can differentiate into each cell type *in vivo* as well as *in vitro*. To keep ES cells undifferentiated, they have to be cultivated under special conditions. Here, the cultivated medium was supplemented with Leukemia inhibiting factor (LIF) and pretested fetal calf serum (FCS). ES cells were grown on feeder cells or on gelatin coated cell culture dishes at 37°C and 5% CO_2. During expansion phase, ES cells were splitted all two days to avoid differentiation of the cells. Genetically modified ES cells were injected into wildtype blastocysts. These modified blastocysts were implanted into pseudo-pregnant foster mothers, which gave birth to genetically divergent pups. These chimeras consist of cells derived from the wildtype blastocyst and to some extent of cells derived from the injected ES cells. Germline chimeras transmit the genetically modified information of the ES cells to the next generation, producing progeny consisting to 100% of the mutant cells.
The ES cell clone E304C05, used here, was derived from the feeder independent E14Tg2A.4 (E14) gene trap line (Skarnes, 2000), while the ES cell clone D045A10 which was derived from a TBV-2 cell line (Hill and Wurst, 1993) was cultured on mouse embryonic fibroblast feeder layer.

5.3.1 Preparation of primary mouse fibroblasts (feeder cells)

Feeder cells are mouse fibroblasts, which have been mitotically inactivated by mitomycin C treatment. Primary fibroblast were obtained from embryos at stage E13.5 under sterile conditions and were expanded for 3-4 days. When the cells are still in an exponential growth phase, medium with a concentration of 10µg/ml mitomycin C is added and incubated for 2 hours at 37°C. After washing two times with PBS, cells are trypsinized and plated on fresh

culture dishes or frozen (-80°C) for later use. Feeder cells were plated at a density of 2 – 2.5 x 104 cells/cm^2 at least several hours or one day prior to plating on ES cells.

5.3.2 Splitting of ES cells

For expansion, ES cells were splitted all two days to avoid differentiation. Medium was discarded, cells were washed with PBS and trypsinized for 5 min at 37°C. The reaction was stopped by adding an equal amount of medium to the cells and the suspension was centrifuged for 4 min at 1200 rpm to get rid of the trypsin. The cell pellet was resuspended in an equal amount of medium and splitted to several fresh culture dishes in an adequate ratio.

5.3.3 Freezing and Thawing of ES cells

For freezing of ES cells, they were washed with PBS and trypsinized for 5 min at 37°C. After detaching the cells from the surface the reaction was stopped by adding an equal amount of medium. To get rid of the trypsin the suspension was centrifuged for 4 min at 1200 rpm. The cell pellet was resuspended in medium and after adding ice cold 2x freezing medium the cells were transferred in 2ml freezing vials and stored in precooled freezing containers at -80°C for short term storage. For long term storage, the vials were then transferred in liquid nitrogen. For freezing multi well plates, cells were trypsinized as described above and 2x freezing medium was added with a final ratio of 1:1. Plates were wrapped in cellulose and frozen at -80°C.

For thawing, cells were put into a water bath with a temperature of 37°C. The thawed cells were diluted with fresh medium and centrifuged to get rid of the DMSO. The cell pellet was resuspended in medium and plated on feeder or gelatin coated plates.

5.3.4 Electroporation of ES cells

To generate targeted mutations in ES cells, the cell plasma membranes need to be permeabilized. Electroporation is the physical way to bring DNA into the cell by performing

short electric impulses. To introduce DNA into the genome the cells were electroporated with a plasmid that expressed a recombinase for cutting the genome at specific sites. For a stable integration of DNA into the genome, a specially designed vector containing human mutant cDNA and an expression plasmid coding for a recombinase were co-electroporated.
For every electroporation 10^6-10^7 cells have been used. By adding trypsin, cells were detached from the culture dish and centrifuged for 4 min at 1200 rpm. For determination of the cell number, 10µl of cell suspension was pipetted into a Neubauer counting chamber. The cell number of one quadrant multiplied with 10.000 corresponded to the number of cells in one ml cell suspension. Afterwards the cells were centrifuged again and the required amount of cells was resuspended in 700µl PBS containing the DNA to be electroporated. For specially designed vectors a maximum of 30µg of total DNA, for the expression vectors an amount of 70µg of total DNA was used for 10^7 cells. The cell suspension containing the DNA was pipetted into an electroporation cuvette and electroporated with 300V and 500µF for 2ms. After the electroporation the cell suspension was allowed to recover for 10 min at room temperature. Cells were diluted with fresh medium and in equal parts plated on 3 x 10 cm gelatin coated culture dishes. The cells were incubated for two days at 37°C and 5% CO_2, with medium change after the first day.

5.3.5 Selection and picking of positive ES cell clones

For the selection of stable transfected clones, two days after the electroporation the normal medium was replaced by medium containing the specific antibiotic. In this case, the antibiotic hygromycin was used with a concentration of 150µg/ml. Cells with stable integration of the foreign DNA were resistant to hygromycin and could form colonies, whereas cells without integration of foreign DNA die during selection. The selection medium was changed every day for about 9 days until round, light breaking colonies had formed and single cells had died.
After washing the cells with PBS, single colonies were picked and transferred to a 96-well plate containing a PBS and trypsin mixture with a ratio of 4:1. For every electroporation about 50 colonies were picked. The 96-well plate was incubated for 10 min at 37°C. After this an equal amount of fresh medium was added and the cells were resuspended and transferred to a feeder or gelatin coated 96-well plate. Medium was changed the next day to

get rid of the trypsin and dead cells. The cells were expanded on 3 x 96-well plates. One of these plates was frozen at -80°C, the others were splitted on gelatin coated 48-well plates and grown for confluence and used for DNA extraction and LacZ staining.

5.3.6 PCR screening of resistant ES cell colonies

The resistant ES cell colonies were screened by PCR. Therefore, cells on gelatin coated plates were washed twice with PBS and immediately used for DNA extraction or dry stored at -20°C. Genomic DNA extraction is described in 5.1.1. For genotyping DNA of ES cell clones, SR/TPO6- and BO-PCR were used (see 4.7.1).

5.3.7 LacZ staining of ES cells

To screen the ES cell colonies for LacZ staining, cells were fixed with 4% paraformaldehyde (PFA) for 20 min at RT, following two washing steps with PBS (5 min each) and one washing step in LacZ-washing buffer. Cells were incubated with 200 µl LacZ-staining solution overnight at 33°C in dark. After removing LacZ-staining solution, cells were washed twice and kept in PBS.

5.3.8 Karyotyping of ES cell clones

For depolymerization of microtubules, cells were treated with colcemid (20 µg/ml medium) for 1h. Afterwards, cells were washed and trypsinized. The medium was removed except for 500 µl after a standard centrifugation and the pellet resuspended by flipping. After adding a hypotonic solution (75mM KCl in H_2O) drop wise for 10 min, the cell suspension was centrifuged again for 10 min at 900 rpm. The pellet was resuspended in 15 ml fixation solution (methanol/acetic acid 3:1) and incubated for 30 min at -20°C. After a centrifugation at 900 rpm for 10 min, the supernatant was discarded and the pellet solved in 1 ml fixation solution. The cell suspension (10-20 µl) was dropped on a water covered object slide and dried overnight. The slides were embedded with DAPI staining solution and the

chromosomal counting was performed with an inverted fluorescent microscope (Axiovert 200M, Zeiss).

5.4 Mouse husbandry

5.4.1 Mouse facilities

All mice were kept and bred at the Helmholtz Centre Munich according to national guidelines. If not mentioned else, five mice at maximum were grouped house in individually ventilated cages (IVC). They were maintained on a 12 hours dark/light cycle with food and water *ad libitum*. The temperature was kept at 22 ± 2°C with a relative humidity of 55 ± 5%. In the German Mouse Clinic (GMC) the mice were housed in smaller IVCs, with a maximum of 4 animals per cage.
To breed the mice, single or double matings were set up. Pups were weaned with an age of three weeks according to their gender. For identification, earmarks were made and tail clips were taken for genotyping.

5.4.2 Generation of mice from ES cells

Female mice (C57Bl6/N or BDF-1) were superovulated for the production of blastocysts (E3.5). For this reason, mice were injected first with 7.5 U pregnant mare's serum gonadotropin (PMSG) and 48 h later with human chorion gonadotropin (hCG). These injections were performed intraperitonial (i.p.) at noon. Directly after the hCG injection female mice were mated with male mice of the same stain for one day. The next day females were separated and sacrificed 3 days post coitum. Blastocysts were dissected of the uteri and flushed with M2 medium. One blastocyst was fixed with a capillary of the micromanipulator and 10-20 ES cells were injected into the blastocoel with a second capillary. CD-1 female mice were used as pseudo-pregnant foster mothers. Pseudo-pregnancy was achieved by mating the females to sterile, vasectomized males. For embryo transfer, foster mothers were anesthetized according to their weight. For the dissection of the uterus and the ovaries, the retroperitoneal cavity was opened. Via a thin cannula up to 10 manipulated blastocysts were transferred into the uterus of the foster mother.

Afterwards, the surgery field was closed and the mice were kept on warming plates until awakening.

5.4.3 Establishment of new mouse lines

Chimeras were born 17 days after the embryo transfer. In the case of TBV-2 ES cells the coded fur color was agouti and the wildtype cells from the blastocysts for black fur color. While E14 ES cells coded for white/agouti fur color and the wildtype cells from the blastocysts for black fur color. The more the contribution of the ES cells were the merrier the fur color of the chimeras.
With an age of 8 weeks chimeras were mated to wildtype C57Bl/6J mice to obtain pups with the modified allele. The offspring of these matings was genotyped for successful germline transmission.

5.5 Behavioral testing

All behavioral tests were performed in the mouse facility of the nuclear biology department at the Helmholtz Centre Munich except the IntelliCage test was accomplished in the GMC. 10 mice of each sex and genotype were transferred with an age of 18 months. The tests were started two weeks after accommodation of the animals.

5.5.1 Memory tests

Y-Maze

The Y-Maze consists of three open arms with an interval of 120°. The arms are connected with an equilateral triangular platform, which results in a Y shape. The Y-Maze is based on the natural tendency of rodents to explore their environment and provide an indication for inactive retrograde working memory. Each mouse was placed at the end of an arm and could explore the Y-Maze for 5 min. The start-arm was frequently changed for every mouse to avoid interference during the exploration phase. The data were analyzed with respect to (1) the latency of the first arm entry, (2) the number of arm entries and (3) the sequence of

entries. Only mice with more than five arm entries were further analyzed. An arm entry was scored if all four paws were inside an arm. After the performance of each mouse the Y-maze was cleaned and dried.

Object Recognition

The object recognition test is used to evaluate cognition, particularly recognition memory, in rodents. The test is based on the natural tendency of rodents to spend more time exploring a new object than a familiar one. Two days before the test, mice had two acclimatization phases. Therefore, the mice were put into an empty cage for 10 min once a day to become familiar with the testing arena. The next day mice had three testing trials in the arena with two identical objects. Each trial had 5 min duration, with an interval of 15 min. Afterards, the mice were housed individually. After 3 and 24 hours one familiar object was replaced by an unfamiliar one and the exploration time of each object was scored. The data were analyzed with respect to (1) exploration time in total, (2) exploration of the familiar and (3) unfamiliar object. After each trial the arena was disinfected and dried.

IntelliCage

The IntelliCage V1.4 system (NewBehavior AG, Switzerland) was used for cognitive screening of the mouse strains (Galsworthy et al. 2005; Knapska et al. 2006). The test was performed in the GMC under supervision of Dr. S. Hölter-Koch. The mice were equipped with a transponder to record individual behavior of the animals. In each corner of the cage, a triangular learning chamber is located containing two water bottles. Mice were separated into two groups and were allowed to explore the cage for five days without limitations. To assess the cognitive function of the animals, they were tested in three different drinking behavior parameters increasing the level of difficulty: (1) least preferred corner of the habituation phase became the new drinking corner (place learning) for seven days, (2) the mouse had to open the diagonal opposite corner (reversal learning) of the place learning for drinking and (3) each mouse started with the corner of the reversal learning and the corner was changed clockwise after drinking (patrolling). The data of each mouse were analyzed and the error rate was scored.

5.5.2 Motor tests

Beam Walk

To assess fine motor coordination the beam walk test was performed. The mice had to traverse a wooden beam, 15 mm in diameter and with a length of 1 m. The beam was placed between to cages, with the housing cage as the final destination. Animals were trained to learn crossing the beam at a stretch. Each mouse had five trials with an interval of 5 min. The number of hind and front paws slips, the number of falls and the time needed to traverse the beam were mapped and analyzed.

Vertical Pole

The vertical pole is another method to assess motor coordination and balance. The pole had a length of 50 cm. Mice were placed at the top of the pole, which is held in a horizontal position and after the mice hanged on the pole with the head upwards, the pole was lifted to a vertical position. To avoid injuries of the animals the pole was wrapped with an insulating tape for a better grip. The mice had to turn downwards and descend to the end of the pole. Each mouse had three training trials. The time needed to turn downwards and the time for descend were measured for three trials. Additionally, each mouse was classified for the performance of the trial.

Ladder

The coordination of the four paws is assessed in the ladder test. The mice had to cross a horizontal ladder with ladder spokes in different intervals. The time to traverse the ladder and the number of front and hind paws slips were counted and analyzed. Each mouse had to perform three trials. After each trial the apparatus was disinfected and dried.

Accelerating Rotarod

The accelerating rotarod is another test for motor coordination and balance using the rotating rod apparatus from Biosep (Letica LE 8200). The rod had a diameter of 4.5 cm and was made of hard plastic material covered with soft rubber foam. The test phase consisted of three trials with 15 min interval. Three mice were placed on a rod rotating with a constant speed of 4 rpm. After all mice were positioned correctly the trial was started. The rotating

rod accelerated from 4 to 400 rpm in 300 sec. Latency and rpm at which each mouse fell off the rotating rod were measured and analyzed. Passive rotations were counted as a fall. After each trial the apparatus was disinfected and dried.

Gait Analysis

Problems with the gait are characteristic features for neurodegenerative diseases. To analyze gait disturbances, mice were tested in the automated gait analysis system "CatWalk" (Noldus, Wageningen). The mouse had to run over an elevated illuminated glass plate in a dark room. The step pattern is recorded with a camera (Pulnix Camera RM-765) and analysed with the "CatWalk" software Version 7.1. Each mouse had to perform three uninterrupted runs.

Grip strength

To measure the muscle strength of forelimbs and combined forelimb/hindlimb the grip strength test was performed. For this reason the commercially available Grip Strength Meter apparatus (Bioseb or TSE) was used. The system is supplied with a single grid (400 x 180 x 200 mm) which connects to the sensor. To measure the grip strength of the forelimbs, the mouse was brought down to the grid so that only the forelimbs could grip it and drawn back until the grid was released. The grip strength value was shown on the screen of the apparatus. To measure grip strength of fore and hind paws, the mouse was brought down to the grid so that all four paws could grip it and drawn back until the grid was released. Each mouse had to perform three trials for forelimbs and forelimbs/hindlimbs grip measurement.

5.6 German Mouse Clinic

In the German Mouse Clinic (GMC) at the Helmholtz Centre Munich mouse models are analyzed for a large scale of comprehensive and standardized methods. The mouse line hTDP-43^{A315T}Rosa was tested in the primary screen for phenotypically analysis. The mouse model was screened in the following areas: behavior, bone and cartilage development, neurology, clinical chemistry, eye development, immunology, allergy, steroid metabolism, energy metabolism, lung function, vision and pain perception, molecular phenotyping, cardiovascular analyses and pathology. All tests were performed according to the

standardised phenotyping screens developed by the EUMORPHIA partners and available at www.empress.har.mrc.ac.uk.

A cohort of mice (10 mice per sex and genotype) were transferred to the GMC with an age of 5 months. After a habituation of two weeks the primary screen was performed according to GMC guidelines (Gailus-Durner et al. 2005).

6 Results

6.1 Generation of hTDP-43 mice

6.1.1 Generation of hTDP-43 ES cells

For generation of ES cells containing human wildtype or mutated TDP-43 cDNA (kindly provided by M. Neumann), vectors were designed for FLP recombinase mediated cassette exchange (RMCE) with FlEx gene trap vectors (Schebelle et al. 2010). Vectors harboring human TDP-43 cDNA between two attB recognition sites were electroporated along with a FlpO expression plasmid to gene trap clones. The gene trap clones (D045A10, E304C05) had insertions of a retroviral SA-βgeo-pA vector in the first intron of the Tardbp mouse locus. By unidirectional recombination the SA-βgeo-pA cassette was replaced and the SA-hTDP43-BGHpA/3'UTR cassette inserted (Fig.4). The following hTDP-43 cDNAs were used: hTDP-43^{WT}BGHpA, hTDP-43^{A315T}BGHpA, hTDP-43^{G348C}BGHpA, hTDP-43^{M337V}BHGpA, hTDP-43^{82aaa}BGHpA, and hTDP-43^{WT}3'UTR and hTDP-43^{A315T}3'UTR.

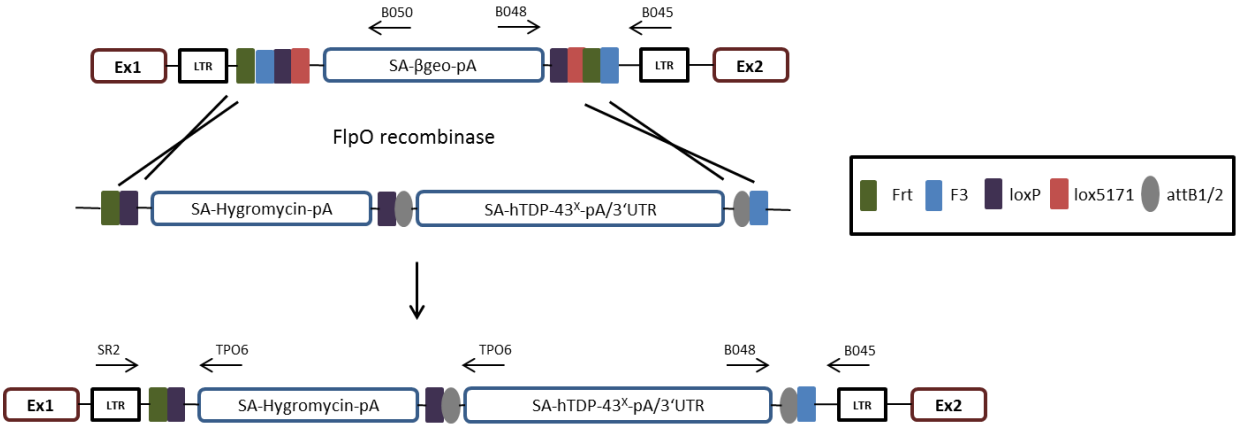

Fig. 4: Illustration of the FlpO mediated cassette exchange *in vitro*.

For each electroporation, 48 hygromycin resistant clones were picked and analyzed for β-gal activity (data not shown). β-gal negative clones were further screened by PCR. Two PCR strategies were used to confirm correctly exchanged ES cell clones: (I) the primers B045/B048/B050 were used to identify false positive clones with inverted β-geo cassettes or random insertions and (II) the SR2/TPO6 PCR was done to identify clones with a correct exchange. All clones with a band size of 426 bp for the B0-PCR and a band size of 261 bp for the SR/TPO6-PCR were considered as positive for the correct exchange (Tab.3).

construct	ES cell clone	positive clones
hTDP-43^{WT}BGHpA	D045A10	**3/6**, **3/8**, **3/15**, 3/19, 3/21, 3/22, 3/23, 3/29, 3/32, 3/40, 3/41
hTDP-43^{A315T}BGHpA	D045A10	**5/1**, **5/10**, 5/14, 5/16, 5/21, 5/23, 5/25, 5/26, 5/27, 5/29, **5/30**, 5/35, 5/36
hTDP-43^{G348C}BGHpA	D045A10	**9/8**, **9/9**, **9/16**, 9/19, 9/21, 9/28, 9/29, 9/31, 9/33, 9/35, 9/37, **9/40**, 9/42
hTDP-43^{M337V}BGHpA	D045A10	13/5, 13/10, 13/11, 13/13, 13/14, 13/18, **13/21**, **13/22**, **13/23**, 13/25, 13/38, 13/43, **13/45**, **13/47**
hTDP-43^{82aaa}BGHpA	D045A10	82/1, 82/11, **82/12**, 82/14, 82/16, 82/18, 82/21, 82/23, **82/25**, 82/26, 82/27, **82/29**, 82/30, **82/35**, 82/36
hTDP-43^{WT}BGHpA	E304C05	3E/2, **3E/6**, **3E/7**, 3E/13, 3E/15, 3E/19, 3E/22, 3E/30, 3E/31, 3E/42
hTDP-43^{WT}3'UTR	E304C05	3U/1, **3U/12**, **3U/19**, 3U/20, 3U/22, 3U/28, 3U/31 , **3U/34**
hTDP-43^{A315T}3'UTR	E304C05	5U/7, 5U/7, 5U/9, 5U/12, 5U/15, **5U/22**, **5U/23**, 5U/29, 5U/32, 5U/34

Tab. 3: Positive clones for electroporations of plasmids with the human TDP-43 cDNAs. Clones used for blastocyst injections are labeled in bold.

6.1.2 Generation of hTDP-43 chimeras

The positive clones of the RMCE were karyotyped and used for blastocyst injections. Injected blastocysts were transferred into the uteri of pseudo-pregnant CD-1 foster mothers. In the case of 46% of all embryo transfers chimeras were born (Tab.4). All male chimeras were mated to C57Bl6/J female mice for germline transmission. Only for hTDP-43^{A315T}BGHpA clone 5/10 gave rise to agouti pups. To overcome this problem constructs were electroporated in an alternative gene trap clone (E304C05) with insertion of the SA-βgeo-pA cassette similar to the previously used gene trap clone (D045A10). The genetically modified ES cell clones were again injected into blastocysts and transferred to CD-1 foster mothers. At the moment all chimeras are bred with C57Bl6/J mice for germline transmission.

ES cell clone	construct	clone	chimeras	germline transmission
D045A10	hTDP43^{WT}BGHpA	3/6	1	no
		3/8	0	
		3/15	0	
	hTDP43^{A315T}BGHpA	5/1	0	
		5/10	5	yes, founder of colony
		5/30	1	no
	hTDP43^{G348C}BGHpA	9/8	0	
		9/9	0	
		9/16	2	no
		9/40	1	no
	hTDP43^{M337V}BGHpA	13/21	0	
		13/22	5	no
		13/23	0	
		13/45	2	no
		13/47	1	no
	hTDP43^{82aaa}BGHpA	82/12	0	
		82/25	0	
		82/29	10	no
		82/35	0	
E304C05	hTDP43^{WT}BGHpA	3E/6	2	in mating
		3E/7	0	
	hTDP43^{WT}3‘UTR	3U/12	0	
		3U/19	0	
		3U/34	4	in mating
	hTDP43^{A315T}3‘UTR	5U/22	0	
		5U/23	7	in mating

Tab. 4: Chimeras born from the injected clones. Number of chimeras and germline transmission is noted. Only for the clone 5/10 a germline transmission was achieved. These pups were used to establish a colony.

6.1.3 Expression of hTDP-43^{A315T} *in vivo*

To start the expression of hTDP-43, the hygromycin cassette had to be excised. Therefore, hTDP-43^{A315T}BGHpA (in the following referred to as hTDP-43^{A315T}) animals were crossed with Rosa26-Cre expressing mice. The Cre recombinase leads to the excision of the hygromycin cassette, which is flanked by two loxP sites and activates the expression of the human TDP-43 isoform (Fig.5).

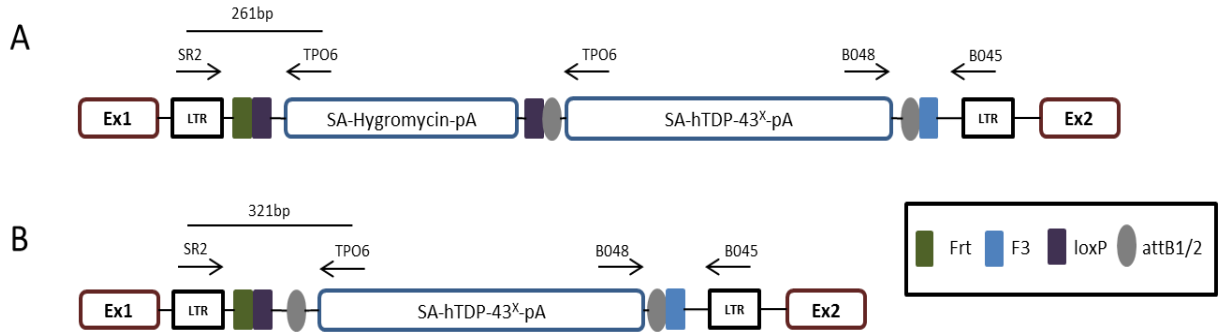

Fig. 5: Illustration of hygromycin excision *in vivo*. (A) Insertion of hygromycin and hTDP-43 in the first intron of the mouse Tardbp locus. (B) The Tardbp allele after successful Cre-mediated hygromycin excision.

Arising pups were genotyped with the SR/TPO6 and pCre PCR. The PCR with primers SR2 and TPO6 was performed to identify animals with an excision of the hygromycin cassette, which yielded either a 321bp band for a correct excision or a 261bp band for no excision of the hygromycin cassette. Mice expressing Cre recombinase and carrying the hTDP-43^{A315T} allele displayed expression of the human mutated TDP-43 protein (Fig.6).

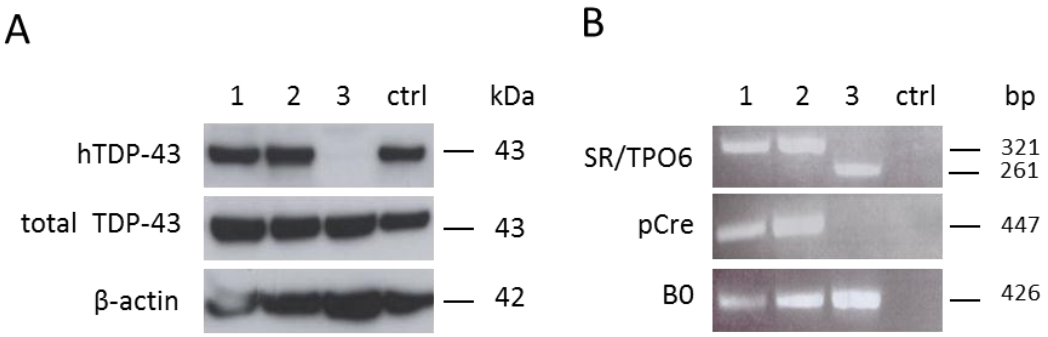

Fig. 6: Expression of hTDP-43^{A315T} in the brain of embryos from hTDP-43^{A315T} x Rosa26Cre mating. Embryos were sacrificed at day E17.5. (A) Western blot analysis from head tissue demonstrates human TDP-43 expression for embryo 1 and 2, ctrl = protein lysates of HEK cells (B) Genotyping of embryo mouse tails with the SR/TPO6, pCre and B0-PCR. Upper band (321bp) displayed successful excision of hygromycin, lower band (261bp) revealed still inserted resistance cassette.

To detect the expected activation of hTDP-43 expression via Cre recombinase, embryos from a hTDP-43^{A315T} x Rosa26Cre mating were sacrificed at stage E17.5. Tails were used for genotyping and protein from head tissue for western blot analysis. As shown in figure 6A embryos 1 and 2 but not 3 exhibited bands of successful hygromycin excision (SR/TPO6-PCR) and carried the Cre recombinase (pCre-PCR). All embryos showed a correct band for the triple B0-PCR, indicating correct hTDP-43^{A315T} insertion. The heads of the embryos were used for protein lysates. Blots were incubated with an antibody for human TDP-43 protein (hTDP-43) and an antibody recognizing both mouse and human TDP-43 isoforms (total TDP-43). The expression of human TDP-43 protein coincided with the results of the genotyping. Only

embryos 1 and 2 showed expression of human TDP-43 but not 3. Total TDP-43 protein could be detected in all protein lysates. As a positive control for the hTDP-43 antibody protein lysates of HEK cells were used.

6.1.4 Conditional expression of hTDP-43^{A315T}

To examine the possibility of conditional expression of human mutant TDP-43 in neuronal tissue only, hTDP-43^{A315T} animals were bred to Nestin-Cre mice (Tronche et al. 1999). In contrast to the ubiquitous expression of TDP-43 by Rosa26Cre, Nestin promoter activity is restricted to the central nervous system (CNS). In order to detect the activation of human TDP-43 in the CNS, several tissues of a one month old hTDP-43^{A315T}Nes mouse were used for protein isolation. For all organs, a mouse specific TDP-43 band was detectable. Human TDP-43 protein however was only detectable in the brain lysate but not in any other tissue (Fig.7).

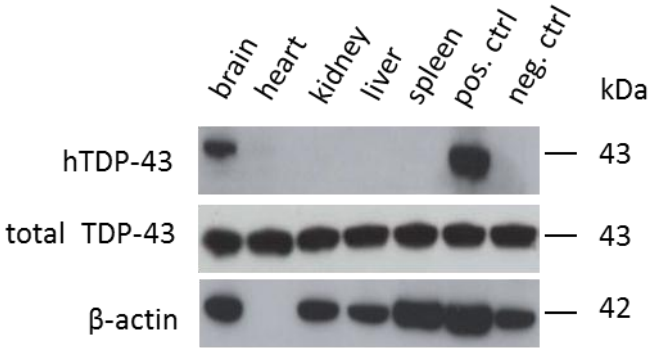

Fig. 7: Conditional expression of human TDP-43. Expression of hTDP-43 was only detectable in the brain but not in any other tissues. Expression of mouse TDP-43 was found in all tissues tested. As a positive control for the hTDP-43 antibody HEK cell protein lysates were used. For a negative control brain lysate was used from a wildtype mouse.

The conditional expression of human TDP-43 was successful. The excision of the hygromycin cassette occurred only in tissues where Cre recombinase was active.

6.1.5 Homozygous lethality of hTDP-43^{A315T}Rosa mice

Heterozygous hTDP-43^{A315T}Rosa mice were viable and fertile. To initiate a putative stronger phenotype, hTDP-43^{A315T}Rosa+/- mice were intercrossed in order to obtain homozygous offspring. Given mendelian inheritance, the following distribution was expected: 25%

wildtype, 25% homozygous and 50% heterozygous mice. However, no homozygous hTDP-43^{A315T}Rosa mice could be detected. After genotyping of 446 pups from hetxhet matings at weaning age, none of the offspring carried the hTDP-43 insertion on both alleles indicating embryonic lethality (Fig.8A).

A

wildtype	heterozygous	homozygous	total
159	287	0	446

B

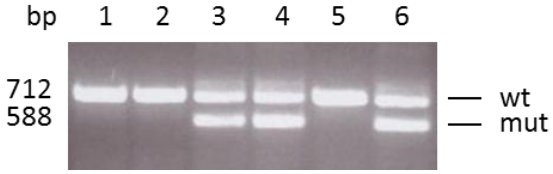

Fig. 8: Homozygous lethality of hTDP-43^{A315T}Rosa mice. (A) Overview about mice genotyped at weaning age of hTDP-43^{A315T}Rosa+/- x hTDP-43^{A315T}Rosa+/- matings. (B) Genotyping of embryos at stage E7.5 from hetxhet matings (number 1-6). Upper band represents the wildtpye TDP-43 allele (712bp), lower band represents the hTDP-43^{A315T} allele (588bp).

To determine the stage of lethality, hetxhet matings were done, plugs were checked at E0.5 and the offspring at embryonic stage 7.5 was sacrificed. The embryonic tissue was used for DNA isolation and genotyping. A triplex PCR was performed using the primers D045for/D045rev/LTRfor. Appearance of one band with a size of 712bp according to wildtype animals, one band with a size of 588bp according to homozygous animals and appearance of both bands (588bp + 712bp) correlated to heterozygous embryos (Fig.8B). For 20 embryos genotyped at E7.5, no homozygous hTDP-43^{A315T}Rosa mouse could be identified indicating lethality before or around gastrulation (E6.5 – E7.5). Therefore, the entire study was done using heterozygotes.

6.2 Analysis of TDP-43 expression level

6.2.1 Elevated TDP-43 levels in hTDP-43^{A315T}Rosa+/- mice

To analyze the expression level of TDP-43 in the mutants compared to controls, a variety of tissues from 6 months old hTDP-43^{A315T}Rosa+/- animals were used for total protein isolation. A western blot was performed with the protein lysates and bands were detected with the antibody recognizing both TDP-43 isoforms. TDP-43 levels were found to be elevated in

brain, spleen, kidney and liver (Fig.9A). Additionally, a number of tissue-specific TDP-43 isoforms could be identified. To determine whether the appearing bands were a result of mRNA splicing or post-translational modification, an additional western blot was performed with an antibody recognizing only the N-terminal human TDP-43 protein. This antibody detected not only the typical 43kDa band but also the 35kDa specific isoform in kidney. Considering the absence of splicing for a cDNA, the kidney-specific TDP-43 isoform seemed to be a matter of post-translational modification.

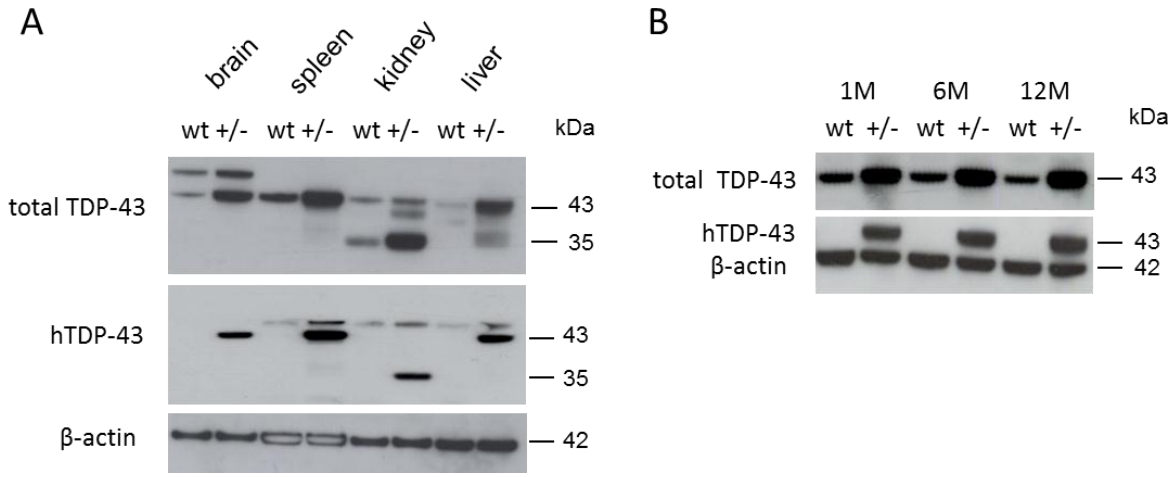

Fig. 9: Elevated TDP-43 levels in hTDP-43^{A315T}Rosa+/- mice. (A) Western blots of various tissue lysates from a 6 months old mutant mouse compared to control probed for total TDP-43 or human TDP-43 revealed tissue-specific pattern as well as increased TDP-43 levels for all organs. (B) Western blots of brain lysates from 1,6, and 12 months old mutants (+/-) compared to controls (wt) using antibodies against total TDP-43 and human TDP-43 showed elevated expression of TDP-43 in the mutants.

To investigate the onset of TDP-43 overexpression, brain lysates of 1, 6 and 12 months old mutants were used for western blot analysis (Fig.9B). Compared to wildtype littermates, heterozygous hTDP-43^{A315T}Rosa mice showed elevated TDP-43 levels already at an age of 1 month.

6.2.2 Down-regulation of endogenous TDP-43

The elevated TDP-43 levels in mutants raised the question, which TDP-43 isoform was over-expressed, the human or the endogenous mouse TDP-43. For this purpose, a quantitative real-time PCR was performed. Brain RNA samples were isolated from three male hTDP-43^{A315T}Rosa+/- animals and three age-matched controls (6 months) and transcribed into cDNA. To differentiate between the endogenous mouse and human TDP-43 mRNAs,

TaqMan® Gene Expression Assays were specifically designed for the particular sequence. The comparison of the mRNA expression levels revealed a down-regulation of endogenous mouse TDP-43 and an overexpression of human mutated TDP-43 (Fig.10) in hTDP-43^{A315T}Rosa+/- mice. The endogenous mouse TDP-43 mRNA level was down-regulated around 80% compared to controls. In contrast, the human mutated TDP-43 mRNA was elevated up to 3-fold.

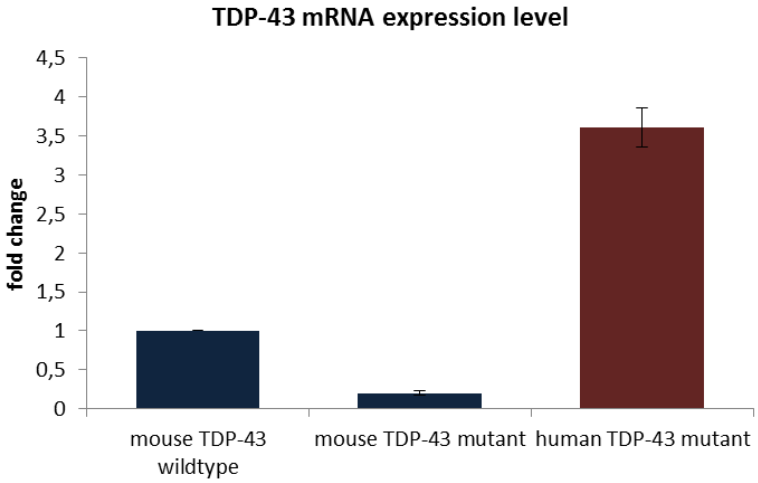

Fig. 10: TDP-43 mRNA expression level. Quantification of mouse and human TDP-43 isoforms via quantitative real-time PCR. Down-regulation of endogenous mouse TDP-43 to about 20% as well as a 3 to 4 fold up-regulation of human TDP-43 in mutants compared to controls.

6.3 Pathological analysis

6.3.1 Insoluble TDP-43

A pathological hallmark of amyotrophic lateral sclerosis (ALS) and a subset of frontotemporal lobar degeneration (FTLD-TDP) is the formation of neuronal insoluble TDP-43 inclusions (Neumann et al. 2006, Arai et al. 2006). To analyze the formation of insoluble TDP-43 inclusions, total protein was isolated from control and mutant brains. The pellet was washed twice and solved in urea buffer. Western blot analyses were performed with soluble and insoluble brain lysates of three and twelve months old heterozygous hTDP-43^{A315T}Rosa mice compared to controls (Fig.11A). Insoluble TDP-43 was detectable in young and old mutants, but not in controls. The amount of insoluble TDP-43 increased with age, while three months old mutants displayed only small amounts of insoluble TDP-43, it was highly detectable in twelve months old mutants. The insoluble form of TDP-43 could be detected with an

antibody recognizing only the human TDP-43 protein as well as with an antibody detecting total TDP-43 species.

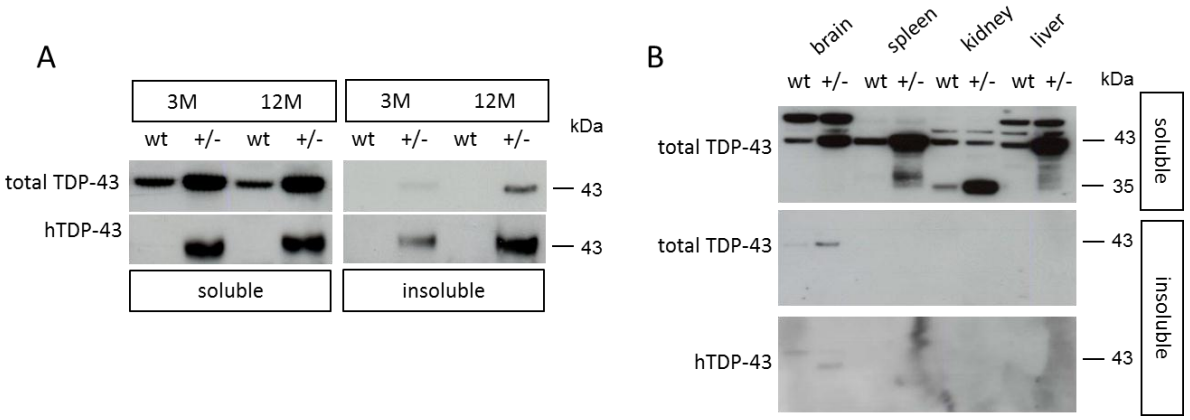

Fig. 11: Insoluble TDP-43 in hTDP-43^{A315T}Rosa mice. (A) Western blot analysis of soluble and insoluble TDP-43. Soluble protein fractions showed increased levels of TDP-43 in mutants (+/-) with both antibodies (total TDP-43 and hTDP-43) but not in wildtpye littermates (wt). Increasing amounts of insoluble TDP-43 were detectable for 3 and 12 months old mutants. No insoluble TDP-43 was found in wildtpye mice. (B) Western blot analysis of soluble and insoluble tissue fractions. Insoluble TDP-43 was only found in brain lysates but not in other tissues.

Despite the increased levels of TDP-43 in all tissues tested, detection of insoluble TDP-43 protein was only possible in brain lysates (Fig.11B). Insoluble TDP-43 could be found in neither spleen, nor kidney, nor liver.

Immunohistochemistry was performed to identify the location of insoluble TDP-43 aggregates in brain and spinal cord of hTDP-43^{A315T}Rosa+/- mice. Paraffin sections were prepared from brain and spinal cord of 15 months old mutants and controls. Stainings with antibodies for TDP-43 (hTDP-43 and total TDP-43) revealed neuronal cytoplasmic inclusions (NCIs) in brain (Fig.12A) and spinal cord (Fig.12B).

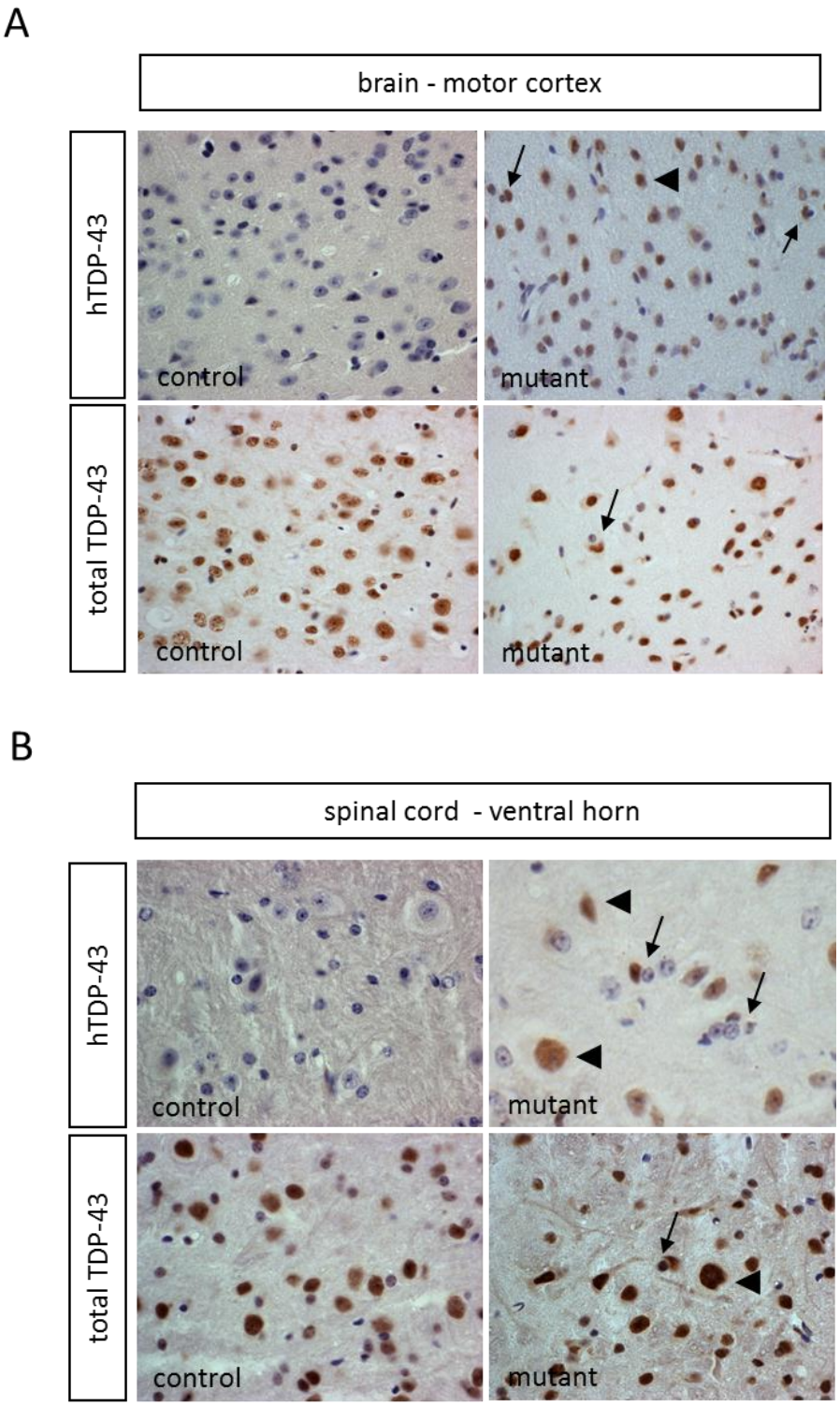

Fig. 12: Immunohistochemistry of brain and spinal cord sections from 15 months old mutants compared to controls. (A) Sections of the motor cortex from hTDP-43^{A315T}Rosa+/- mice compared to controls. (B) Sections of the ventral horn of the spinal cord from hTDP-43^{A315T}Rosa+/- mice compared to controls. NCIs are highlighted with arrows and normal nuclear staining with arrowheads.

Neuronal cytoplasmic inclusions of TDP-43 could be mainly detected in the motor cortex and to some extent in hippocampal neurons of the brain. In the spinal cord, TDP-43 aggregates were located in the ventral horn.

6.3.2 Ubiquitination of TDP-43

The identity of the ubiquitinated protein in amyotrophic lateral sclerosis (ALS) and frontotemporal lobar degeneration (FTLD-U) was unknown a long time. Neumann et al. (2006) discovered TDP-43 as the major protein in these neurodegenerative diseases. In order to detect ubiquitin positive inclusions in hTDP-43^{A315T}Rosa+/- mice, brain and spinal cord sections were prepared from mutants and stained with an antibody recognizing poly-Ubiquitin. Ubiquitin-positive inclusions could be detected in brain (Fig.13A) as well as in spinal cord (Fig.13B) sections of one year old mutants. These inclusions were mainly located in the cortex of the brain and the ventral horn of the spinal cord.

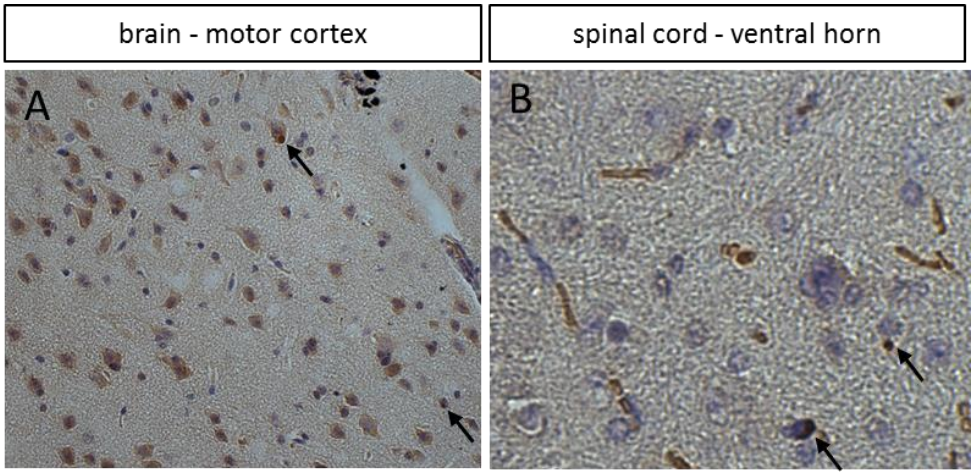

Fig. 13: Immunohistochemistry of brain (A) and spinal cord (B) sections of one year old mutants with an antibody recognizing poly-Ubiquitin. Neuronal cytoplasmic inclusions are highlighted with an arrow.

To investigate ubiquitination of TDP-43, a double immunofluorescence labeling with antibodies recognizing both TDP-43 isoforms and poly-Ubiquitin was performed (Fig.14). In the controls, TDP-43 (green) localized mainly to the nucleus and the staining for poly-ubiquitin (red) was rather weak in brain as well as in spinal cord sections (Fig.14A,C). For sections of heterozygous mutants, cytoplasmic TDP-43 inclusions could be detected in neurons of brain and spinal cord (Fig.14B,D). These neuronal cytoplasmic inclusions were mainly located in the motor cortex and the anterior horn of the spinal cord and co-labeled for poly-ubiquitin (yellow).

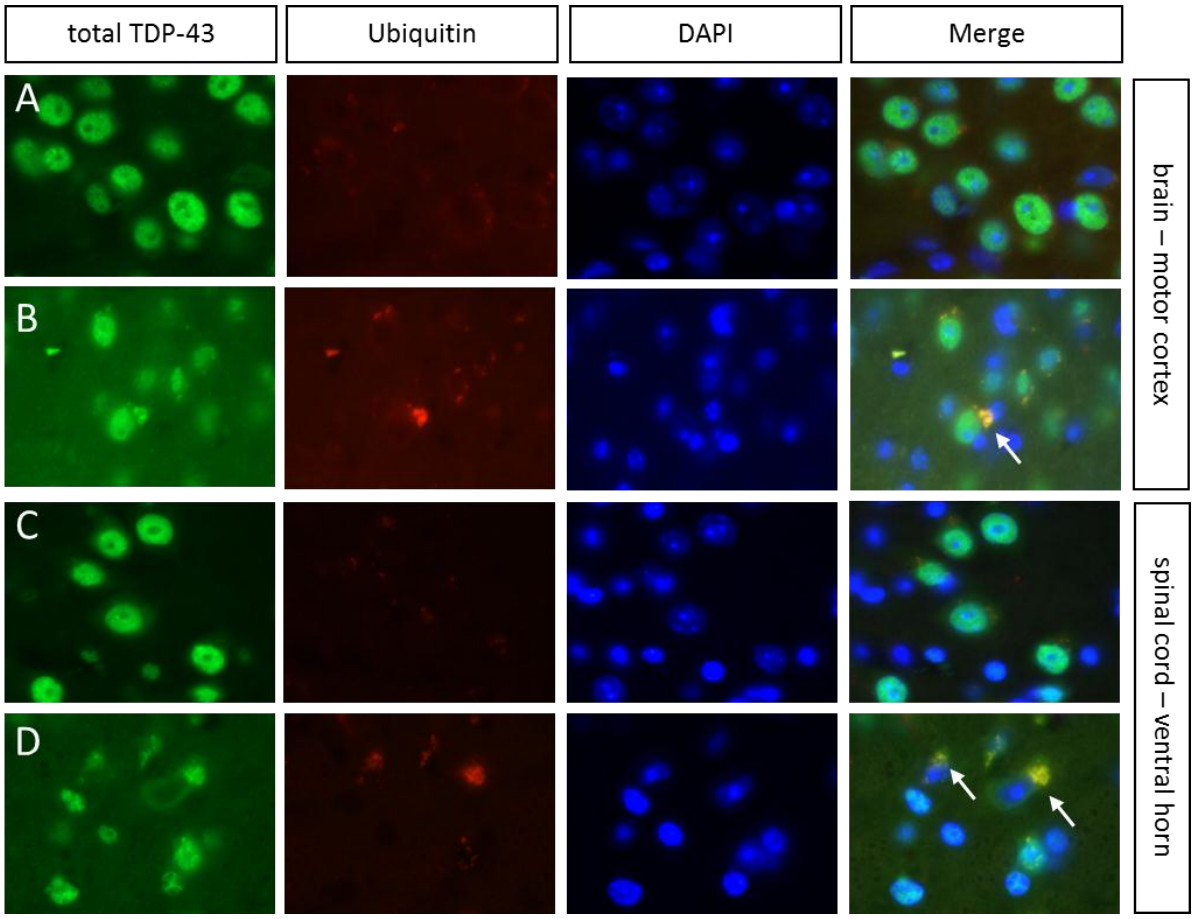

Fig. 14: Double immunofluorescence labeling of brain and spinal cord sections from one year old mutants and controls. (A+C) Nuclear TDP-43 staining of brain and spinal cord sections. Poly-ubiquitin labeling was rather weak. No co-labeling of TDP-43 and poly-ubiquitin could be detected. (B+D) Nuclear and cytoplasmic TDP-43 in neurons of brain and spinal cord. Cytoplasmic TDP-43 inclusions co-labeled with poly-ubiquitin.

Other previously described pathological features of TDP-43 are (I) hyper-phosphorylation of the protein at several serine residues and (II) the cleavage in C-terminal fragments (Neumann et al. 2006). In order to check putative hyper-phosphorylation in mice carrying the A315T mutation, soluble and insoluble brain lysates were established and analyzed by western blot with an antibody recognizing the pathologically phosphorylated serine residues (kindly provided by E. Kremmer). As a positive control, brain lysate of a wildtype mouse was *in vitro* phosphorylated with casein kinase I to mimic the serine residue phosphorylation (Kametani et al. 2009). Neither for the soluble nor for the insoluble brain lysates of one year old mutants was a band for the TDP-43 hyper-phosphorylation detectable (Fig.15). Only the *in vitro* phosphorylated brain samples displayed a positive signal for the used antibody.

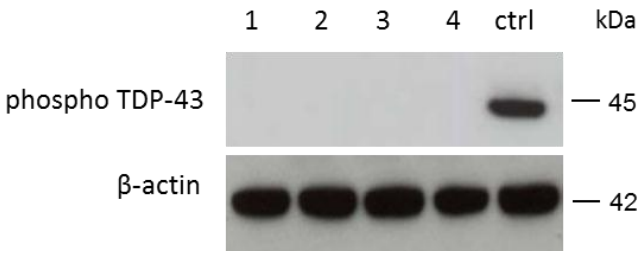

Fig. 15: Western blot anaylsis of soluble wildtype (1) and mutant (2) and insoluble wildtpye (3) and mutant (4) brain lysates using antibody specific for hyper-phosphorylated TDP-43. Signal was only detectable for the *in vitro* phosphorylated brain lysate (ctrl).

To detect C-terminal fragments of TDP-43 in hTDP-43^{A315T}Rosa+/- mice, brain lysates of mutants and controls were used for western blot analyses. Although several antibodies detecting the C-terminus of TDP-43 were tested, no pathological cleavage of TDP-43 could be found in old mutants compared to controls.

6.3.3 Motor neuron degeneration

A characteristic hallmark of amyotrophic lateral sclerosis (ALS) is the degeneration of upper and lower motor neurons. To detect motor neuron degeneration, spinal cord paraffin sections of 18 months old hTDP-43^{A315T}Rosa+/- and control animals were prepared. The sciatic motor pool of the lumbar spinal cord region was used for counting of the motor neurons after staining the serial sections with Nissl reagent (cresylviolet). Three animals per genotype were counted and scored. The number of motor neurons was found to be significantly reduced in mutants compared to controls (Fig.16). However, to validate the obtained results, motor neurons of three months old hTDP-43^{A315T}Rosa+/- and control animals were counted additionally. Again a significant reduction of motor neurons in the sciatic motor pool was determined indicating a developmental phenotype but not a progressive neurodegeneration.

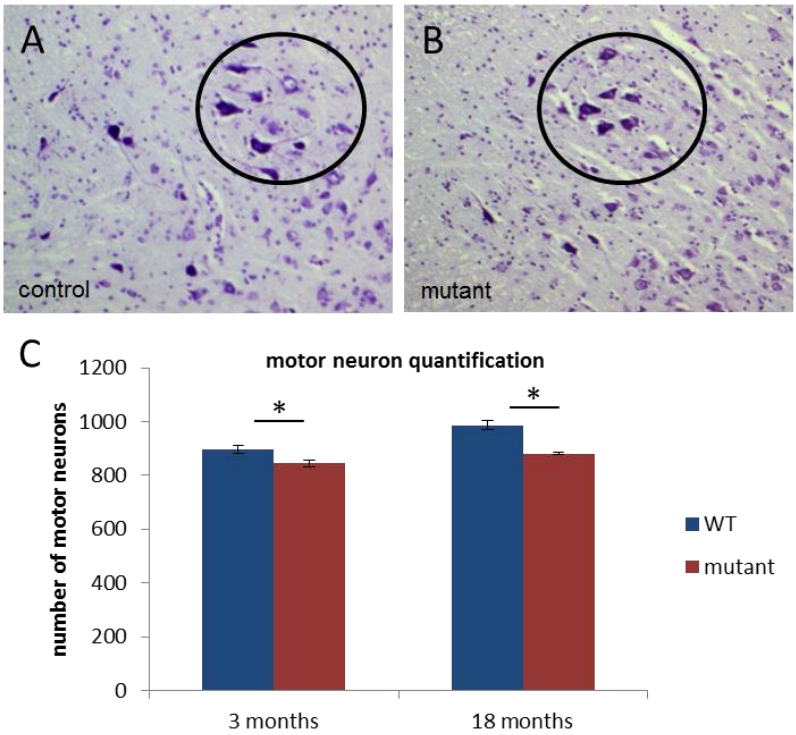

Fig. 16: Quantification of motor neurons. (A-B) Nissl staining of spinal cord sections revealed motor neurons in the sciatic motor pool. (C) Significantly decreased number of motor neurons in the lumbar area of 3 and 18 months old mutants compared to age-matched controls (* = t-test, $P < 0.05$).

6.4 Phenotypic analysis

6.4.1 Reduced body weight in hTDP-43 mutants

hTDP-43^{A315T}Rosa+/- mice were viable and fertile. No obvious phenotype was detectable for young mutants compared to controls. With an age of three months a reduction in body weight was verifiable during normal breeding conditions. In order to examine the loss of body weight, cohorts of mice were continuously weighed and the body weight was documented. The cohorts consisted of ten mice per sex and genotype. The body weight increased consistently with age for hTDP-43^{A315T}Rosa+/- and wildtype mice. However, already at an age of three months a significant reduction in body weight was detectable for males but not for females (Fig.17). This was also seen in animals at an age of eight months. Again significant loss of body weight for male mutants compared to controls but females displayed similar weight as wildtype mice. For aged cohorts (15 months) a weight deficit of 14% for male and 12% for female mutants was detected as compared to wildtype animals of

the same age. The older the mutants grow the more obvious became the body weight decrease.

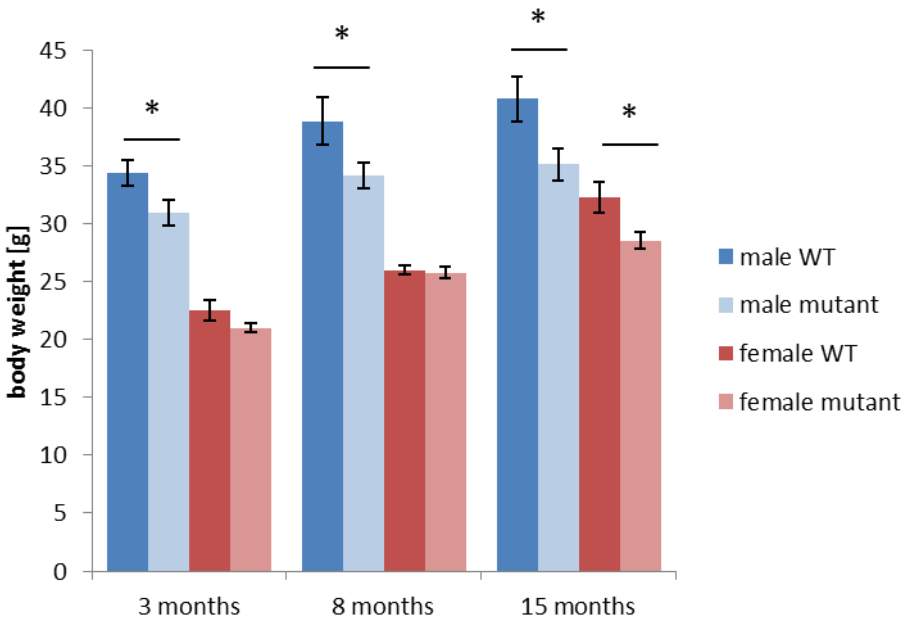

Fig. 17: Body weight measurements of different aged cohorts compared to controls. Male mutants displayed significant reduced body weight compared to controls already with an age of three months. A significant loss of body weight was detected with an age of 15 months for females but not for younger mice (* = t-test, $P < 0.05$).

6.4.2 Behavioral analysis

6.4.2.1 Motor tests

In the light that the number of motor neurons were negatively affected in the hTDP-43^{A315T}Rosa+/- animals, a cohort of ten mice per sex and genotype were tested in the following motor coordination tests: beam walk, vertical pole, ladder, cat walk, accelerating rotarod and grip strength. At the beginning of the tests all mice had an age of 18 months.

In the gait analysis mutant mice (male and female) revealed significantly more gait disturbances as controls. A selection of significantly altered test results is summarized in figure 18. In general, mutants showed a trend towards spending more time standing on four paws as compared to wildtype animals (Fig.18A). Furthermore, the time at which the largest part of a paw contacts the glass plate was significantly altered for the left hind paws (Fig.18B). The most severe gait phenotype was detectable in the performance of diagonal coordination. Normally for diagonal paw pairs, the target paw typically moves synchronously with the anchor (“coupling”) (Noldus 2007). In the mutants, the diagonal phase dispersion

and the diagonal coupling were disturbed. The temporal relationship of diagonal paws (RF-LH, LF-RH) within a step cycle was found to be significantly altered (Fig.18C-D). Additionally affected parameters are summarized in appendix (see 9.3.1).

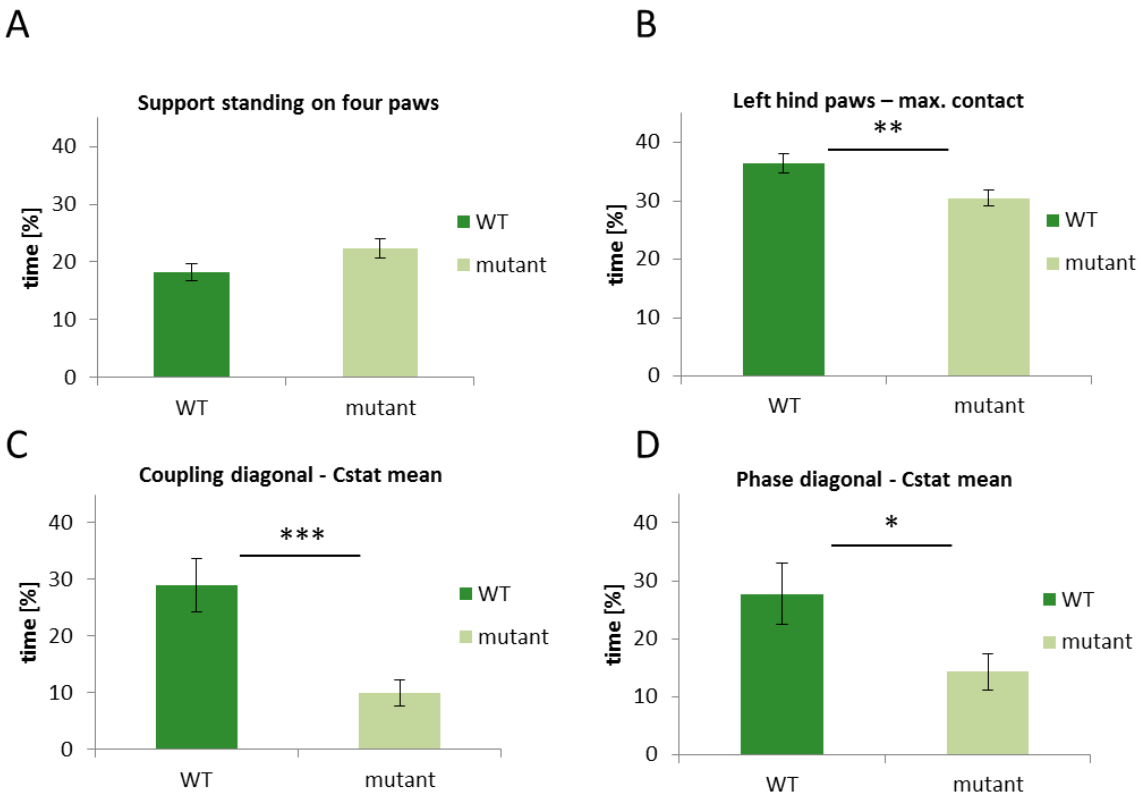

Fig. 18: Gait analysis of 15 months old mutants compared to controls with the "CatWalk" system. (A) Mutants showed a trend to spend more time standing on four paws. (B) Time of maximal contact spent on left hind paws was altered in mutants. (C-D) The diagonal inter-paw coordination was the most severe affected parameter(* = t-test, $P < 0.05$; ** = t-test, $P < 0.01$; *** = t-test, $P < 0.001$) (Cstat mean = statistic that represents Phase dispersions using circular statistics).

For all other motor tests (beam walk, vertical pole, ladder, accelerating rotarod and grip strength) no significant changes were detectable (Fig.19). Only in the vertical pole test, female hTDP-43^{A315T}Rosa+/- mice revealed a trend for a longer turning duration compared to wildtype animals (Fig.19B). These results indicate motor deficits that hint to either cerebellar, motor cortex or spinal cord abnormalities.

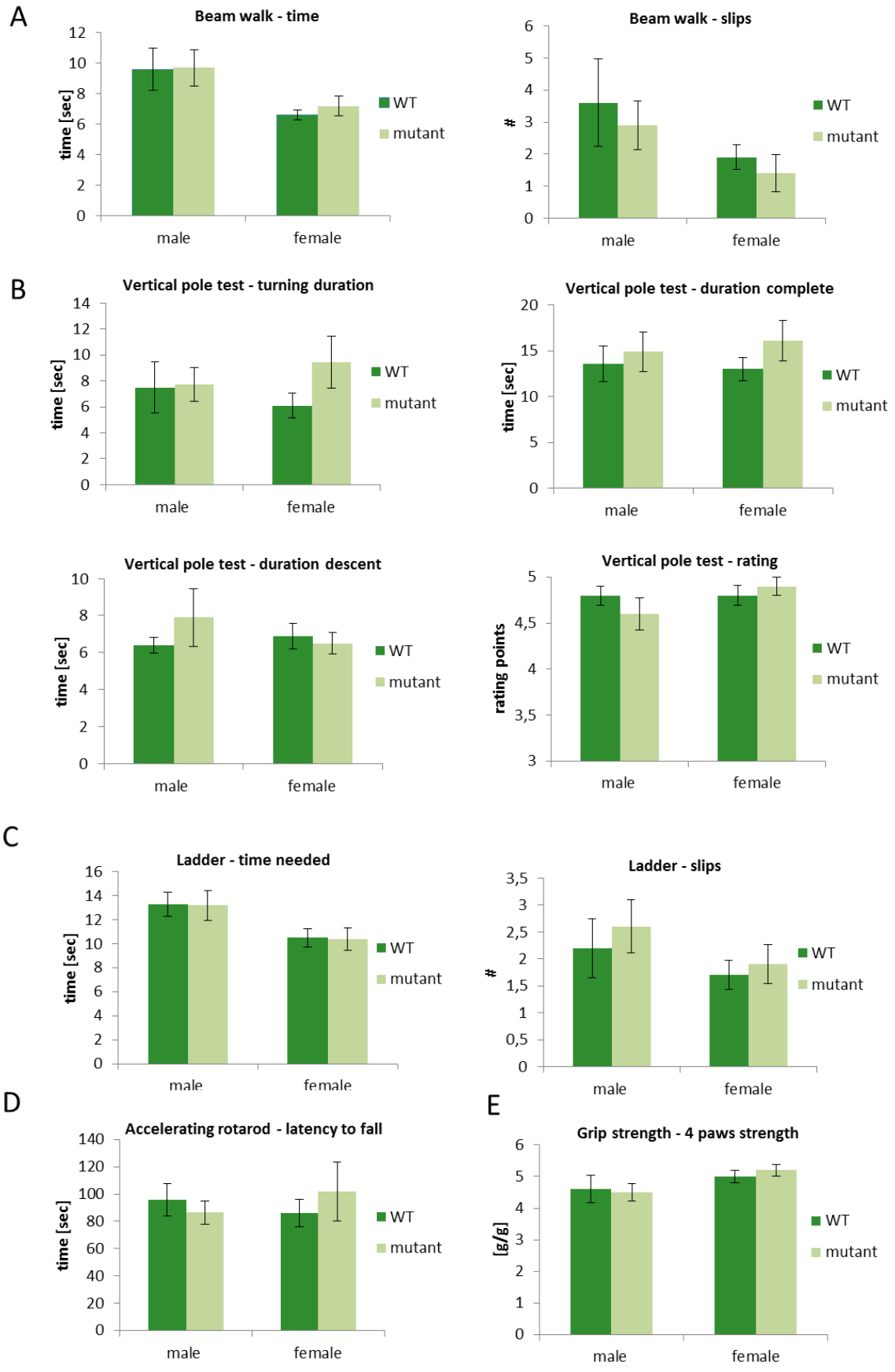

Fig. 19: Motor tests of 15 months old hTDP-43^{A315T}Rosa+/- mice. In the beam walk (A), ladder (C), accelerating rotarod (D) and grip strength (E) mutants were comparable to controls. A trend was detectable for longer turning duration of female mutants in the vertical pole test (B) (trend = t-test, 0.1>P<0.05).

6.4.2.2 Memory tests

Patients suffering from amyotrophic lateral sclerosis (ALS) occasionally develop a form of dementia (Lillo and Hodges 2009); therefore a series of tests was performed in order to detect problems with memory function. To check working memory, the y-maze test was done. The number of spontaneous alternations (SPAs), alternate arm returns (AARs) and same arm returns (SARs) was scored and evaluated. Female hTDP-43^{A315T}Rosa+/- mice displayed a trend towards unusually more same arm returns (SARs) compared to controls (Fig.20C), meaning female mutants had a tendency to leave one arm of the y-maze, go to the center and return to the same arm they came from. No changes were detectable for spontaneous alternations (SPAs) as well as alternate arm returns (AARs) (Fig.20A-B).

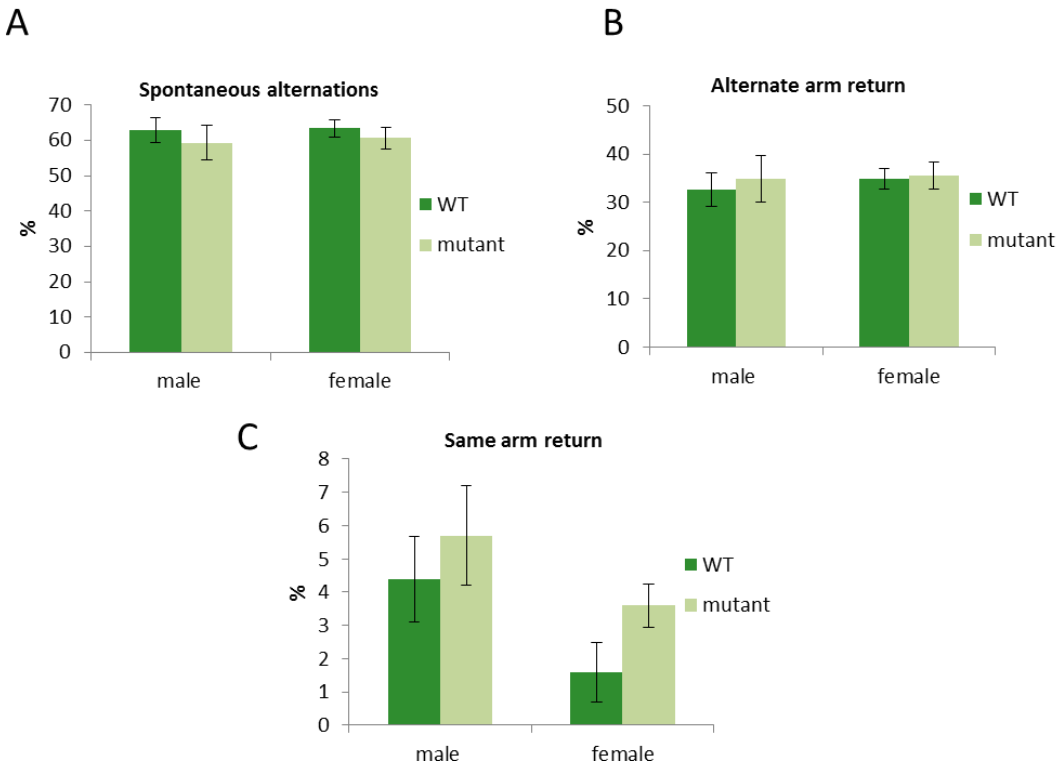

Fig. 20: Y-maze test of 15 months old mutants compared to controls. Spontaneous alternations (A) and alternate arm returns (B) were comparable to wildtype mice. (C) Female mutants revealed a trend towards more same arm returns compared to controls. This was not detectable for male mutants (trend = t-test, 0.1>P<0.05).

For object recognition task, a test addressing non spatial memory, a cohort of mice was trained for three times with two identical objects in an empty cage (each trial 5 minutes). After 3h and 24h one familiar object was replaced by a new unfamiliar one. The exploration time for each object was scored and analyzed (Fig.21). Neither after 3 hours nor after 24 hours genotype related differences could be observed in comparison to control animals.

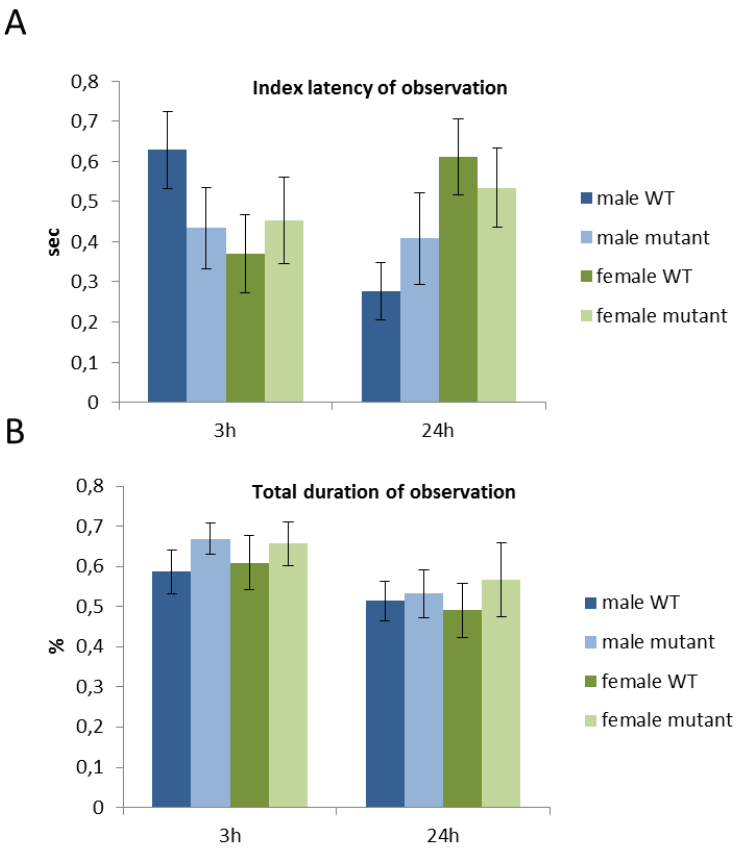

Fig. 21: Object recognition test. (A) The latency of observation was not affected in mutants when compared to controls. Only male mutants displayed a trend towards decreased observation of the unfamiliar object after 3h. (B) The total duration of observation was similar for all genotypes.

In the IntelliCage system, 20 months old hTDP-43^{A315T}Rosa+/- female mice were tested compared to female controls (wildtype n=7, mutant n=8). The animals were tested for three different memory parameters increasing the level of difficulty: (1) place learning, (2) reversal learning and (3) patrolling (Fig.22). Mutant mice behaved comparable to controls, even for the more difficult patrolling phase.

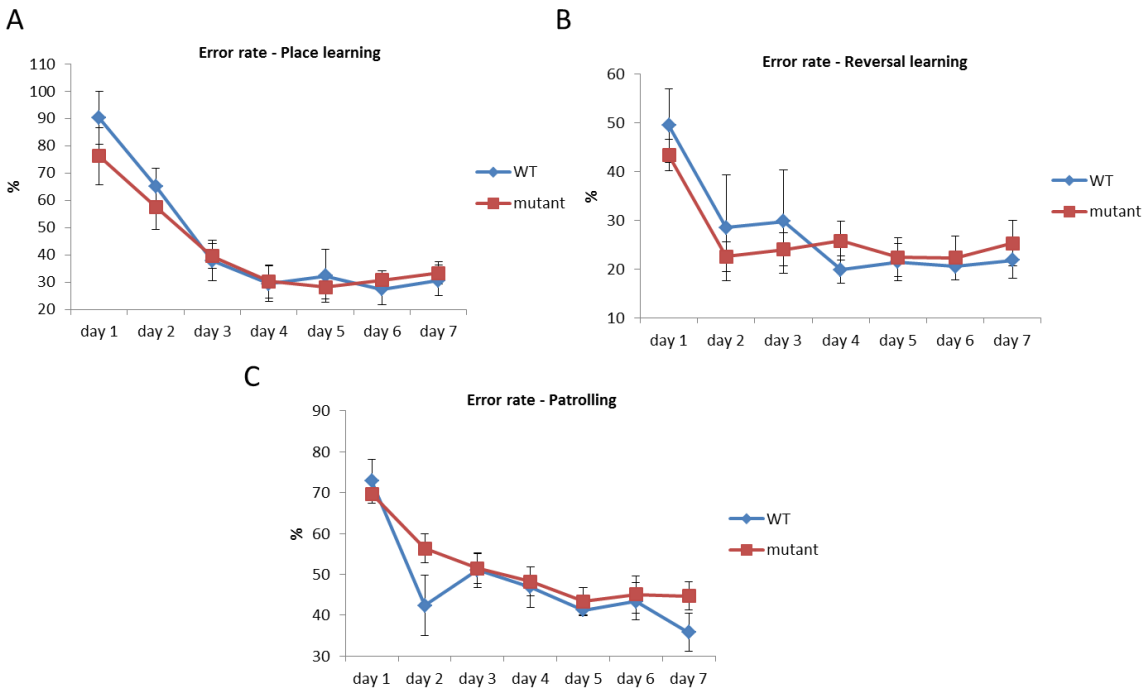

Fig. 22: IntelliCage system. A significant difference could be detected neither for place learning (A), nor for reversal learning (B), nor for patrolling (C) in 20 months old female mutants compared to controls.

6.4.3 Phenotypic analysis in the German Mouse Clinic

Due to unexpected differences between hTDP-43^{A315T}Rosa+/- mice and controls, regarding the body weight (see Fig.17) a cohort of mice was transferred to the German Mouse Clinic (GMC) to obtain more detailed information about their constitution. Subsequently, only results from the GMC with significant genotypic differences are listed.

6.4.3.1 Behavioral analysis

In the behavioral screen mutants were tested in open field and accelerating rotarod compared to controls (Fig.23). The analyses were performed under supervision of Dr. S. Hölter-Koch or Dr. L. Becker. In the open field, male mutants exhibited decreased locomotor activity compared to male controls with an opposite effect in the female mutants (Fig.23B). The same was found for the rearing activity. Decreased rearing activity detectable for male mutants with opposite effect for female mutants compared to wildtype littermates (Fig.23A). There were no significant genotype effects on anxiety-related behavior such as

center time and center distance (data not shown).

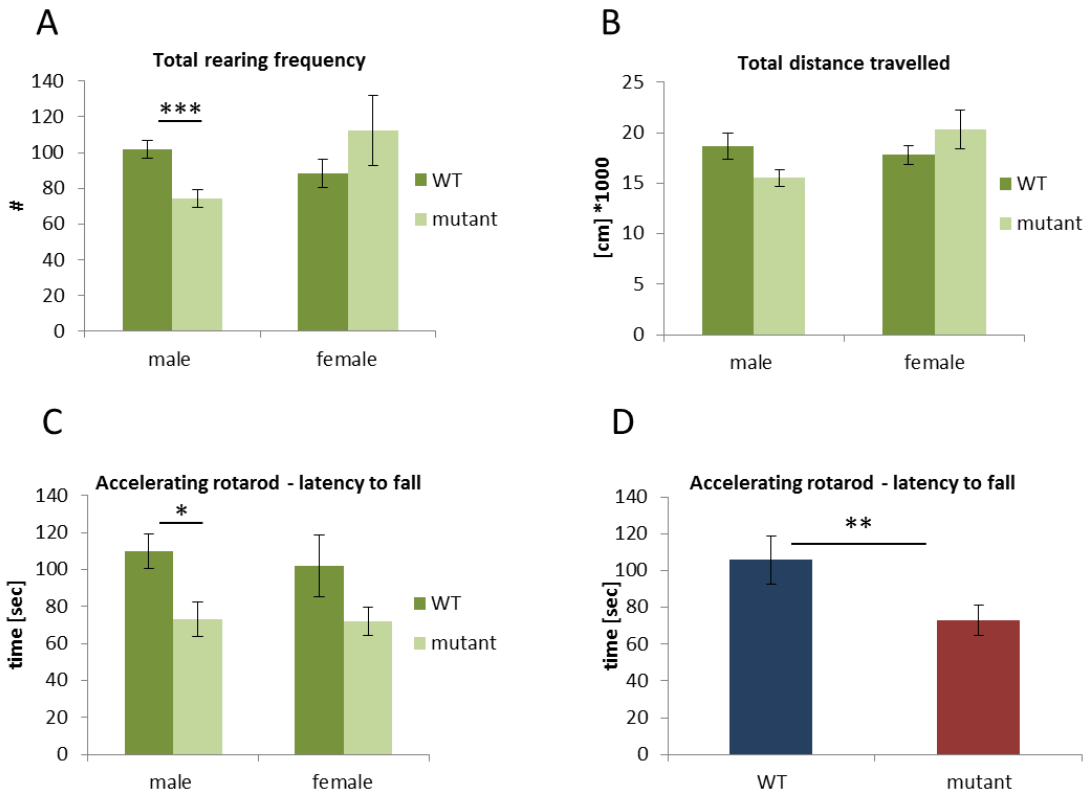

Fig. 23: Behavioral analyses of 5 months old hTDP-43^{A315T}Rosa+/- mice compared to controls in the GMC. (A-B) Open field analysis of mutants revealed significant decreased rearing activity in males with an opposite effect in females (A). The total distance travelled was decreased in male mutants with an opposite effect in female mutants (B). (C-D) In the accelerating rotarod male mutants showed an elevated tendency to fall from the rod, female mutants had a trend to decreased time spent on the rod (C). Pooled data of male and female mice displayed a significant genotype effect (D) (* = t-test, $P < 0.05$; ** = t-test, $P < 0.01$; *** = t-test, $P < 0.001$).

To check motor coordination, ten mice per sex and genotype were tested in the accelerating rotarod. Interestingly, male and female mutants exhibited increased tendency to fall from the rod compared to wildtype littermates (Fig.23C-D).

6.4.3.2 Clinical Chemistry

In the clinical chemistry screen ten mice per sex and genotype were tested for the following parameters: fasted blood lipid values, clinical-chemical analysis and hematology. All tests were accomplished under supervision of Dr. B. Rathkolb. Analysis of blood plasma samples were performed using *ad libitum* fed and overnight fasted mutant and wildtpye mice. Significant genotype related differences were detected in total cholesterol levels of overnight fasted and *ad libitum* fed male mice. In fed male mutants the total cholesterol

level was increased compared to controls, while it was decreased in fasted male mice. Triglyceride levels were found to be decreased in female fasted animals compared to wildtype littermates (Fig.24A). Glucose levels were slightly increased in the group of *ad libitum* fed mice, for both males and female mutants.

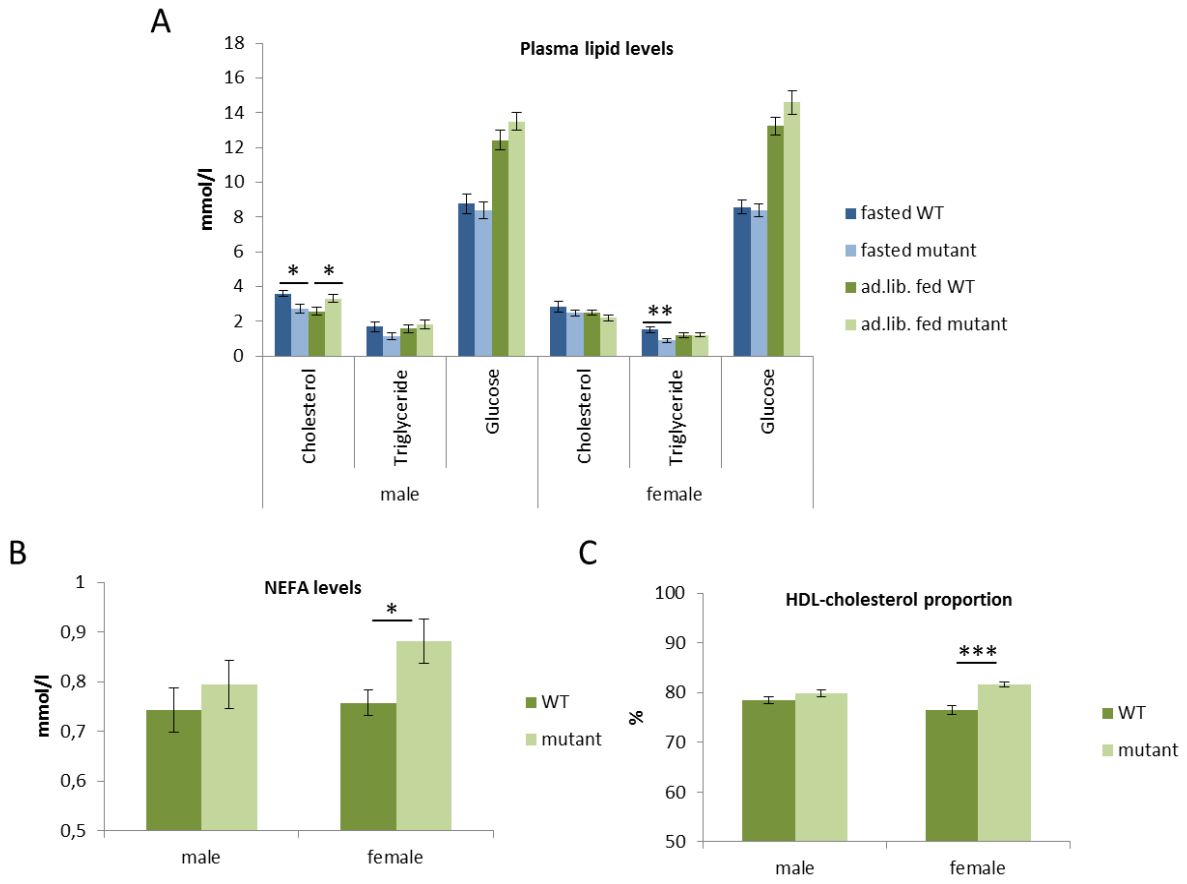

Fig. 24: Analyses of blood plasma samples in the GMC. (A) Significant changes in cholesterol levels of *ad libitum* and fasted male mice. Reduction of triglyceride levels in fasted females. Both sexes displayed elevated glucose level under normal breeding conditions. (B) The amount of non-esterified fatty acids (NEFA) was increased in fasted female mutants compared to controls. (C) The ratio of HDL- to total cholesterol was raised for females (* = t-test, $P < 0.05$; ** = t-test, $P < 0.01$; *** = t-test, $P < 0.001$).

Additionally, significantly increased non-esterified fatty acids (NEFA) were detected for fasted female mutants (Fig.24B). The ratio of HDL cholesterol to total cholesterol was significantly elevated in fasted females compared to controls, indicating a reduction of non-HDL cholesterol in this group (Fig.24C). These results suggest that the mutants either have a problem with lipid recovery or their energy input is higher as compared to controls.

6.4.3.3 Gene expression analysis

In order to identify candidate genes, whose expression is changed in the hTDP-43^{A315T}Rosa+/- mice a global gene expression study was performed at the institute of experimental genetics under supervision of Dr. M. Horsch. For this purpose, RNA was isolated from total brain samples and analyzed on a microarray chip. The microarray chip contained samples of >46.000 different transcripts covering the entire murine transcriptome. The 10 most differentially expressed genes are listed in table 5. The complete list with all 50 genes, whose expression profile was significantly altered, can be found in the appendix (see 9.3.3). In general, genes were down-regulated in mutants.

#	gene symbol	gene name	mean ratio
1	Lhx1	LIM homeobox protein 1	2,06
2	Eno1	enolase 1, alpha	1,65
3	Masp2	mannan-binding lectin serine peptidase 2	2,62
4	Klk1b22	kallikrein 1-related peptidase b22	-5,38
5	Actc1	actin, alpha	-2,47
6	Myl3	myosin, light polypeptide 3	-2,94
7	Mup1	major urinary protein 1	-2,55
8	Hoxb7	homeobox B7	-2,39
9	Myl2	myosin, light polypeptide 2	-2,77
10	Mup2	major urinary protein 2	-2,60

Tab. 5: Gene expression analysis of 12 months old brain samples revealed several genes, whose expression profile was altered in hTDP-43^{A315T}Rosa+/- mice compared to controls.

6.5 Effects of TDP-43 on putative targets

6.5.1 Effects of TDP-43 on expression level

Several TDP-43 targets were predicted by different publications (Polymenidou et al. 2010, Tollervey et al. 2010). Some of them were chosen to be analyzed in detail at the post-transcriptional level. In order to examine the mRNA expression level of putative TDP-43 targets, a semi-quantitative reverse transcription PCR (RT-PCR) and a quantitative real-time PCR (qRT-PCR) were performed. The qRT-PCR was examined using TaqMan® Gene Expression assays. Fus and progranulin (Grn) are known to be involved in sporadic and/or familiar forms of ALS and FTLD. The mRNA levels of Grn were unaffected in hTDP-43^{A315T}Rosa+/- mice compared to controls for both the RT- and qRT-PCR, while the Fus mRNA levels were increased in the RT-PCR (~ 20%) and unchanged for the more sensitive qRT-PCR (Fig.25). The decreased mRNA levels for Htt in the semi-quantitative RT-PCR could not be confirmed for qRT-PCR. In contrast, decreased expression levels were detected for the mRNA of Parkin (Park2) for both quantification methods. The mRNA expression level of Park2 was down-regulated of among 80% (Fig.25B) in mutants compared to wildtype animals.

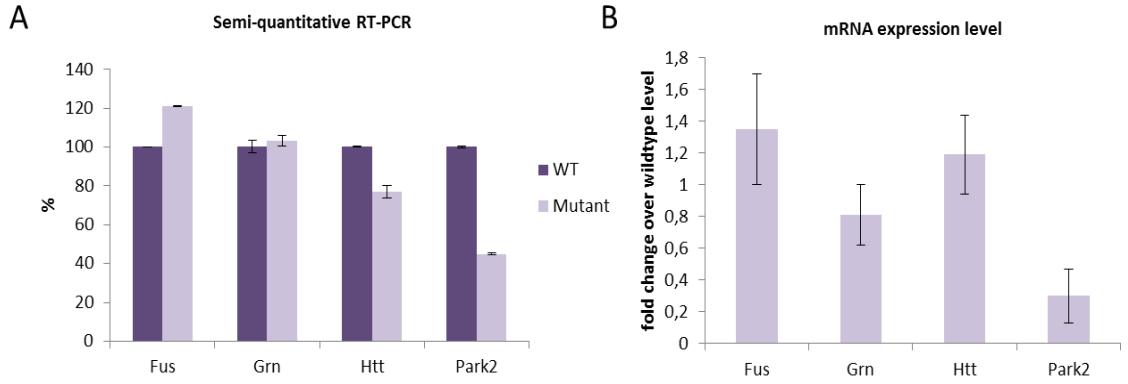

Fig. 25: Quantification of mRNA expression levels. (A) semi-quantitative RT-PCR of putative TDP-43 targets. Increased levels for Fus and decreased levels for Htt and Park2 were observed. No changes in the expression level of Grn. (B) Quantitative RT-PCR of putative targets revealed no changes in the expression levels of Fus, Grn and Htt. The expression level of Park2 was significantly affected.

Western blot analyses were performed additionally, to validate the results of the mRNA quantification. Brain lysates of three and 15 months old hTDP-43^{A315T}Rosa+/- and wildtype mice were prepared and incubated with the particular antibody to observe general and age-related changes in the protein expression levels (Fig.26). The protein levels of Fus and Grn were comparable to controls (Fig.26A-B), coincident with the result for the mRNA levels. The

Htt level was found unchanged (Fig.26C). The protein expression level of Parkin was 70% down-regulated in agreement with mRNA quantification (Fig.26D).

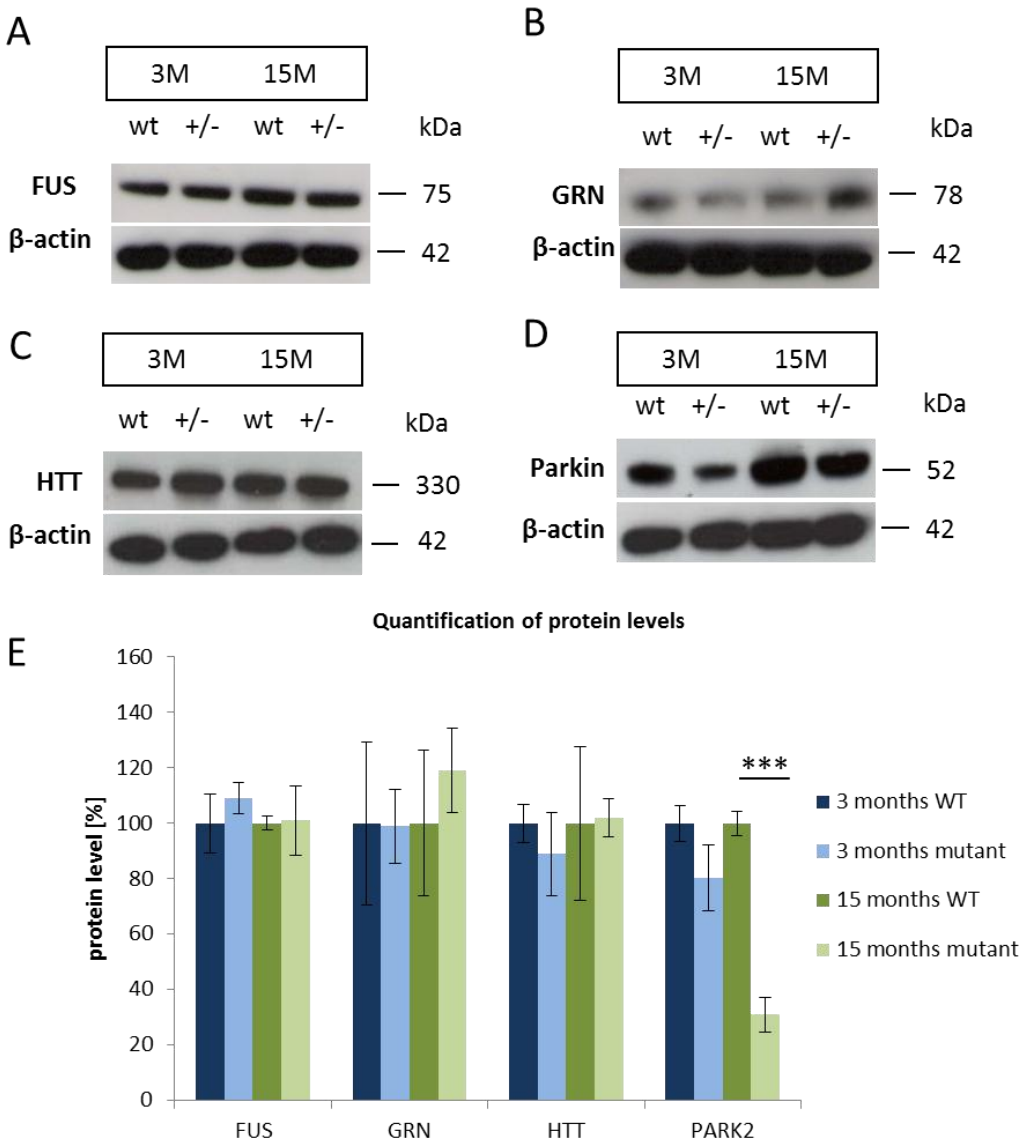

Fig. 26: Protein level quantification of putative TDP-43 targets. (A-D) Western blot analyses of 3 and 15 months old mutants compared to controls. No changes for FUS (A), GRN (B) and HTT (C) levels detectable. In old mutants the amount of Parkin protein is significantly reduced (D). (E) Quantification of western blots (*** = t-test, $P < 0.001$).

In order to check whether the decreased Parkin expression has an effect on CD36, a new target of Parkin described by Kim et al. (2011), liver lysates of 3 and 15 months old mice were analyzed for their protein expression (Fig.27A). Indeed a significant reduction of CD36 protein expression level was detected in old mutants. The protein level was approximately 50% down-regulated compared to controls. These data indicate an involvement of TDP-43 in

fat metabolism as CD36 is a fatty acid translocase and is probably implicated in fatty acid metabolism and associated abnormalities.

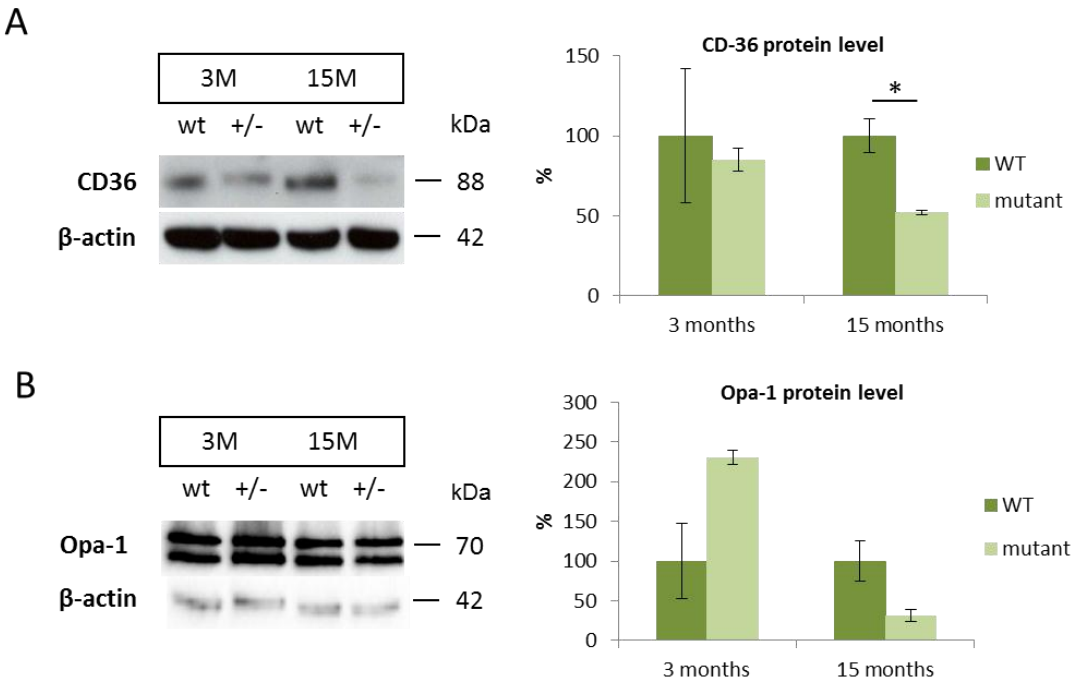

Fig. 27: Western blot analyses and quantification of CD36 and Opa-1. (A) Significant reduction of CD36 in liver lysates of 15 months old mutants compared to controls. (B) Brain lysates of 3 and 15 months old mutants compared to controls revealed a high tendency towards increased Opa-1 in young and decreased Opa-1 in old mutants (* = t-test, $P < 0.05$; trend = t-test, $0.1>P<0.05$).

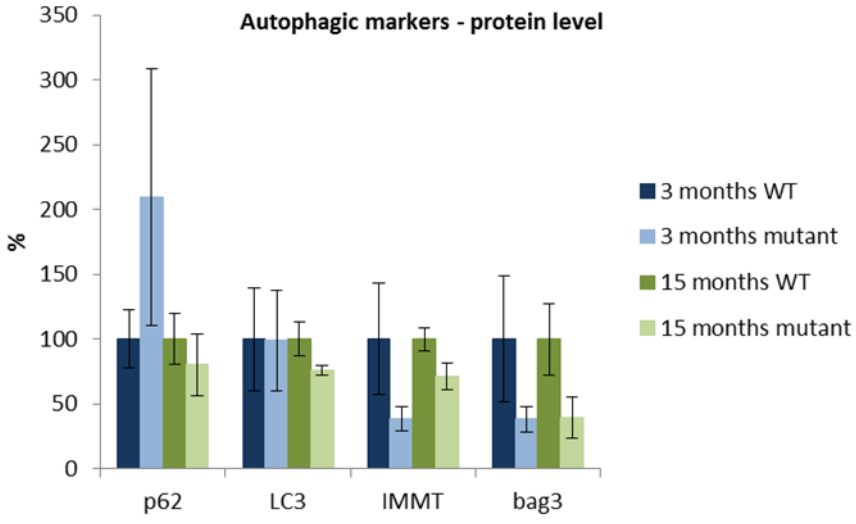

Fig. 28: Western blot analyses showed no significant changes in the protein level of autophagic markers. The marker bag3 revealed a trend for a decreased protein level in young and old mutants compared to controls (trend = t-test, $0.1>P<0.05$).

In addition, several autophagic and mitochondrial markers were analyzed in order to reveal abnormalities in autophagy or mitochondrial function and/or morphology (in collaboration

with A. Reichert). No alterations in the protein expression levels were detectable for autophagic/mitochondrial markers including p62, LC3, BAG3 and IMMT (Fig.28). Only for bag3 a trend towards decreased protein level was observed in young as well as in old mutants compared to controls.
Interestingly, the optic atrophy 1 (OPA-1), a protein involved in mitochondrial morphology, was found to be increased in 3 months old mutants and in contrast decreased in 15 months old mutants indicating dysfunction of the highly dynamic fission and fusion process of mitochondria (Fig.27B).

6.5.2 Effects of TDP-43 on alternative splicing

Polymenidou et al. (2010) claimed that TDP-43 mediates alternative splicing of mRNA targets. To detect alternatively spliced mRNAs in mutants, a semi-quantitative reverse transcription PCR was performed using primers for following targets: Dst, Dclk1, Kcnip2, Kncd3, Sema3F and Sort1. The ratio of exon inclusion to exon exclusion was calculated for hTDP-43^{A315T}Rosa+/- and control animals using brain samples (Fig.29). No splicing alterations were observed of selected RNAs, neither for exon inclusion nor for exon exclusion.

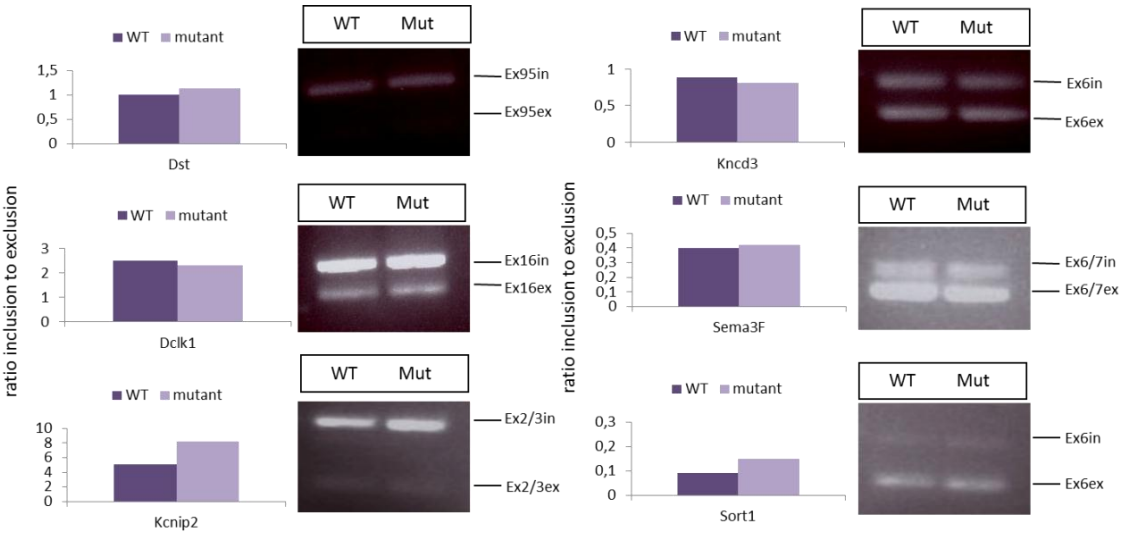

Fig. 29: Semi-quantitative RT-PCR analysis of selected RNA targets. No changes in the ratio of exon inclusion to exon exclusion in mutants compared to controls. Representative gel pictures of RT-PCR products from wildtype and mutant brain samples were quantified using ImageJ.

6.6 Cloning of hTDP-43^{x}3'UTR vectors

6.6.1 Splicing variants of TDP-43 3'UTR

TDP-43 regulates itself negatively through a feedback loop by binding to its own 3'UTR sequence (Polymenidou et al. 2010, Ayala et al. 2010). Due to this finding, vectors were created containing 3'UTR sequence instead of the BGH polyA sequence together with human wildtype or mutant TDP-43 cDNA. For cloning of the TDP-43 3'UTR, a rapid amplification of 3' ends was performed using brain sample of control animals (Fig.30A). Interestingly, two splicing variants were detected with a size of 828bp and 247bp. After sequencing and alignment with a predicted 3'UTR sequence (ensemble data base), accordance of 785bp was detected for splicing variant 1 and of 202bp for splicing variant 2 (Fig.30B). Moreover, a putative TDP-43 binding site (TDPBR) could be identified in the spliced region predicted by Ayala et al. (2010). The splicing product of 828bp was used for further cloning reactions.

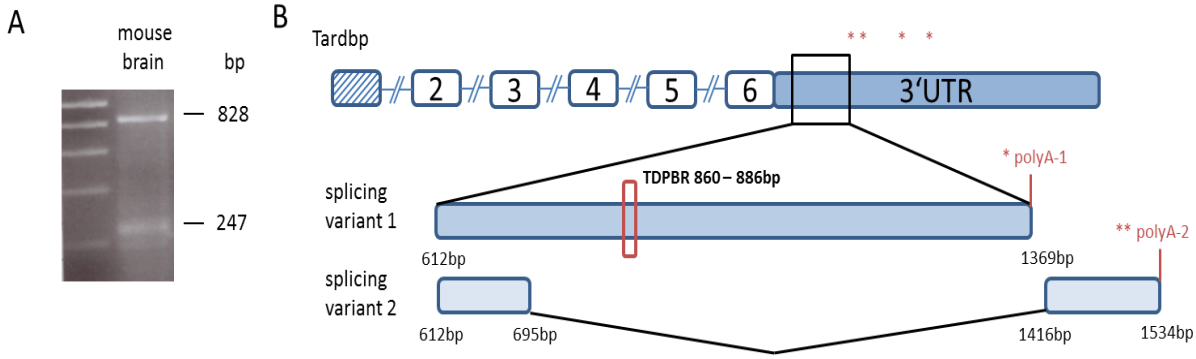

Fig. 30: 3'RACE of brain samples revealed two splicing variants for the mouse TDP-43 3'UTR. (A) Representative gel picture from the 3'RACE displayed a band at 828bp and 247bp for mouse RNA. (B) Illustration of TDP-43 3'UTR splicing variants. Putative TDP-43 binding region (TDPBR) is boxed in red. Putative polyA signals are presented by red stars.

6.6.2 Construction of hTDP-43^{x}3'UTR vectors

To generate ES cells expressing human TDP-43 cDNA together with the 3'UTR sequence under control of the endogenous promoter, the BGH polyA sequence was replaced by TDP-43 3'UTR. For this purpose, the 828bp 3'UTR sequence was cloned into a pCR®II-TOPO vector and first digested with SpeI, blunted and afterwards digested with XbaI. Vectors containing human TDP-43 cDNA (pENTR-hTDP-43) were opened with SacI, blunted and additionally digested with XbaI to get rid of BGH polyA. The opened pENTR-hTDP-43 vectors and the

digested 3'UTR sequence were ligated and plasmids were transformed into DH5α competent bacteria. Ampicillin resistant clones were screened by digestion of the plasmids with EcoRI, where the vectors with successfully inserted 3'UTR showed four bands (2.5kb, 1.1kb, 750bp and 60bp) and the pENTR-hTDP-43 vectors displayed only a linear band (4kb). Afterwards, the successfully cloned plasmids containing hTDP-43 cDNA and mouse 3'UTR, were used for Gateway® reaction into a destination vector (pEX-Dest) and electroporated into the gene trap clone E304C05 (see Tab.3-4).

7 Discussion

TDP-43 was found to be one of the major proteins aggregating in ALS and FTLD (Neumann et al. 2006). Several mutations were identified in the gene *TARDBP* encoding for TDP-43 in ALS and FTLD patients. The majorities of these mutations are located in the conserved C-terminal glycine-rich region and are dominant missense mutations. The C-terminal domain of TDP-43 was reported to be involved in protein-protein interactions. To date it is unclear whether the TDP-43 neuronal inclusions are the trigger or a consequence of the neurodegenerative diseases. Moreover, until now it is under consideration if the nuclear clearance of TDP-43 and the cytoplasmic aggregation lead to a toxic-gain-of-function in the cytoplasm or a loss-of-function in the nucleus.

7.1 Generation of hTDP-43^{A315T} animals

In order to investigate the effects of a human ALS causative TDP-43 point mutation (A315T), I generated a mouse model expressing the human mutant cDNA under control of the endogenous Tardbp promoter. For this purpose, a new protocol for efficient FLP-mediated RMCE in gene trap ES cell clones was used established by Schebelle et al. (2010). After successful germline transmission, mice were crossed with Rosa26Cre animals to initiate ubiquitous expression of the human mutant TDP-43 protein. Arising pups were used to investigate correct expression of the human cDNA. I could show that only pups having an excision of the hygromycin selection cassette expressed the human TDP-43 cDNA under control of the endogenous promoter (Fig.6). Despite numerous attempts, I was unable to generate mice expressing the human wildtype TDP-43 cDNA under control of the endogenous promoter. Therefore, another gene trap clone with a similar insertion of the retroviral SA-βgeo-pA vector in the first intron of the Tardbp mouse locus was used in order to achieve germline transmission.

Due to the fact that the inserted hygromycin cassette was flanked by loxP sites, also conditional expression of the human TDP-43 cDNA should be possible. For this purpose, mice were bred to Nestin-Cre animals (Tronche et al. 1999) leading to an expression of human TDP-43 in the central nervous system only (Fig.7). Because of no obvious phenotype for heterozygous hTDP-43^{A315T}Rosa animals the conditional expression was not necessary in this

study. In summary, the FLP-mediated RMCE in combination with gene trap clones is a useful tool to generate mouse models expressing any sequence under control of the appropriate promoter.

7.2 TDP-43 expression level

7.2.1 Overexpression of human TDP-43 in mutants

Homozygous loss of TDP-43 was shown to result in perinatal lethality between E3.5 – E7.5 (Wu et al. 2010, Sephton et al. 2010) indicating an essential role of TDP-43 for early embryonic development. Even a postnatal deletion of TDP-43 using a tamoxifen-inducible mouse model resulted in rapid lethality (Chiang et al. 2010). In addition, an overexpression of either wildtype or mutant TDP-43 *in vivo* led to enhanced toxicity (Wegorzweska et al. 2009, Stallings et al. 2010, Xu et al. 2010). Despite the expression of human TDP-43 under control of the endogenous promoter elevated TDP-43 levels (~ 3-fold) were observed already in younger animals (Fig.9). After performing a quantitative real-time PCR, a reduction of mouse TDP-43 of 80% was observed while the human TDP-43 isoform was up-regulated to about 3-fold (Fig.10). The increase in human TDP-43 could not only be detected in brain but also in other tissues (spleen, kidney and liver) (Fig.9). In addition, neither homozygous adults nor homozygous embryos could be observed indicating embryonic lethality between E3.5 and E7.5 before gastrulation. These results for embryonic lethality indicate toxicity because of the high TDP-43 levels. Beyond that a down-regulation of endogenous TDP-43 mRNA and protein was reported for mouse models overexpressing exogenous TDP-43 (Igaz et al. 2011, Xu et al. 2010). Taken together these data all indicate that the expression level of TDP-43 is tightly regulated during embryogenesis as well as in adulthood.

7.2.2 Involvement of the 3'UTR

After generating hTDP-43^{A315T} animals, it was published that TDP-43 regulates itself through a negative feedback loop by binding on its own 3'UTR (Ayala et al. 2010, Polymenidou et al. 2010). To clarify whether the missing 3'UTR or the inserted mutation is responsible for the increased TDP-43 levels, new vectors were cloned containing mouse 3'UTR instead of the

BGH polyA. In order to clone the mouse 3'UTR, RNA was isolated out of wildtype mouse brain and used for a 3'RACE which revealed two splicing variants of the 3'UTR (Fig. 30), a strong unspliced 828bp band, referred to as splicing variant 1, and a weaker spliced 247bp band, referred to as splicing variant 2. The 828bp band, was used for further cloning reactions. The newly generated vectors were used for FLP-mediated RMCE and successful exchanged ES cell clones were injected into blastocysts. Currently the arising chimeras are bred to C57Bl6/J females to achieve germline transmission.

Meanwhile an *in vitro* study was performed showing that ES cells expressing either wildtype or mutant TDP-43 together with mouse 3'UTR under control of the endogenous promoter had an expression level comparable to unaffected ES cells. ES cells expressing either wildtype or mutant TDP-43 together with BGH polyA revealed elevated TDP-43 levels comparable to the mutant mice (Stribl et al. unpublished). These data indicate that the 3'UTR is essential to control TDP-43 level *in vitro* and *in vivo* and that the mutation A315T is not involved in the abnormal regulation of the protein. However, a slight increase for TDP-43 protein level was determined in cells expressing the mutant human cDNA with or without 3'UTR indicating that the mutation has some influence on the expression level respectively on the degradation of the mutant protein.

The mechanisms involved in the autoregulation of the protein are still unclear. TDP-43 binding sites were found in the 3'UTR of the TDP-43 pre-mRNA (Ayala et al. 2010, Polymenidou et al. 2010). Polymenidou et al. (2010) claimed that this binding leads to an alternatively spliced 3'UTR with a premature termination codon which causes the degradation of the mRNA by nonsense-mediated decay (NMD). This mechanism was also shown to be involved in the autoregulation of several other RNA-binding proteins (Rossbach et al. 2009, Wollerton et al. 2004, Sureau et al. 2001). In agreement with the data published by Polymenidou et al. (2010), splicing variant 2 was present at very low levels and revealed splicing of a 732bp long fragment containing a putative TDP-43 binding site (Fig.30). This indicates that the 247bp 3'UTR fragment is a substrate for NMD.

In contrast, Ayala et al. (2010) showed that TDP-43 autoregulation is may be associated with the exosome complex. However, they also found mRNA isoforms which were regulated by NMD. An alternative hypothesis was brought up by Yu et al. (2012) who demonstrate that TDP-43 associates with FMRP and STAU1 to regulate SIRT1 mRNA and that depletion of any one of these proteins resulted in destabilization of SIRT1 mRNA. In addition, STAU1 was

found to mediate mRNA decay by binding to 3'UTRs via Alu elements (Gong and Maquat 2011). In applying this to the autoregulation of *TARDBP*, an overexpression of TDP-43 would further stabilize the *TARDBP* transcript, which is in contrast to the results of the hTDP-43 mouse model.

Interestingly, a mutation in the 3'UTR of an ALS and FTLD-MND patient resulted in a two-fold increase of TDP-43 thereby indicating an essential role of the 3'UTR also in humans (Gitcho et al. 2009). A dysfunction in the negative feedback loop of TDP-43 could contribute to TDP-43 pathology in neurodegenerative diseases as a primary or secondary pathological feature with or without TDP-43 mutations. Once TDP-43 is sequestered to the cytoplasm, due to protein modification, cellular stress or modified binding partners, the absence of TDP-43 in the nucleus would activate the autoregulation and thereby elevate the levels of TDP-43. The increase in protein level could lead to an overstrained degradation mechanism and thus promote the formation of insoluble aggregates as it was the case for hTDP-43^{A315T} mice. To understand the exact mechanism of the negative feedback loop and the associated machinery would be of great importance to develop therapeutic approaches.

7.3 Phenotypic changes in hTDP-43^{A315T}Rosa mice

As mentioned (see 3.2.4) ALS and FTLD patients show a characteristic TDP-43 pathology. The clearance of TDP-43 from the nucleus and its mislocalization to the cytoplasm followed by abnormal cleavage in C-terminal fragments, hyper-phosphorylation at several serine residues, and the ubiquitination of the protein and the formation of insoluble inclusions (Neumann et al. 2006) are characteristic features in the course of the disease. The degeneration of neurons and glial cells leads to muscle weakness and spasticity or behavioral and language dysfunctions. However, none of the generated mouse models to date were able to mimic all the characteristic features of ALS/FTLD. In this work, I used the hTDP-43^{A315T}Rosa mouse to study the role of mutant TDP-43 during development and its possible involvement in neurodegenerative disease.

7.3.1 Pathological and biochemical profile

To check for the presence of insoluble TDP-43 inclusions in mutant mice, paraffin sections and detergent-insoluble protein fractions were performed. The western blot analysis revealed detergent-insoluble TDP-43 in mutants but not in controls with increasing level the older the animals were (Fig.11). For the immunohistochemical stainings I could detect neuronal cytoplasmic TDP-43 inclusions in the brain primarily in the motor cortex and in the anterior horn of the spinal cord. The results demonstrate that the expression of the mutant TDP-43 protein has an effect on its localization and solubility. Furthermore this mouse model is one of the first displaying the existence of insoluble TDP-43 protein as it is detectable in ALS/FTLD patients. Interestingly, increased TDP-43 levels were found in brain, spleen, kidney and liver, insoluble TDP-43, however, could only be discovered in brain but not in any other tested tissue (Fig.11). This shows that (1) the formation of insoluble TDP-43 is independent of elevated TDP-43 levels and (2) the mechanisms involved in the formation of insoluble TDP-43 are restricted to the central nervous system while other cell types remain unaffected.

TDP-43 is considered to be disposed by the ubiquitin-proteasome system (UPS), consistent with the ubiquitination of TDP-43 in ALS and FTLD patients and the ubiquitination of overexpressed TDP-43 in transgenic mice (for review see Lee et al. 2011). We asked whether ubiquitinated TDP-43 would be also present in hTDP-43^{A315T}Rosa mice. Ubiquitin inclusions could be found in brain and spinal cord sections of one year old mutants (Fig.13). While only a slight staining for ubiquitin was detectable in wildtype littermates, the staining was much stronger in mutants. Furthermore, some neurons revealed nuclear clearance of TDP-43 and the formation of TDP-43 inclusions in the cytoplasm. These inclusions overlapped with ubiquitin in the brain cortex and anterior horn of the spinal cord (Fig.14). While ubiquitinated inclusions are a common feature in TDP-43 mouse models, the inclusions rarely or never included TDP-43 itself (Wegorzewska et al. 2009, Xu et al. 2011, Xu et al. 2010). Given the facts I could show that there is an ubiquitination of TDP-43 in hTDP-43^{A315T}Rosa mice for all TDP-43 inclusions (Fig. 14). These results recapitulate the TDP-43 pathology found in ALS and FTLD patients (Neumann et al. 2006).

To investigate the hyper-phosphorylation and C-terminal cleavage of TDP-43, custom-made antibodies were used in western blot analyses (kindly provided by E. Kremmer). I could

neither detect a hyper-phosphorylation of TDP-43 (Fig.15) nor the development of C-terminal fragments (data not shown) in soluble and insoluble protein fractions. In contrast to the formation of TDP-43 inclusions and the ubiquitination of the protein mentioned above the two characteristic features of hyper-phosphorylation and C-terminal cleavage of TDP-43 could not be verified. In other mouse models C-terminal fragments were present but only in the detergent-soluble protein fraction (Wegorzewska et al. 2009, Wils et al. 2010, Xu et al. 2011, Swarup et al. 2011), in contrast to observations in human patients. This leads to the hypothesis that the detected C-terminal fragments are not a cause of TDP-43 pathology and are rather indicating proteolytic cleavage of full-length TDP-43, although splice variants or cryptic transcription start sites. Moreover, not all TDP-43 mouse models exhibit C-terminal fragments while showing similar neurodegenerative phenotypes, indicating that TDP-43-mediated neurodegeneration is independent of C-terminal fragments (Shan et al. 2010, Igaz et al. 2011). Concerning TDP-43 hyper-phosphorylation it is under consideration whether phosphorylation is a cause or effect of aggregation. As a matter of fact, cell culture studies revealed that phosphorylation of TDP-43 was not required for the development of C-terminal fragments and aggregation of the protein (Dormann et al. 2009, Zhang et al. 2009). These studies indicated that additional approaches are required to determine the effects of C-terminal fragments on the course of disease and the influence on normal TDP-43 function.

Neurodegenerative diseases are characterized by the loss of specific neurons in the central or peripheral nervous system which are unique for each disorder. For ALS, in particular upper and lower motor neurons are degenerated. This neurodegeneration leads to a devastating phenotype, including muscle weakness and spasticity. To investigate possible degeneration of motor neurons in the spinal cord of hTDP-43^{A315T}Rosa mice, paraffin sections were prepared and stained and motor neurons in the sciatic motor pool were counted. A significant reduction of 10% in the number of motor neurons was observed for three months as well as for 18 months old animals (Fig.16). This indicates that the loss of neurons is not due to neurodegeneration but it is more likely a developmental defect. Possible reasons could be that (1) the already high levels of human TDP-43 at an age of one month initiated the degeneration of neurons or (2) defects in the embryonic neurogenesis. To clarify this issue it would be important to investigate motor neuron development in embryos of various stages.

7.3.2 Behavioral analysis

In most of the behavioral motor tests, hTDP-43^{A315T}Rosa mice had a performance comparable to wildtype controls. For the gait analysis with the “CatWalk” system, various gait disturbances could be detected. Especially in the performance of diagonal coordination, mutants revealed abnormalities in diagonal coupling and phase dispersion (Fig.18). Interestingly, females seemed to be more affected than males. These data gave a hint to deficits in motor coordination as known for ALS patients.

However, in all other motor tests with 15 months old animals no more obvious deficits could be detected. Therefore, it would be interesting to test an older cohort of mice to see whether the problems with motor coordination worsen with age. Moreover, the missing phenotype could be attributed to the age of the tested animals. Younger mice are more interested in participation of behavioral test than older ones. However, because of the lack of motivation the realization of the tests was quite difficult and not comparable to younger mice. This could also explain the significant differences found in the accelerating rotarod performed in the GMC (Fig.23). For this approach five months old mutants and controls were tested and analyzed. In addition, a cohort of six months old animals had been checked previously in all motor tests and displayed significant abnormalities for the ladder and the gait analysis (see appendix 9.3.2). In summary, it can be suggested that young as well as old hTDP-43^{A315T}Rosa mice exhibit slight problems with motor coordination. This coincided with the reduction of motor neurons detected in younger animals and the conclusion that the decrease in motor neurons is not age-related.

A small group of ALS patients is known to develop a form of dementia as well as a quarter of FTLD patients show evidence of motor neuron disease, which interconnects the two neurodegenerative diseases ALS and FTLD (Lillo and Hodges 2009). To investigate possible cognitive impairments in this mouse model, different memory tests were performed with 15 months old animals. In all of the memory tests, hTDP-43^{A315T}Rosa mice behaved comparable to wildtype controls. Only in the y-maze, a test for working memory, female mutants revealed a trend towards more same arm returns (SARs) compared to controls. For the object recognition test and the IntelliCage no obvious differences were detectable.

In summary, hTDP-43^{A315T}Rosa mice showed no cognitive impairments which is consistent with the data of Gitcho et al. (2008) presenting a family with the mutation A315T. This

family, suffering on MND, displayed a slow progression of the disease with no cognitive impairments.

7.4 TDP-34 and its targets

7.4.1 TDP-43 and alternative splicing

TDP-43 is known to promote exon 9 skipping of the cystic fibrosis transmembrane conductance regulator (CFTR) (Buratti et al. 2001), exon 7 inclusion of the SMN2 gene (Bose et al. 2008) and alternative splicing of SKAR (Fiesel et al. 2012). Other studies using high-throughput sequencing of RNA isolated by crosslinking immunoprecipitation (HITS-CLIP) identified a large amount of RNA species with binding sites for TDP-43, mainly located to introns, 3'UTRs and non-coding RNAs (Polymenidou et al. 2010, Tollervey et al. 2010). Furthermore, these TDP-43 binding sites were enriched around exons with evidence of either alternative exon inclusion or exon exclusion. After TDP-43 knockdown in the striatum of mouse brains about 203 exons were identified revealing alternative exon inclusion or exclusion (Polymenidou et al. 2010). Some of the TDP-43 targets for alternative splicing from this study were analyzed in the hTDP-43^{A315T}Rosa mouse model. After RNA isolation a semi-quantitative RT-PCR was performed and the ratio of inclusion to exclusion was determined. As it appeared in this mouse model alternative splicing seemed to be unaffected (Fig.29). The analysis underlined that the mutant protein, which comprises approximately 90% of all TDP-43 in this mouse, can entirely perceive the splice function of TDP-43. This could be explained by the fact that these mice show an overexpression of TDP-43 while RNAs of knockdown tissues were used for the iCLIP analysis. However, before generalizing these results of alternative splicing further analyses of more putative TDP-43 splice targets are necessary.

7.4.2 TDP-43 and gene expression

As mentioned in the introduction, one of the TDP-43 functions is the regulation of gene transcription. To identify new genes regulated by TDP-43 a microarray analysis was performed using RNA of one year old hTDP-43^{A315T}Rosa and control animals. About 50 genes were determined that were differentially expressed in mutants (Tab.5 and appendix 9.3.3). Three of them were up-regulated while all other identified genes were significantly decreased indicating that 3-fold overexpression of TDP-43 negatively effects gene regulation. An interesting finding was the gene Lhx1 (LIM homeobox protein 1), which is known to be involved in the development of the spinal cord by coordinating motor neuron migration (Palmesino et al. 2010). The abnormal regulation of Lhx1 could be an explanation for the decreased number of motor neurons found in 3 and 18 months old mutants.

Another gene determined with the microarray analysis was Mup1 (major urinary protein 1). Mup1 is a regulator of lipid and glucose metabolism in mice (Zhou et al. 2009) thereby links TDP-43 to the results of the clinical chemistry study and to the reduced body weight in mutants. To verify the results obtained from the microarray analysis, quantitative real-time PCRs have to be performed for each abnormal regulated gene. Additionally, all determined genes are analyzed using bioinformatical tools to find out whether genes cluster in particular pathways that are of importance in the onset and course of the disease.

7.5 Involvement of TDP-43 in lipid metabolism

TDP-43 was found to preferentially bind to UG-rich repeats of single-stranded RNA. In the last years several putative mRNA targets of TDP-43 were identified containing such UG-rich binding sites including *Fus*, *Progranulin*, *Parkin*, *Htt*, *Hdac6* and *Mapt* RNA (Polymenidou et al. 2010, Tollervey et al. 2010). Some of them were used to analyze their mRNA and protein levels. RNA and protein brain samples of hTDP-43^{A315T}Rosa and control animals were used in semi-quantitative RT-PCR, quantitative real-time PCR and western blotting. The expression levels of *Fus*, *Grn* and *Htt* mRNAs were unchanged as well as the protein levels in heterozygous mutants. Interestingly, *Parkin* mRNA was 80% down-regulated as well as the protein (Fig.25,26). Mutations in the Parkin gene (*PARK2*) cause autosomal recessive, juvenile-onset Parkinson disease (PD) (Kitada et al. 1998). Kim et al. (2011) claimed that

Parkin is lipid-dependent regulated and modulates fat uptake in mice and human cells linking lipid metabolism to neurodegenerative diseases.

The loss of body weight is a feature frequently observed in ALS patients and its cause range from reduction in skeletal muscle mass to abnormal lipid metabolism (Funalot et al. 2009, Dupuis et al. 2004). In the mouse model hTDP-43^{A315T}Rosa a reduction of body weight in males and females was determined. Male mutants showed significant less body weight at all stages of life compared to wildtype animals, while a significant loss of body weight for female mutants was only detectable in old animals (Fig.17). In order to investigate this phenotype in detail, blood plasma samples were analyzed for several lipid parameters of 5 months old mutants compared to controls (Fig.24). The animals were either fed *ad libitum* or fasted overnight. For male fasted mice a significant reduction in cholesterol was detected. The opposite effect was observed for *ad libitum* fed mice which showed an increase in cholesterol level. In addition, a slight decrease in triglyceride was found for male fasted mice. Overnight fasted female mutants revealed a significant reduction in triglyceride level. In the group of *ad libitum* fed mice for both sexes the glucose levels were slightly increased. Furthermore, fasted female mutants revealed significant changes in NEFA levels and in the ratio of HDL cholesterol to total cholesterol.

All these data indicate that hTDP-43^{A315T}Rosa mice have problems with lipid metabolism which corresponds to recent studies in ALS patients. A different ALS mouse model with a mutation in SOD1 showed a similar phenotype (Kim et al. 2011). After a fasting period of six hours, mice were tested for cholesterol, LDL, HDL/LDL ratio and glucose levels. Mutant mice revealed a decrease in cholesterol, LDL and HDL/LDL ratio, while the serum glucose levels were unaffected. Basal serum cholesterol and LDL were lower in male but not in female ALS mice. Our findings are consistent with these data in the case of the occurrence of hypolipidemia in male mutant mice with no association to decreased serum glucose levels. But these findings are inconsistent with Dupuis et al. (2008) who showed hypermetabolism in patients with ALS. To gain more insight into the deregulation of fat metabolism for this mouse model a challenge by a high-fat diet could be useful.

The reasons for the abnormal lipid metabolism in animal models as well as in ALS patients have not been found yet. In this study, the PD-related protein Parkin was found to be down-regulated. Furthermore, a recently discovered target of Parkin, the fatty acid translocase CD36, was decreased in parallel to Parkin (Kim et al. 2011). The decrease of Parkin as well as

CD36 progressed with age, indicating an age-dependent phenotype (Fig.27A). CD36 is a member of the class B scavenger receptors which are high density lipoprotein receptors (Acton et al. 1996). Several studies showed that CD36 mediates the uptake of high density lipoproteins *in vivo* and *in vitro* (Brundert et al. 2011) and is involved in fatty acid oxidation (McFarlan et al. 2012). These studies indicate that Parkin plays a role in lipid metabolism by affecting the level of CD36 and thereby introduce a metabolism phenotype in hTDP-43^{A315T}Rosa mice.

7.6 TDP-43 and mitochondrial function

Parkin, an E3 ubiquitin ligase, is encoded by the gene *PARK2* (Shimura et al. 2000). Mutations in PARK2 are involved in autosomal recessive-juvenile Parkinson's disease, a widespread neurodegenerative disorder affecting dopaminergic neurons in the midbrain leading to progressive movement dysfunctions (Kitada et al. 1998). Parkin was found to be dramatically down-regulated in mice overexpressing mutant human TDP-43 cDNA (Fig.26). Parkin mediates ubiquitination and thereby tags substrates for proteasome-dependent degradation (Shimura et al. 2000, Zhang et al. 2000). Therefore a loss of parkin function was thought to cause aggregation of proteins and thereby leading to neurodegeneration. Moreover, some studies indicate that Parkin is also meditating mono-ubiquitination, a non-proteolytic modification (Doss-Pepe et al. 2005, Hampe et al. 2006).

In addition to the ubiquitination of substrates, Parkin was found to play a role in the maintenance of mitochondrial integrity. Several studies claimed that Parkin acts along with PINK1, another PD-related protein, in mitochondrial quality control (Palacino et al. 2004, Ziviani et al. 2010). Damaged mitochondria in the cell are recognized and eliminated by Parkin through an autophagic process called mitophagy (Narendra et al. 2008). Several studies claimed a relationship between mitochondrial dysfunction and neurodegenerative diseases such as AD, PD and ALS (for review see Swerdlow 2011). Interestingly, the mitochondrial associated protein OPA-1 was abnormally regulated in mutant TDP-43 mice (Fig.27B). OPA-1 regulates mitochondrial fusion, a process for the recovery of damaged mitochondria (Cipolat et al. 2004). The level of OPA-1 was up-regulated in 3 months old mutants, but in contrast down-regulated in 15 months old mutants, indicating a deregulation of OPA-1 in mice expressing mutant hTDP-43. The elevated OPA-1 level in young animals

hypothesizes a tendency to more mitochondrial fusion, while the decrease in OPA-1 could promote more fission of mitochondria. However, these data are a hint to dysfunction of mitochondria in hTDP-43^{A315T}Rosa mice. This correlates with studies of patients with ALS documenting mitochondrial damage in motor neurons of the spinal cord and muscles (Sasaki and Iwata 1996, Siklos et al. 1996). Furthermore, abnormal mitochondrial morphology (aggregated, fragmented or swollen mitochondria) was detected in several cell and animal models of familial ALS (Jung et al. 2002, Raimondi et al. 2006, Xu et al. 2010, Coussee et al. 2011, Xu et al. 2011).

All these findings suggest that the down-regulation of Parkin in hTDP-43^{A315T}Rosa mice either leads to the accumulation of TDP-43 by loss of ubiquitination for the proteasome system or to mitochondrial dysfunction by abnormally regulated target genes of Parkin. To deepen the understanding, further approaches have to be performed with regards to the role of Parkin in ALS and the connection between TDP-43 and mitochondrial function.

8 References

Abramoff, M.D., Magelhaes, P.J., and Ram, S.J. (2004) Image Processing with ImageJ. *Biophotonics International 11*, 36-42.

Acton S., Rigotti A., Landschulz K. T., Xu S., Hobbs H. H., Krieger M. (1996) Identification of scavenger receptor SR-BI as a high density lipoprotein receptor. *Science* 271: 518–520.

Amador-Ortiz C, Lin WL, Ahmed Z, Personett D, Davies P, Duara R, Graff-Radford NR, Hutton ML, Dickson DW. (2007) TDP-43 immunoreactivity in hippocampal sclerosis and Alzheimer's disease. *Ann Neurol.* 61(5):435-45.

Arai T, Hasegawa M, Akiyama H, Ikeda K, Nonaka T, Mori H, Mann D, Tsuchiya K, Yoshida M, Hashizume Y, Oda T. (2006)TDP-43 is a component of ubiquitin-positive tau-negative inclusions in frontotemporal lobar degeneration and amyotrophic lateral sclerosis. *Biochem Biophys Res Commun* 351(3):602-611.

Ayala YM, Pantano S, D'Ambrogio A, Buratti E, Brindisi A, Marchetti C, Romano M, Baralle FE. (2005) Human, Drosophila, and C.elegans TDP43: nucleic acid binding properties and splicing regulatory function. *J Mol Biol* 348(3):575-588.

Ayala YM, Zago P, D'Ambrogio A, Xu YF, Petrucelli L, Buratti E, Baralle FE. (2008) Structural determinants of the cellular localization and shuttling of TDP-43. *J Cell Sci* 121(Pt 22):3778-3785.

Ayala YM, De Conti L, Avendaño-Vázquez SE, Dhir A, Romano M, D'Ambrogio A, Tollervey J, Ule J, Baralle M, Buratti E, Baralle FE. (2011) TDP-43 regulates its mRNA levels through a negative feedback loop. *EMBO J* 30(2):277-288.

Baker M, Mackenzie IR, Pickering-Brown SM, Gass J, Rademakers R, Lindholm C, Snowden J, Adamson J, Sadovnick AD, Rollinson S, Cannon A, Dwosh E, Neary D, Melquist S, Richardson A, Dickson D, Berger Z, Eriksen J, Robinson T, Zehr C, Dickey CA, Crook R, McGowan E, Mann D, Boeve B, Feldman H, Hutton M. (2006) Mutations in progranulin cause tau-negative frontotemporal dementia linked to chromosome 17. *Nature* 442(7105):916-919.

Benajiba L, Le Ber I, Camuzat A, Lacoste M, Thomas-Anterion C, Couratier P, Legallic S, Salachas F, Hannequin D, Decousus M, Lacomblez L, Guedj E, Golfier V, Camu W, Dubois B, Campion D, Meininger V, Brice A. (2009) TARDBP mutations in motoneuron disease with frontotemporal lobar degeneration. *Ann Neurol.* 65(4):470-3.

Bose JK, Wang IF, Hung L, Tarn WY, Shen CK. (2008) TDP-43 overexpression enhances exon 7 inclusion during the survival of motor neuron pre-mRNA splicing. *J Biol Chem*. 283(43):28852-9.

Brandmeir NJ, Geser F, Kwong LK, Zimmerman E, Qian J, Lee VM, Trojanowski JQ. (2008) Severe subcortical TDP-43 pathology in sporadic frontotemporal lobar degeneration with motor neuron disease. *Acta Neuropathol* 115(1):123-131.

Brundert M, Heeren J, Merkel M, Carambia A, Herkel J, Groitl P, Dobner T, Ramakrishnan R, Moore KJ, Rinninger F. (2011) Scavenger receptor CD36 mediates uptake of high density lipoproteins in mice and by cultured cells. *J Lipid Res.* 52(4):745-58.

Buratti E, Dörk T, Zuccato E, Pagani F, Romano M, Baralle FE. (2001) Nuclear factor TDP-43 and SR proteins promote in vitro and in vivo CFTR exon 9 skipping. *EMBO J* 20(7):1774-84.

Buratti E, **Baralle FE**. (2008) Multiple roles of TDP-43 in gene expression, splicing regulation, and human disease. *Front Biosci* 13:867-878.

Buratti E, De Conti L, Stuani C, Romano M, Baralle M, Baralle F. (2010) Nuclear factor TDP-43 can affect selected microRNA levels. *FEBS J* 277(10):2268-2281.

Chen YZ, Bennett CL, Huynh HM, Blair IP, Puls I, Irobi J, Dierick I, Abel A, Kennerson ML, Rabin BA, Nicholson GA, Auer-Grumbach M, Wagner K, De Jonghe P, Griffin JW, Fischbeck KH, Timmerman V, Cornblath DR, Chance PF. (2004) DNA/RNA helicase gene mutations in a form of juvenile amyotrophic lateral sclerosis (ALS4). *Am J Hum Genet* 74: 1128-1135.

Chen-Plotkin AS, Lee VM, Trojanowski JQ. (2010) TAR DNA-binding protein 43 in neurodegenerative disease. *Nat Rev Neurol* 6(4):211-220.

Chiang PM, Ling J, Jeong YH, Price DL, Aja SM, Wong PC. (2010) Deletion of TDP-43 down-regulates Tbc1d1, a gene linked to obesity, and alters body fat metabolism. *Proc Natl Acad Sci U S A* 107(37):16320-16324.

Chow CY, Zhang Y, Dowling JJ, Jin N, Adamska M, Shiga K, Szigeti K, Shy ME, Li J, Zhang X, Lupski JR, Weisman LS, Meisler MH. (2007) Mutation of FIG4 causes neurodegeneration in the pale tremor mouse and patients with CMT4J. *Nature* 448: 68-72.

Cipolat S, Martins de Brito O, Dal Zilio B, Scorrano L. (2004) OPA1 requires mitofusin 1 to promote mitochondrial fusion. *Proc Natl Acad Sci USA.* 101: 15927 – 15932.

Colombrita C, Zennaro E, Fallini C, Weber M, Sommacal A, Buratti E, Silani V, Ratti A. (2009) TDP-43 is recruited to stress granules in conditions of oxidative insult. *J Neurochem* 111(4):1051-61.

Coussee E, De Smet P, Bogaert E, Elens I, Van Damme P, Willems P, Koopman W, Van Den Bosch L, Callewaert G. (2011) G37R SOD1 mutant alters mitochondrial complex I activity, Ca(2+) uptake and ATP production. *Cell Calcium.* 49(4):217-25.

Cruts M, Kumar-Singh S, Van Broeckhoven C. (2006) Progranulin mutations in ubiquitin-positive frontotemporal dementia linked to chromosome 17q21. *Curr Alzheimer Res* 3(5):485-491.

Dormann D, Capell A, Carlson AM, Shankaran SS, Rodde R, Neumann M, Kremmer E, Matsuwaki T, Yamanouchi K, Nishihara M, Haass C. (2009) Proteolytic processing of TAR DNA binding protein-43 by caspases produces C-terminal fragments with disease defining properties independent of progranulin. *J Neurochem* 110(3):1082-1094.

Doss-Pepe EW, Chen L, Madura K. (2005) Alpha-synuclein and parkin contribute to the assembly of ubiquitin lysine 63-linked multiubiquitin chains. *J Biol Chem.* 280(17):16619-24.

Dupuis L, Oudart H, René F, Gonzalez de Aguilar JL, Loeffler JP. (2004) Evidence for defective energy homeostasis in amyotrophic lateral sclerosis: benefit of a high-energy diet in a transgenic mouse model. *Proc Natl Acad Sci U S A.* 101(30):11159-64.

Elden AC, Kim HJ, Hart MP, Chen-Plotkin AS, Johnson BS, Fang X, Armakola M, Geser F, Greene R, Lu MM, Padmanabhan A, Clay-Falcone D, McCluskey L, Elman L, Juhr D, Gruber PJ, Rüb U, Auburger G, Trojanowski JQ, Lee VM, Van Deerlin VM, Bonini NM, Gitler AD. (2010) Ataxin-2 intermediate-length polyglutamine expansions are associated with increased risk for ALS. *Nature.* 466(7310):1069-75.

Fiesel FC, Weber SS, Supper J, Zell A, Kahle PJ. (2012) TDP-43 regulates global translational yield by splicing of exon junction complex component SKAR. *Nucleic Acids Res* 40(6):2668-82.

Funalot B, Desport JC, Sturtz F, Camu W, Couratier P. (2009) High metabolic level in patients with familial amyotrophic lateral sclerosis. *Amyotroph Lateral Scler.* 10(2):113-117.

Gailus-Durner V, Fuchs H, Becker L, Bolle I, Brielmeier M, Calzada-Wack J, Elvert R, Ehrhardt N, Dalke C, Franz TJ, Grundner-Culemann E, Hammelbacher S, Hölter SM, Hölzlwimmer G, Horsch M, Javaheri A, Kalaydjiev SV, Klempt M, Kling E, Kunder S, Lengger C, Lisse T, Mijalski T, Naton B, Pedersen V, Prehn C, Przemeck G, Racz I, Reinhard C, Reitmeir P, Schneider I, Schrewe A, Steinkamp R, Zybill C, Adamski J, Beckers J, Behrendt H, Favor J, Graw J, Heldmaier G, Höfler H, Ivandic B, Katus H, Kirchhof P, Klingenspor M, Klopstock T, Lengeling A, Müller W, Ohl F, Ollert M, Quintanilla-Martinez L, Schmidt J, Schulz H, Wolf E, Wurst W, Zimmer A, Busch DH, de Angelis MH. (2005) Introducing the German Mouse Clinic: open access platform for standardized phenotyping. *Nat Methods* 2(6):403-404.

Galsworthy MJ, Amrein I, Kuptsov PA, Poletaeva II, Zinn P, Rau A, Vyssotski A, Lipp HP. (2005) A comparison of wild-caught wood mice and bank voles in the Intellicage: assessing exploration, daily activity patterns and place learning paradigms. *Behav Brain Res* 157(2):211-7.

Geser F, Winton MJ, Kwong LK, Xu Y, Xie SX, Igaz LM, Garruto RM, Perl DP, Galasko D, Lee VM, Trojanowski JQ. (2008) Pathological TDP-43 in parkinsonism-dementia complex and amyotrophic lateral sclerosis of Guam. *Acta Neuropathol.* 115(1):133-45.

Geser F, Martinez-Lage M, Robinson J, Uryu K, Neumann M, Brandmeir NJ, Xie SX, Kwong LK, Elman L, McCluskey L, Clark CM, Malunda J, Miller BL, Zimmerman EA, Qian J, Van Deerlin V, Grossman M, Lee VM, Trojanowski JQ. (2009) Clinical and pathological continuum of multisystem TDP-43 proteinopathies. *Arch Neurol* 66(2):180-189.

Gitcho MA, Baloh RH, Chakraverty S, Mayo K, Norton JB, Levitch D, Hatanpaa KJ, White CL 3rd, Bigio EH, Caselli R, Baker M, Al-Lozi MT, Morris JC, Pestronk A, Rademakers R, Goate AM, Cairns NJ. (2008) TDP-43 A315T mutation in familial motor neuron disease. *Ann Neurol*. 63(4):535-8.

Gitcho MA, Bigio EH, Mishra M, Johnson N, Weintraub S, Mesulam M, Rademakers R, Chakraverty S, Cruchaga C, Morris JC, Goate AM, Cairns NJ. (2009) TARDBP 3'-UTR variant in autopsy-confirmed frontotemporal lobar degeneration with TDP-43 proteinopathy. *Acta Neuropathol.* 118(5):633-45.

Gong C, Maquat LE. (2011) lncRNAs transactivate STAU1-mediated mRNA decay by duplexing with 3' UTRs via Alu elements. *Nature.* 470(7333):284-8.

Greenway MJ, Andersen PM, Russ C, Ennis S, Cashman S, Donaghy C, Patterson V, Swingler R, Kieran D, Prehn J, Morrison KE, Green A, Acharya KR, Brown RH Jr, Hardiman O. (2006) ANG mutations segregate with familial and 'sporadic'amyotrophic lateral sclerosis. *Nat Genet* 38: 411-413.

Gregory RI, Yan KP, Amuthan G, Chendrimada T, Doratotaj B, Cooch N, Shiekhattar R. (2004) The Microprocessor complex mediates the genesis of microRNAs. Nature 432(7014):235-240.

Gros-Louis F, Gaspar C, Rouleau GA.(2006) Genetics of familial and sporadic amyotrophic lateral sclerosis. *Biochim Biophys Acta* 1762:956–972.

Hadano S, Hand CK, Osuga H, Yanagisawa Y, Otomo A, Devon RS, Miyamoto N, Showguchi-Miyata J, Okada Y, Singaraja R, Figlewicz DA, Kwiatkowski T, Hosler BA, Sagie T, Skaug J, Nasir J, Brown RH Jr, Scherer SW, Rouleau GA, Hayden MR, Ikeda JE. (2001) A gene encoding a putative GTPase regulator is mutated in familial amyotrophic lateral sclerosis 2. *Nat Genet* 29:166-173.

Hampe C, Ardila-Osorio H, Fournier M, Brice A, Corti O. (2006) Biochemical analysis of Parkinson's disease-causing variants of Parkin, an E3 ubiquitin-protein ligase with monoubiquitylation capacity. *Hum Mol Genet.* 15(13):2059-75.

Hardiman O, van den Berg LH, Kiernan MC. (2011) Clinical diagnosis and management of amyotrophic lateral sclerosis. *Nat Rev Neurol* 7(11):639-649.

Hasegawa M, Arai T, Akiyama H, Nonaka T, Mori H, Hashimoto T, Yamazaki M, Oyanagi K. (2007) TDP-43 is deposited in the Guam parkinsonism-dementia complex brains. *Brain.* 130(Pt 5):1386-94.

Hasegawa M, Arai T, Nonaka T, Kametani F, Yoshida M, Hashizume Y, Beach TG, Buratti E, Baralle F, Morita M, Nakano I, Oda T, Tsuchiya K, Akiyama H. (2008) Phosphorylated TDP-43 in frontotemporal lobar degeneration and amyotrophic lateral sclerosis. *Ann Neurol* 64(1):60-70.

Haverkamp LJ, Appel V, Appel SH. (1995) Natural history of amyotrophic lateral sclerosis in a database population. Validation of a scoring system and a model for survival prediction. *Brain* 118 (Pt 3):707-719.

Hill DP, Wurst W. (1993) Gene and enhancer trapping: mutagenic strategies for developmental studies. *Curr Top Dev Biol* 28:181-206.

Hutton M, Lendon CL, Rizzu P, Baker M, Froelich S, Houlden H, Pickering-Brown S, Chakraverty S, Isaacs A, Grover A, Hackett J, Adamson J, Lincoln S, Dickson D, Davies P, Petersen RC, Stevens M, de Graaff E, Wauters E, van Baren J, Hillebrand M, Joosse M, Kwon JM, Nowotny P, Che LK, Norton J, Morris JC, Reed LA, Trojanowski J, Basun H, Lannfelt L, Neystat M, Fahn S, Dark F, Tannenberg T, Dodd PR, Hayward N, Kwok JB, Schofield PR, Andreadis A, Snowden J, Craufurd D, Neary D, Owen F, Oostra BA, Hardy J, Goate A, van Swieten J, Mann D, Lynch T, Heutink P. (1998) Association of missense and 5'-splice-site mutations in tau with the inherited dementia FTDP-17. *Nature* 393(6686):702-5.

Igaz LM, Kwong LK, Lee EB, Chen-Plotkin A, Swanson E, Unger T, Malunda J, Xu Y, Winton MJ, Trojanowski JQ, Lee VM. (2011) Dysregulation of the ALS-associated gene TDP-43 leads to neuronal death and degeneration in mice. *J Clin Invest* 121(2):726-738.

Jung C, Higgins CM, Xu Z. (2002) Mitochondrial electron transport chain complex dysfunction in a transgenic mouse model for amyotrophic lateral sclerosis. *J Neurochem.* 83(3):535-45.

Kabashi E, Valdmanis PN, Dion P, Spiegelman D, McConkey BJ, Vande Velde C, Bouchard JP, Lacomblez L, Pochigaeva K, Salachas F, Pradat PF, Camu W, Meininger V, Dupre N, Rouleau GA. (2008) TARDBP mutations in individuals with sporadic and familial amyotrophic lateral sclerosis. *Nat Genet.* 40(5):572-4.

Kametani F, Nonaka T, Suzuki T, Arai T, Dohmae N, Akiyama H, Hasegawa M. (2009) Identification of casein kinase-1 phosphorylation sites on TDP-43. *Biochem Biophys Res Commun.* 382(2):405-9.

Kawahara Y, Mieda-Sato A. (2012) TDP-43 promotes microRNA biogenesis as a component of the Drosha and Dicer complexes. *Proc Natl Acad Sci U S A* 109(9):3347-3352.

Kim KY, Stevens MV, Akter MH, Rusk SE, Huang RJ, Cohen A, Noguchi A, Springer D, Bocharov AV, Eggerman TL, Suen DF, Youle RJ, Amar M, Remaley AT, Sack MN. (2011) Parkin is a lipid-responsive regulator of fat uptake in mice and mutant human cells. *J Clin Invest*. 121(9):3701-12.

Kim SM, Kim H, Kim JE, Park KS, Sung JJ, Kim SH, Lee KW. (2011) Amyotrophic lateral sclerosis is associated with hypolipidemia at the presymptomatic stage in mice. *PLoS One*. 6(3):e17985.

Kitada T, Asakawa S, Hattori N, Matsumine H, Yamamura Y, Minoshima S, Yokochi M, Mizuno Y, Shimizu N. (1998) Mutations in the parkin gene cause autosomal recessive juvenile parkinsonism. *Nature*. 392(6676):605-8.

Knapska E, Walasek G, Nikolaev E, Neuhäusser-Wespy F, Lipp HP, Kaczmarek L, Werka T. (2006) Differential involvement of the central amygdala in appetitive versus aversive learning. *Learn Mem* 13(2):192-200.

Kwiatkowski TJ Jr, Bosco DA, Leclerc AL, Tamrazian E, Vanderburg CR, Russ C, Davis A, Gilchrist J, Kasarskis EJ, Munsat T, Valdmanis P, Rouleau GA, Hosler BA, Cortelli P, de Jong PJ, Yoshinaga Y, Haines JL, Pericak-Vance MA, Yan J, Ticozzi N, Siddique T, McKenna-Yasek D, Sapp PC, Horvitz HR, Landers JE, Brown RH Jr. (2009) Mutations in the FUS/TLS gene on chromosome 16 cause familial amyotrophic lateral sclerosis. *Science* 323: 1205-1208.

Lagier-Tourenne C, Cleveland DW. (2009) Rethinking ALS: the FUS about TDP-43. *Cell* 136(6):1001-1004.

Lee EB, Lee VM, Trojanowski JQ. (2011) Gains or losses: molecular mechanisms of TDP43-mediated neurodegeneration. *Nat Rev Neurosci* 13(1):38-50.

Levine B, Kroemer G. (2008) Autophagy in the pathogenesis of disease. *Cell* 132(1):27-42.

Li HY, Yeh PA, Chiu HC, Tang CY, Tu BP. (2011) Hyperphosphorylation as a defense mechanism to reduce TDP-43 aggregation. *PLoS One* 6(8):e23075.

Lillo P, Hodges JR. (2009) Frontotemporal dementia and motor neurone disease: overlapping clinic-pathological disorders. *J Clin Neurosci*. 16(9):1131-5.

Ling SC, Albuquerque CP, Han JS, Lagier-Tourenne C, Tokunaga S, Zhou H, Cleveland DW. (2010) ALS-associated mutations in TDP-43 increase its stability and promote TDP-43 complexes with FUS/TLS. *Proc Natl Acad Sci U S A* 107(30):13318-13323.

Maruyama H, Morino H, Ito H, Izumi Y, Kato H, Watanabe Y, Kinoshita Y, Kamada M, Nodera H, Suzuki H, Komure O, Matsuura S, Kobatake K, Morimoto N, Abe K, Suzuki N, Aoki M, Kawata A, Hirai T, Kato T, Ogasawara K, Hirano A, Takumi T, Kusaka H, Hagiwara K, Kaji R, Kawakami H. (2010) Mutations of optineurin in amyotrophic lateral sclerosis. *Nature.* 465(7295):223-6.

McFarlan JT, Yoshida Y, Jain SS, Han XX, Snook LA, Lally J, Smith BK, Glatz JF, Luiken JJ, Sayer RA, Tupling AR, Chabowski A, Holloway GP, Bonen A. (2012) In Vivo, fatty acid translocase (CD36) critically regulates skeletal muscle fuel selection, exercise performance and training-induced adaptation of fatty acid oxidation. *J Biol Chem.*

Mercado PA, Ayala YM, Romano M, Buratti E, Baralle FE. (2005) Depletion of TDP 43 overrides the need for exonic and intronic splicing enhancers in the human apoA-II gene. *Nucleic Acids Res*. 33(18):6000-10.

Mitchell JD, Borasio GD. (2007) Amyotrophic lateral sclerosis. *Lancet* 369(9578):2031-2041.

Morita M, Al-Chalabi A, Andersen PM, Hosler B, Sapp P, Englund E, Mitchell JE, Habgood JJ, de Belleroche J, Xi J, Jongjaroenprasert W, Horvitz HR, Gunnarsson LG, Brown RH Jr. (2006) A locus on chromosome 9p confers susceptibility to ALS and frontotemporal dementia. *Neurology* 66(6):839-844.

Narendra D, Tanaka A, Suen DF, and Youle RJ. (2008) Parkin is recruited selectively to impaired mitochondria and promotes their autophagy. *J Cell Biol* 183: 795–803.

Neary D, Snowden JS, Gustafson L, Passant U, Stuss D, Black S, Freedman M, Kertesz A, Robert PH, Albert M, Boone K, Miller BL, Cummings J, Benson DF. (1998) Frontotemporal lobar degeneration: a consensus on clinical diagnostic criteria. *Neurology* 51(6):1546-1554.

Neumann M, Sampathu DM, Kwong LK, Truax AC, Micsenyi MC, Chou TT, Bruce J, Schuck T, Grossman M, Clark CM, McCluskey LF, Miller BL, Masliah E, Mackenzie IR, Feldman H, Feiden W, Kretzschmar HA, Trojanowski JQ, Lee VM. (2006) Ubiquitinated TDP-43 in frontotemporal lobar degeneration and amyotrophic lateral sclerosis. *Science* 314: 130-133.

Neumann M, Kwong LK, Sampathu DM, Trojanowski JQ, Lee VM. (2007) TDP-43 proteinopathy in frontotemporal lobar degeneration and amyotrophic lateral sclerosis: protein misfolding diseases without amyloidosis. *Arch Neurol.* 64(10):1388-94.

Neumann M, Kwong LK, Lee EB, Kremmer E, Flatley A, Xu Y, Forman MS, Troost D, Kretzschmar HA, Trojanowski JQ, Lee VM. (2009) Phosphorylation of S409/410 of TDP-43 is a consistent feature in all sporadic and familial forms of TDP-43 proteinopathies. *Acta Neuropathol* 117(2):137-149.

Nishimura AL, Mitne-Neto M, Silva HC, Richieri-Costa A, Middleton S, Cascio D, Kok F, Oliveira JR, Gillingwater T, Webb J, Skehel P, Zatz M. (2004) A mutation in the vesicle-trafficking protein VAPB causes late-onset spinal muscular atrophy and amyotrophic lateral sclerosis. *Am J Hum Genet* 75: 822-831.

Noldus (2007) CatWalk^{TM} Reference manual Version 7.1

Orlacchio A, Babalini C, Borreca A, Patrono C, Massa R, Basaran S, Munhoz RP, Rogaeva EA, St George-Hyslop PH, Bernardi G, Kawarai T. (2010) SPATACSIN mutations cause autosomal recessive juvenile amyotrophic lateral sclerosis. *Brain* 133:591-598.

Ou SH, Wu F, Harrich D, García-Martínez LF, Gaynor RB. (1995) Cloning and characterization of a novel cellular protein, TDP-43, that binds to human immunodeficiency virus type 1 TAR DNA sequence motifs. *J Virol* 69(6):3584-3596.

Palacino JJ, Sagi D, Goldberg MS, Krauss S, Motz C, Wacker M, Klose J, and Shen J. (2004) Mitochondrial dysfunction and oxidative damage in parkin-deficient mice. *J Biol Chem* 279: 18614–18622.

Palmesino E, Rousso DL, Kao TJ, Klar A, Laufer E, Uemura O, Okamoto H, Novitch BG, Kania A. (2010) Foxp1 and lhx1 coordinate motor neuron migration with axon trajectory choice by gating Reelin signalling. *PLoS Biol.* 8(8):e1000446.

Polymenidou M, Lagier-Tourenne C, Hutt KR, Huelga SC, Moran J, Liang TY, Ling SC, Sun E, Wancewicz E, Mazur C, Kordasiewicz H, Sedaghat Y, Donohue JP, Shiue L, Bennett CF, Yeo GW, Cleveland DW. (2011) Long pre-mRNA depletion and RNA missplicing contribute to neuronal vulnerability from loss of TDP-43. *Nat Neurosci* 14(4):459-468.

Raimondi A, Mangolini A, Rizzardini M, Tartari S, Massari S, Bendotti C, Francolini M, Borgese N, Cantoni L, Pietrini G. (2006) Cell culture models to investigate the selective vulnerability of motoneuronal mitochondria to familial ALS-linked G93ASOD1. *Eur J Neurosci.* 24(2):387-99.

Ratnavalli E, Brayne C, Dawson K, Hodges JR. (2002) The prevalence of frontotemporal dementia. *Neurology* 58(11):1615-1621.

Rosen DR. (1993) Mutations in Cu/Zn superoxide dismutase gene are associated with familial amyotrophic lateral sclerosis. *Nature* 364(6435):362.

Rossbach O, Hung LH, Schreiner S, Grishina I, Heiner M, Hui J, Bindereif A. (2009) Auto- and cross-regulation of the hnRNP L proteins by alternative splicing. *Mol Cell Biol.* 29(6):1442-51.

Rowland LP. (2001) "How amyotrophic lateral sclerosis got its name: the clinical-pathologic genius of Jean-Martin Charcot". *Arch Neurol* 58 (3): 512–515.

Sasaki S, Iwata M. (1996) Ultrastructural study of the synapses of central chromatolytic anterior horn cells in motor neuron disease. *J Neuropathol Exp Neurol.* 55(8):932-9.

Schebelle L, Wolf C, Stribl C, Javaheri T, Schnütgen F, Ettinger A, Ivics Z, Hansen J, Ruiz P, von Melchner H, Wurst W, Floss T. (2010) Efficient conditional and promoter-specific in vivo expression of cDNAs of choice by taking advantage of recombinase-mediated cassette exchange using FlEx gene traps. *Nucleic Acids Res* 38(9):e106.

Schwab C, Arai T, Hasegawa M, Yu S, McGeer PL. (2008) Colocalization of transactivation-responsive DNA-binding protein 43 and huntingtin in inclusions of Huntington disease. *J Neuropathol Exp Neurol.* 67(12):1159-65.

Sephton CF, Good SK, Atkin S, Dewey CM, Mayer P 3rd, Herz J, Yu G. (2010) TDP-43 is a developmentally regulated protein essential for early embryonic development. *J Biol Chem* 285(9):6826-34.

Shan X, Chiang PM, Price DL, Wong PC. (2010) Altered distributions of Gemini of coiled bodies and mitochondria in motor neurons of TDP-43 transgenic mice. *Proc Natl Acad Sci U S A* 107(37):16325-16330.

Shimura H, Hattori N, Kubo S, Mizuno Y, Asakawa S, Minoshima S, Shimizu N, Iwai K, Chiba T, Tanaka K, Suzuki T. (2000) Familial Parkinson disease gene product, parkin, is a ubiquitin-protein ligase. *Nat Genet.* 25(3):302-5.

Siklós L, Engelhardt J, Harati Y, Smith RG, Joó F, Appel SH. (1996) Ultrastructural evidence for altered calcium in motor nerve terminals in amyotropic lateral sclerosis. *Ann Neurol.* 39(2):203-16.

Skarnes WC. (2000) Gene trapping methods for the identification and functional analysis of cell surface proteins in mice. *Methods Enzymol* 328:592-615.

Skibinski G, Parkinson NJ, Brown JM, Chakrabarti L, Lloyd SL, Hummerich H, Nielsen JE, Hodges JR, Spillantini MG, Thusgaard T, Brandner S, Brun A, Rossor MN, Gade A, Johannsen P, Sørensen SA, Gydesen S, Fisher EM, Collinge J. (2005) Mutations in the endosomal ESCRTIII-complex subunit CHMP2B in frontotemporal dementia. *Nat Genet* 37(8):806-808.

Sreedharan J, Blair IP, Tripathi VB, Hu X, Vance C, Rogelj B, Ackerley S, Durnall JC, Williams KL, Buratti E, Baralle F, de Belleroche J, Mitchell JD, Leigh PN, Al-Chalabi A, Miller CC, Nicholson G, Shaw CE. (2008) TDP-43 mutations in familial and sporadic amyotrophic lateral sclerosis. *Science.* 319(5870):1668-72.

Stallings NR, Puttaparthi K, Luther CM, Burns DK, Elliott JL. (2010) Progressive motor weakness in transgenic mice expressing human TDP-43. *Neurobiol Dis* 40(2):404-414.

Sureau A, Gattoni R, Dooghe Y, Stévenin J, Soret J. (2001) SC35 autoregulates its expression by promoting splicing events that destabilize its mRNAs. *EMBO J.* 20(7):1785-96.

Swarup V, Phaneuf D, Bareil C, Robertson J, Rouleau GA, Kriz J, Julien JP. (2011) Pathological hallmarks of amyotrophic lateral sclerosis/frontotemporal lobar degeneration in transgenic mice produced with TDP-43 genomic fragments. *Brain* 134(Pt 9):2610-2626.

Swerdlow RH. (2011) Role and treatment of mitochondrial DNA-related mitochondrial dysfunction in sporadic neurodegenerative diseases. *Curr Pharm Des.* 17(31):3356-73.

Tollervey JR, Curk T, Rogelj B, Briese M, Cereda M, Kayikci M, König J, Hortobágyi T, Nishimura AL, Zupunski V, Patani R, Chandran S, Rot G, Zupan B, Shaw CE, Ule J. (2011) Characterizing the RNA targets and position-dependent splicing regulation by TDP-43. *Nat Neurosci* 14(4):452-458.

Tronche, F., Kellendonk, C., Kretz, O., Gass, P., Anlag, K., Orban, P.C., Bock, R., Klein, R., and Schutz, G. (1999) Disruption of the glucocorticoid receptor gene in the nervous system results in reduced anxiety. *Nat Genet 23*, 99-103.

Uryu K, Nakashima-Yasuda H, Forman MS, Kwong LK, Clark CM, Grossman M, Miller BL, Kretzschmar HA, Lee VM, Trojanowski JQ, Neumann M. (2008) Concomitant TAR-DNA-binding protein 43 pathology is present in Alzheimer disease and corticobasal degeneration but not in other tauopathies. *J Neuropathol Exp Neurol.* 67(6):555-64.

Vance C, Rogelj B, Hortobagyi T, De Vos KJ, Nishimura AL, Sreedharan J, Hu X, Smith B, Ruddy D, Wright P, Ganesalingam J, Williams KL, Tripathi V, Al-Saraj S, Al-Chalabi A, Leigh PN, Blair IP, Nicholson G, de Belleroche J, Gallo JM, Miller CC, Shaw CE. (2009) Mutations in FUS, an RNA processing protein, cause familial amyotrophic lateral sclerosis type 6. *Science* 323:1208-1211.

Van Deerlin VM, Sleiman PM, Martinez-Lage M, Chen-Plotkin A, Wang LS, Graff-Radford NR, Dickson DW, Rademakers R, Boeve BF, Grossman M, Arnold SE, Mann DM, Pickering-Brown SM et al. (2010) Common variants at 7p21 are associated with frontotemporal lobar degeneration with TDP-43 inclusions. *Nat Genet.* 42(3):234-9.

Wang HY, Wang IF, Bose J, Shen CK. (2004) Structural diversity and functional implications of the eukaryotic TDP gene family. *Genomics* 83(1):130-139.

Watts GD, Wymer J, Kovach MJ, Mehta SG, Mumm S, Darvish D, Pestronk A, Whyte MP, Kimonis VE. (2004) Inclusion body myopathy associated with Paget disease of bone and frontotemporal dementia is caused by mutant valosin-containing protein. *Nat Genet* 36(4):377-381.

Wegorzewska I, Bell S, Cairns NJ, Miller TM, Baloh RH. (2009) TDP-43 mutant transgenic mice develop features of ALS and frontotemporal lobar degeneration. *Proc Natl Acad Sci U S A* 106(44):18809-18814.

Wegorzewska I, Baloh RH. (2011) TDP-43-based animal models of neurodegeneration: new insights into ALS pathology and pathophysiology. *Neurodegener Dis* 8(4):262-274.

Wils H, Kleinberger G, Janssens J, Pereson S, Joris G, Cuijt I, Smits V, Ceuterick-de Groote C, Van Broeckhoven C, Kumar-Singh S. (2010) TDP-43 transgenic mice develop spastic paralysis and neuronal inclusions characteristic of ALS and frontotemporal lobar degeneration. *Proc Natl Acad Sci U S A* 107(8):3858-3863.

Wollerton MC, Gooding C, Wagner EJ, Garcia-Blanco MA, Smith CW. (2004) Autoregulation of polypyrimidine tract binding protein by alternative splicing leading to nonsense-mediated decay. *Mol Cell.* 13(1):91-100.

Wu LS, Cheng WC, Hou SC, Yan YT, Jiang ST, Shen CK. (2010) TDP-43, a neuro-pathosignature factor, is essential for early mouse embryogenesis. *Genesis* 48(1):56-62.

Xu YF, Gendron TF, Zhang YJ, Lin WL, D'Alton S, Sheng H, Casey MC, Tong J, Knight J, Yu X, Rademakers R, Boylan K, Hutton M, McGowan E, Dickson DW, Lewis J, Petrucelli L. (2010) Wild-type human TDP-43 expression causes TDP-43 phosphorylation, mitochondrial aggregation, motor deficits, and early mortality in transgenic mice. *J Neurosci* 30(32):10851-10859.

Xu YF, Zhang YJ, Lin WL, Cao X, Stetler C, Dickson DW, Lewis J, Petrucelli L. (2011) Expression of mutant TDP-43 induces neuronal dysfunction in transgenic mice. *Mol Neurodegener* 6:73.

Yu Z, Fan D, Gui B, Shi L, Xuan C, Shan L, Wang Q, Shang Y, Wang Y. (2012) Neurodegeneration-associated TDP-43 Interacts with Fragile X Mental Retardation Protein (FMRP)/Staufen (STAU1) and Regulates SIRT1 Expression in Neuronal Cells. *J Biol Chem.* [Epub ahead of print]

Zhang Y, Gao J, Chung KK, Huang H, Dawson VL, Dawson TM. (2000) Parkin functions as an E2-dependent ubiquitin- protein ligase and promotes the degradation of the synaptic vesicle-associated protein, CDCrel-1. *Proc Natl Acad Sci U S A.* 97(24):13354-9.

Zhang YJ, Xu YF, Cook C, Gendron TF, Roettges P, Link CD, Lin WL, Tong J, Castanedes-Casey M, Ash P, Gass J, Rangachari V, Buratti E, Baralle F, Golde TE, Dickson DW, Petrucelli L. (2009) Aberrant cleavage of TDP-43 enhances aggregation and cellular toxicity. *Proc Natl Acad Sci U S A* 106(18):7607-7612.

Zhang YJ, Gendron TF, Xu YF, Ko LW, Yen SH, Petrucelli L. (2010) Phosphorylation regulates proteasomal-mediated degradation and solubility of TAR DNA binding protein-43 C-terminal fragments. *Mol Neurodegener*. 5:33.

Zhou H, Huang C, Chen H, Wang D, Landel CP, Xia PY, Bowser R, Liu YJ, Xia XG. (2010) Transgenic rat model of neurodegeneration caused by mutation in the TDP gene. *PLoS Genet* 6(3):e1000887.

Zhou Y, Jiang L, Rui L. (2009) Identification of MUP1 as a regulator for glucose and lipid metabolism in mice. *J Biol Chem.* 284(17):11152-11159.

Ziviani E, Tao RN, Whitworth AJ. (2010) Drosophila parkin requires PINK1 for mitochondrial translocation and ubiquitinates mitofusin. *Proc Natl Acad Sci U S A.* 107(11):5018-23.

9 Appendix

9.1 Abbreviations

A	purine base/amino acid adenine
Ac	acetate
ACTB	actin, beta (endogenous control)
ad.lib.	*ad libitum* fed
adSA	adenoviral splice acceptor
ALS	amyotrophic lateral sclerosis
amp	ampicillin
ATP	adenosine triphosphate
attB	attachment site in the donor vector (RMCE)
attL	attachment site in the acceptor vector (RMCE)
attR	attachment site in the donor vector (RMCE)
βgeo	β-galactosidase / neomycinphosphotransferase
BAG3	BAG family molecular chaperone regulator 3
BCA	bicinchoninic acid
BGH	bovine growth hormone
bp	basepair
BSA	bovine serum albumin
°C	celsius degree
C	amino acid cysteine / pyrimidine base cytosine
c	centi (10^{-2})
$CaCl_2$	calcium chloride
CD36	Cluster of Differentiation 36
cDNA	complementary desoxyribonucleic acid
C. elegans	*Caenorhabditis elegans*
CHAPS	3-[(3-cholamidopropyl)dimethylammonio]-1-propanesulfonate
CNS	central nervous system
CO_2	carbon dioxide
CRE	induces recombination
C-terminus	carboxy terminus

CTP	cytosine triphosphate
Da	Dalton
DAB	3-3'Diaminobenzidine
DAPI	4',6-diamidino-2-phenylindole
DH5α	*E.coli* strain
DMEM	modified Eagle Medium after Dulbecco
DMSO	Dimethyl sulfoxide
DNA	desoxyribonucleic acid
DNase	desoxyribonuclease
dNTP	desoxyribonucleotide triphosphate
DTT	dithiotreitol
E	embryonic day
E14	ES E14 Tg2A.4 cells
E. coli	*Escherichia coli*
e.g.	exempli gratia, for example
EDTA	ethylendiamintetraacetate
EGTA	ethylenglycol-bis-(b-aminoethylether)-N,N,N´,N´-tetraacetate
ES cells	embryonic stem cells
F	Farad
fALS	familiar amyotrophic lateral sclerosis
FCS	fetal calf serum
FGF	fibroblast growth factor
Fig.	figure
Flp	Flippase
FlpO	optimized Flippase
FMRP	Fragile X Mental Retardation Protein
FTD	frontotemporal dementia
FTLD	frontotemporal lobar degeneration
FTLD-MND	FTLD with motor neuron disease
FTLD-U	FTLD with ubiquitin-positive inclusions
FRT	FLP recombinase target
FUS	fused in sarcoma

g	acceleration of gravity (9.81 m/s2)
g	gram
G	amino acid glycine
G	purine base guanine
GMC	german mouse clinic
GRN	Progranulin
GGTC	german gene trap consortium
h	hour(s)
hCG	human chorion gonadotropin
HCl	hydrochloric acid
HDL	high density lipoprotein
het	heterozygous
HIV	human immunodeficiency virus
hnRNP(s)	heterogeneous nuclear ribonucleoprotein(s)
HPRT	hypoxanthine phosphoribosyltransferase
HTT	Huntington
i.p.	intraperitoneal (injection)
IF	immunofluorescence
IHC	immunohistochemistry
IMMT	mitochondrial inner membrane protein
IVC	individually ventilated cages
kb	kilo base pairs
kDa	kilo Dalton
kg	kilogram
Klenow	large fragment of *E. coli* DNA polymerase I
l	liter
lacZ	β-galactosidase
LB	Luria Broth
LC3	microtubule-associated protein 1 light chain 3
LDL	low-density lipoprotein
Lhx1	LIM homeobox protein 1
LIF	leukemia inhibiting factor

loxP	locus of crossing over of P1 phage
µ	micro (10^{-6})
m	milli (10^{-3})
m	meter
M	molar (mol/l)
M	amino acid methionine
M	months
MAPT	microtubule associated protein tau
$MgCl_2$	magnesium chloride
min	minute(s)
miRNA	micro ribonucleic acid
MND	motor neuron disease
MOPS	3-(N-morpholino)propanesulfonic acid
mPrp	mouse prion protein
mRNA	messenger ribonucleic acid
Mup1	major urinary protein 1
mut	mutant
n	nano (10^{-9})
n	sample size
NaCl	sodium chloride
NaOAc	sodium acetate
NCI	neuronal cytoplasmic inclusion
n.d.	not determined
NEFA	non-esterified fatty acid
NES	nuclear export signal
NH_4OAc	ammonium acetate
NII	neuronal intranuclear inclusions
NLS	nuclear localization signal
NMD	nonsense-mediated decay
NP-40	Nonidet P-40
nt	nucleotide(s)
OD	optical density

OPA-1	optic atrophy 1
ORF	open reading frame
ovn	overnight
p	pico (10^{-12})
P	p-value (statistical analysis)
pA	polyadenylation signal
PBS	phosphate buffered saline
PCR	polymerase chain reaction
PD	Parkinson's disease
PFA	paraformaldehyde
pH	potential hydrogen
PI	protease/phosphatase inhibitor
PiD	Pick's disease
PMSG	pregnant mare's serum gonadotropin
PNFA	progressive nonfluent aphasia
qRT-PCR	quantitative real time polymerase chain reaction
RIPA	protein lysis buffer
RMCE	recombinase mediated cassette exchange
RNA	ribonucleic acid
RNase	ribonuclease
rpm	rounds per minute
RRM	RNA recognition motif
RT	room temperature
RT-PCR	reverse transcription polymerase chain reaction
SA	splice acceptor
sALS	sporadic amyotrophic lateral sclerosis
SD	semantic dementia
SDS	sodium dodecyl sulfate
SDS-PAGE	sodium dodecyl sulfate polyacrylamide gel electrophoresis
sec or s	second(s)
SEM	standard error of the mean
SIRT1	Sirtuin-1

SOD1	superoxide dismutase 1
ssDNA	single-stranded desoxyribonucleic acid
ssRNA	single-stranded ribonucleic acid
STAU1	Staufen homolog 1
T	amino acid threonine
T	pyrimidine base thymine
Tab.	table
TAE	tris acetate with EDTA
Tardbp	TAR DNA-binding protein gene
TBE	tris borate with EDTA
TBS	tris buffered saline
TBS(T)	tris buffered saline (with Tween)
TBV2	wild-type ES cell line from a 129S2 mouse embryo
TDP-43	TAR DNA-binding protein 43
TDPBR	TDP-43 binding region
TE	tris-EDTA
temp.	temperature
Tris	trishydroxymethyl-aminoethane
U	unit(s)
UPS	ubiquitin proteasome system
UTR	untranslated region of a gene
UV	ultra-violet
V	volt(s)
V	amino acid valine
VCP	valosin-containing protein
vol.	volume or volumetric content
wt	wildtype
x	symbol for crosses between mouse strains

9.2 Index of figures and tables

Figures:

Tables:

9.3 Supplementary data

9.3.1 CatWalk analysis

Parameter	male	t-test	female	t-test	all	t-test
general			BOS front paws support diagonal support four	* trend trend	support diagonal support four	trend trend
left front paws	swing speed	trend	duty cycle	**		
right hind paws	print length	*				
left hind paws	intensity swing speed	trend trend	intensity swing duty cycle max contact stand index	* trend trend * **	max contact stand index	** *
front paws			duty cycle	*		
hind paws	print length swing speed	* trend	swing duty cycle stand index	trend trend trend	max contact stand index	trend trend
phase diagonal			RF-LH C_{stat} mean LF-RH C_{stat} mean	trend trend	RF-LH C_{stat} mean	*
phase girdle	LH-RH mean	trend				
phase ipsilateral			LF-LH mean	trend		
coupling diagonal	RF-LH mean RF-LH C_{stat} mean	* ***	RF-LH mean LF-RH mean LF-RH C_{stat} mean LF-RH AMT RH-LF mean RH-LF mitsmatches RH-LF C_{stat} mean	trend * trend * * trend *	RF-LH mean RF-LH C_{stat} mean	** ***
coupling ipsilateral	LH-LF mean LH-LF $_{Cstat}$ mean	trend trend	RH-RF ANT	**	LH-LF C_{stat} mean	trend

Tab. 6: CatWalk analysis parameters with a trend or significant result are shown for 15 months old hTDP-43^{A315T}Rosa+/- mice in comparison to controls (*P < 0.05, **P < 0.01, ***P < 0.001, trend = 0.01 > P < 0.05).

9.3.2 Overview behavioral analysis

	Test	female 5M	male 15M	female 15M
Motor tests	CatWalk	n.s.	significant	significant
	Beam Walk	n.s.	n.s.	n.s.
	Pole test	n.s.	n.s.	trend (turning duration)
	Ladder	significant	n.s.	n.s.
	Rotarod	n.s.	n.s.	n.s.
	Grip strength	n.s.	n.s.	n.s.
Memory tests	Y-maze	n.d.	n.s.	trend (same arm return)
	Object recognition	n.d.	n.s.	n.s.
	IntelliCage	n.d.	n.s.	n.s.

Tab. 7: There were significant differences in the motor tests of 5 and 15 months old mutant mice compared to age matched controls. 5 months old females had more slips on the ladder and some significant changes in the CatWalk. 15 months old female mutants displayed longer turning duration on top of the pole, but that was not significant. In all memory test mutants behaved comparable to controls. Again females showed a trend for same arm returns (SARs) in the Y-maze (trend = t-test, $0.1 > P < 0.05$; significant = t-test, $P < 0.05$).

9.3.3 Gene expression analysis

Gene symbol	Gene name	Mean ratio
Lhx1	LIM homeobox protein 1	2,06
Eno1	enolase 1, alpha	1,65
Masp2	mannan-binding lectin serine peptidase 2	2,62
Klk1b22	kallikrein 1-related peptidase b22	-5,38
Actc1	actin, alpha	-2,47
Myl3	myosin, light polypeptide 3	-2,94
Mup1	major urinary protein 1	-2,55
Hoxb7	homeobox B7	-2,39
Myl2	myosin, light polypeptide 2	-2,77
Mup2	major urinary protein 2	-2,60
Vmo1	vitelline membrane outer layer 1	-2,00
Mylc2b	myosin, light chain 12B	-1,65
Cyp4a14	cytochrome P450, family 4, subfamily a, polypeptide 14	-1,76
Snx3	sorting nexin 3	-1,94
Tcfap2c	transcription factor AP-2, gamma	-1,84
Atg3	autophagy-related 3	-1,57
Dbt	dihydrolipoamide branched chain transacylase E2	-1,64
Rab34	RAB34, member of RAS oncogene family	-1,69
Popdc2	popeye domain containing 2	-1,63
Clstn1	calsyntenin 1	-1,79
Clpx	caseinolytic peptidase X	-1,53
Hoxc6	homeobox C6	-2,42
Nhp2l1	NHP2 non-histone chromosome protein 2-like 1	-1,50
Mb	myoglobin	-1,86
Ccdc59	coiled-coil domain containing 59	-1,50
Olfr42	olfactory receptor 263	-1,79
Casp9	caspase 9	-2,15
Tcf20	transcription factor 20	-1,86
Cyp2a5	cytochrome P450, family 2, subfamily a, polypeptide 5	-2,50

Peg10	paternally expressed 10	-1,47
Vwa5a	von Willebrand factor A domain containing 5A	-1,56
Pik3r4	phosphatidylinositol 3 kinase, regulatory subunit 4, p150	-1,83
Tardbp	TAR DNA binding protein	-1,50
Atad2	ATPase family, AAA domain containing 2	-1,64
Polr2k	polymerase (RNA) II (DNA directed) polypeptide K	-1,66
Nppa	natriuretic peptide type A	-2,13
Ccdc53	coiled-coil domain containing 53	-1,55
H2-T23	histocompatibility 2, T region locus 23	-1,67
Atp13a5	ATPase type 13A5	-1,74
Tmem201	transmembrane protein 201	-1,62
Slco3a1	solute carrier organic anion transporter family, member 3a1	-1,86
Tcf20	transcription factor 20	-1,64
Ppm1h	protein phosphatase 1H	-1,64
Bpil3	BPI fold containing family B, member 6	-1,56
Ppa2	pyrophosphatase 2	-1,46
Veph1	ventricular zone expressed PH domain homolog 1	-1,55
Bpifb4	BPI fold containing family B, member 4	-1,71
Gpr124	G protein-coupled receptor 124	-1,52
Pde6d	phosphodiesterase 6D, cGMP-specific, rod, delta	-1,65

Tab. 8: Gene expression analysis of 12 months old hTDP-43^{A315T}Rosa+/- mice compared to controls.

Danksagung

Danke an …

… Prof. Dr. Wolfgang Wurst für die Möglichkeit diese Arbeit am Institut für Entwicklungsgenetik anzufertigen sowie für die Begeisterung für mein Forschungsthema und die daraus entstandenen hilfreichen und motivierenden Diskussionen

… PD Dr. Thomas Floss für die gute Betreuung während der ganzen Doktorarbeit, die Unterstützung bei wissenschaftlichen Problemen, die zahlreichen hilfreichen Gespräche und die entspannte Arbeitsatmosphäre

… Prof. Dr. Dr. Christian Haass für die Teilnahme am Thesis Committee und die Begeisterung für mein Thema sowie für die Teilnahme an der Prüfungskommission

… Prof. Dr. Erwin Grill für die Übernahme des Vorsitzes der Prüfungskommission

… Dr. Daniela Vogt Weisenhorn für die Unterstützung bei histologischen Fragen und die Hilfe bei Fragen jeglicher Art

… Dr. Sabine Hölter Koch für die Hilfe rund um Verhaltensversuche

… Lisa und Bettina für die Hilfe bei der Durchführung von Tests und deren Auswertung

… Helga, Irina, Michi, Anke, Anja und Susanne für die allgegenwärtige Hilfsbereitschaft bei kleineren oder größeren Problemen, die entstandenen Freundschaften und die tolle Zeit während der letzten Jahre. Ohne euch wäre es nicht dasselbe gewesen!

… das ganze IDG für die tolle Arbeitsatmosphäre und die allgegenwärtige Hilfsbereitschaft

… Olli für deine endlose Geduld, andauernde Unterstützung und dein Verständnis während der letzten Jahre und dafür dass du es auch in „dunklen“ Zeiten geschafft hast mich zum Lachen zu bringen

… meine Mama und meine Schwester für eure moralische Unterstützung und den Zuspruch während der ganzen Zeit

… meinen Papa, der es leider nicht mehr miterleben durfte, aber ohne den ich nicht da wäre wo ich heute bin